REPORT No. 885

FLIGHT INVESTIGATION ON A FIGHTER-TYPE AIRPLANE OF FACTORS WHICH AFFECT THE LOADS AND LOAD DISTRIBUTIONS ON THE VERTICAL TAIL SURFACES DURING RUDDER KICKS AND FISHTAILS

By John Boshar

SUMMARY

Results are presented of a flight investigation conducted on a fighter-type airplane to determine the factors which affect the loads and load distributions on the vertical tail surfaces in maneuvers. An analysis is made of the data obtained in steady flight, rudder kicks, and fishtail maneuvers.

For the rudder kicks, the significant loads were the "deflection load" resulting from an abrupt control deflection and the "dynamic load" consisting of a load corresponding to the new static equilibrium condition for the rudder deflected plus a load due to a transient overshoot. The deflection load is proportional to the angular acceleration which in turn is dependent upon the rate and amount of control deflection and upon the directional response characteristics of the airplane. The dynamic load had an angular acceleration load superposed on it as a result of the rudder being reversed at the time of maximum sideslip. The critical loads on the rudder were associated with the deflection load, and those on the fin, with the dynamic load.

The minimum time to reach the maximum control deflection attainable by the pilot in any flight condition was found to be a constant.

In the fishtail maneuvers, it was found that the pilot tends to deflect the rudder in phase with the natural frequency of the airplane. At the condition of resonance the load on the fin and that on the rudder are approximately 90° out of phase. The maximum loads measured in fishtails were of the same order of magnitude as those from a rudder kick in which the rudder is returned to zero at the time of maximum sideslip.

INTRODUCTION

The problem of evolving methods for designing the tail surfaces of fighter-type airplanes for the dynamic effects which occur in maneuvers has received much attention in recent years. In the case of the horizontal tail, methods by which the loads may be determined for an arbitrary type of elevator motion have been introduced (references 1 and 2) and the type of control deflection to be assumed in design has been specified (reference 3).

In the case of the vertical tail, however, the current design specifications consider only steady-state conditions for loads associated with a specified steady yaw or a specified rudder angle. Indications have been that the loads on the vertical tail are more critical in maneuvers than in steady-flight conditions. For instance, in reference 4, critical vertical-tail loads in rolling pull-out maneuvers were shown to be related to the ratio of aileron power and the static directional-stability derivative of the airplane; whereas, in reference 5 the dynamic loads in abrupt rudder kicks or in fishtail maneuvers were shown to reach high values. For some time, therefore, there has existed a need for a systematic flight investigation to evaluate the factors which influence the vertical-tail loads.

The purpose of the present paper is to present the results of a flight investigation of the factors which affect the loads and the load distributions on the vertical tail surfaces in rudder kicks and fishtail maneuvers. An attempt has been made to isolate the effects of power, of speed, of initial sideslip, and of rate, amount, and direction of control deflection. Emphasis has been placed upon the presentation of the experimental results in the light of theoretical considerations.

SYMBOLS

δ_r	rudder deflection angle, degrees
$\dot{\delta}_r$	maximum rate of rudder deflection, degrees per second
δ_e	elevator deflection angle, degrees
β	sideslip angle, degrees
F_r	pedal force, pounds
N_v	normal force on vertical tail, pounds
N_r	normal force on rudder, pounds
N_f	normal force on fin, pounds
N_{v_1}	first load peak on vertical tail, pounds
N_{r_1}	first load peak on rudder, pounds
N_{f_1}	first load peak on fin, pounds
N_{v_2}	second load peak on vertical tail, pounds
N_{r_2}	second load peak on rudder, pounds
N_{f_2}	second load peak on fin, pounds
C_{N_v}	normal-force coefficient on vertical tail (N_v/qS_v)
C_{N_r}	normal-force coefficient on rudder (N_r/qS_v)
C_{N_f}	normal-force coefficient on fin (N_f/qS_v)

With the foregoing symbols, the prefix Δ represents an increment; for maneuvers, it indicates the maximum increment measured from the initial steady-flight value; for steady sideslip, it represents an increment measured from the trim value for wings level.

V airspeed, miles per hour
V_e equivalent airspeed, miles per hour ($V\sigma^{1/2}$)
S_v total vertical tail area, square feet
x_v distance from center of gravity to rudder hinge line (absolute value), feet
q dynamic pressure, pounds per square foot $\left(\frac{1}{2}\rho V^2\right)$
I_Z moment of inertia about Z-axis, pound-foot-second^2
T_c thrust coefficient ($T/\rho V^2 D^2$)
T propeller thrust, pounds
Q_c torque coefficient ($Q/\rho V^2 D^3$)
Q propeller torque, pound-feet
D propeller diameter, feet
b wing span, feet
S wing area, square feet
P pressure coefficient ($(p-p_0)/q$)
p local static pressure
p_0 free-stream static pressure
N' yawing moment, foot-pounds
ρ mass density of air, slugs per cubic foot
ρ_0 mass density of air at sea level, slugs per cubic foot
C_n yawing-moment coefficient, tail off (N'/qSb)
$\sigma=\frac{\rho}{\rho_0}$
$\dot{\psi}$ maximum yawing velocity, radians per second
$\ddot{\psi}$ angular acceleration in yaw, radians per second^2
$\ddot{\psi}_1$ first maximum angular acceleration in yaw, radians per second^2
$\ddot{\psi}_2$ second maximum angular acceleration in yaw, radians per second^2
$\dot{\theta}$ maximum pitching velocity, radians per second
$\ddot{\theta}_1$ first maximum angular acceleration in pitch, radians per second^2
Δt time interval during which maneuver is allowed to continue before rudder is returned to zero, seconds
$\Delta\alpha$ increment in angle of attack of vertical tail, degrees
$\frac{dC_n}{d\beta}$ rate of change of yawing-moment coefficient with sideslip angle (tail off)
$\left(\frac{dC_N}{d\beta}\right)_v$ measured rate of change of normal-force coefficient on vertical tail with angle of sideslip, including the effect of rudder deflection
$\frac{d\beta}{d\delta_r}$ rate of change of sideslip with change in rudder angle (from steady sideslip measurements)
$\left(\frac{dC_L}{d\delta_r}\right)_v$ estimated rate of change of lift coefficient with control deflection for isolated vertical tail (1.10 per radian)
$\left(\frac{dC_L}{d\alpha}\right)_v$ estimated rate of change of lift coefficient with angle of attack for isolated vertical tail (1.43 per radian)
$\left(\frac{d\alpha}{d\delta_r}\right)_v$ estimated rudder effectiveness (0.77)

DEFINITIONS

Deflection load: Maximum increment in load due to abrupt control deflection at the start of maneuver (first load peak).

Dynamic load: Maximum increment in load including load due to the static balance condition for rudder deflected, load due to transient overshoot, and load due to rudder reversal (second load peak).

U-type control manipulation: Hypothetical control manipulation in which both the initial kick and the return of rudder have the same amount and rate of control deflection.

APPARATUS

Test airplane.—The investigation was conducted on a modified Curtiss P-40K airplane which is a low-wing fighter airplane with a gross weight of about 8200 pounds and equipped with a V-1710-F4R Allison engine rated at 1000 horsepower at a pressure altitude of 10,800 feet. Figure 1 shows photographs of the test airplane. Figure 2 presents a three-view drawing of the airplane; table I contains a list of some pertinent geometric characteristics.

The military equipment, radio, and fuselage gas tanks were removed to permit the installation of the recording instruments. The airplane was flown with a center-of-gravity location of 29.5 percent of the mean aerodynamic chord.

Tail surfaces.—In order to improve the directional stability characteristics and to permit the pilot to fly more easily

(a) One-quarter front view.

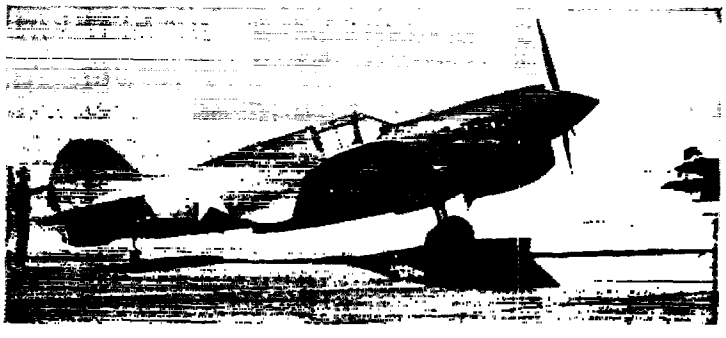

(b) Side view.

FIGURE 1.—Test airplane.

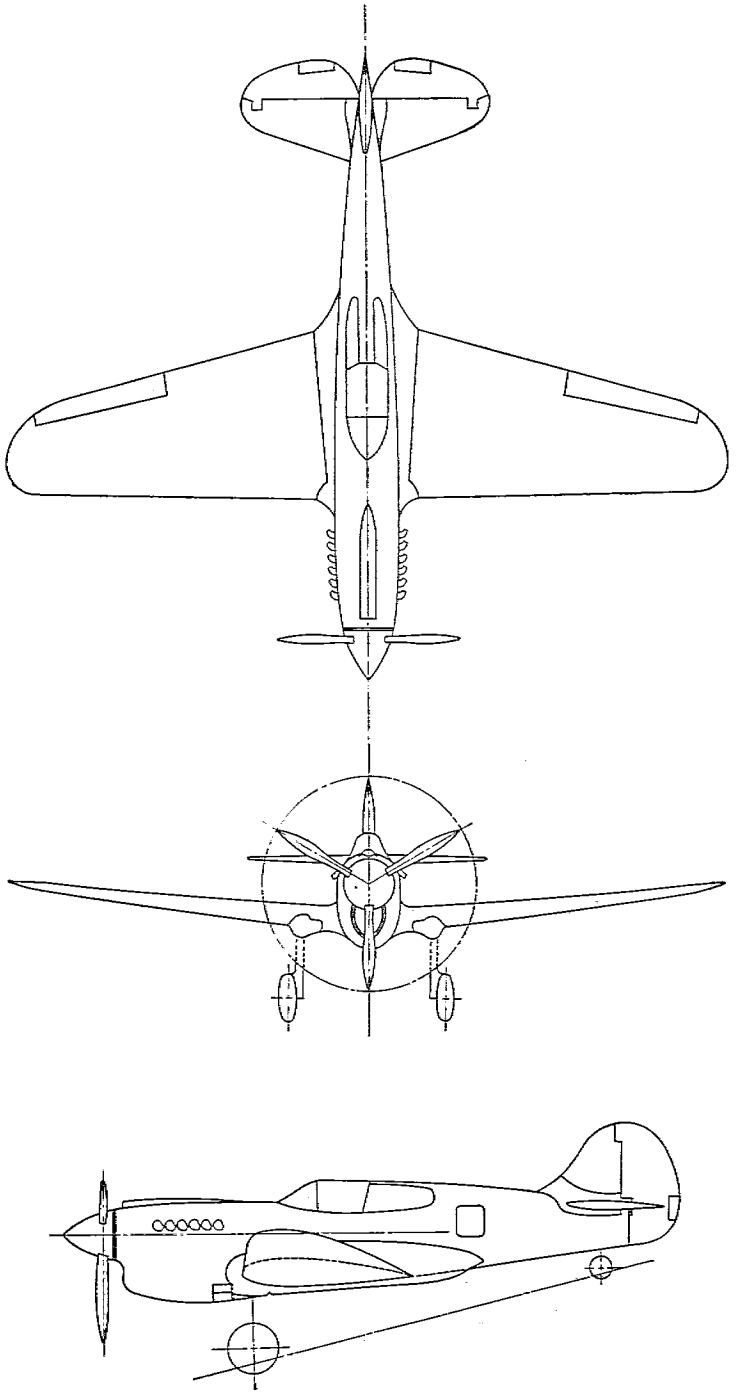

FIGURE 2.—Three-view drawing of test airplane. List of geometric characteristics is given in table I.

through the speed range with only one setting of the rudder-trim tab, a fin extension was added (see fig. 3), and the fin offset was changed from 1½° left to 0° offset as suggested in reference 6.

The horizontal tail surfaces were unchanged with the exception of the fairing added at the juncture of the fin and horizontal tail to cover the pressure lines. The amount of protuberance of this fairing is shown in the photographs in figure 4.

Orifices were installed opposite each other on the left and right sides of the vertical tail at the locations shown in figure 5.

Flight instruments.—Instruments installed to measure the differential pressures, the control forces, the control deflections, and the motions of the airplane were as follows:

(1) Multicell manometers to measure the differential pressures over the vertical tail surface at the points shown in figure 5.

(2) An NACA airspeed recorder with the swivelling static head located approximately one chord forward of the right wing tip. (See fig. 1 (a).)

(3) Control-force recorders which measured the forces exerted by the pilot on the stick (aileron and elevator) and on the rudder pedals.

(4) NACA electrical control-position recorders which measured the elevator- and rudder-control positions at points on these controls near the fuselage center line.

(5) A sideslip-angle recorder mounted approximately one-half chord above and one chord forward of the left wing tip. (See fig. 1 (a).)

(6) Accelerometers which recorded transverse and normal accelerations at points 59 and 152 inches behind the center of gravity.

(7) Turnmeters which measured the angular velocities in yaw, pitch, and roll.

(8) A timer used to synchronize all records.

Prior to each test the pilot noted the manifold pressure, the pressure altitude, the airspeed, and the cockpit settings of the rudder, elevator, and aileron trim tabs.

TEST PROGRAM

The test program may be divided into three parts: (1) tests conducted to obtain steady-flight data, (2) tests in which rudder kicks were made, and (3) tests in which fishtail maneuvers were made. All speeds mentioned are equivalent airspeeds.

Steady-flight runs.—Inasmuch as the vertical-tail loads on an airplane are related to its steady-sideslip characteristics, a number of steady-flight runs were made at various values of steady sideslip and speed, and at two power conditions. The data were recorded after the pilot had trimmed the airplane at the test condition. Runs were obtained through a speed range of 100 to 380 miles per hour with power on (power for level flight or rated power when necessary) and 100 to 220 miles per hour with power off.

Rudder kicks.—Rudder kicks (single abrupt rudder deflections) are useful in the study of the directional stability characteristics of an airplane and for the investigation of the effects of rate, amount, and direction of control deflection on the vertical-tail loads.

A total of approximately 50 left and right rudder kicks were made during which pressure distributions were measured. Of these runs, approximately 30 were kicks from the wings-level condition and 20 were kicks against

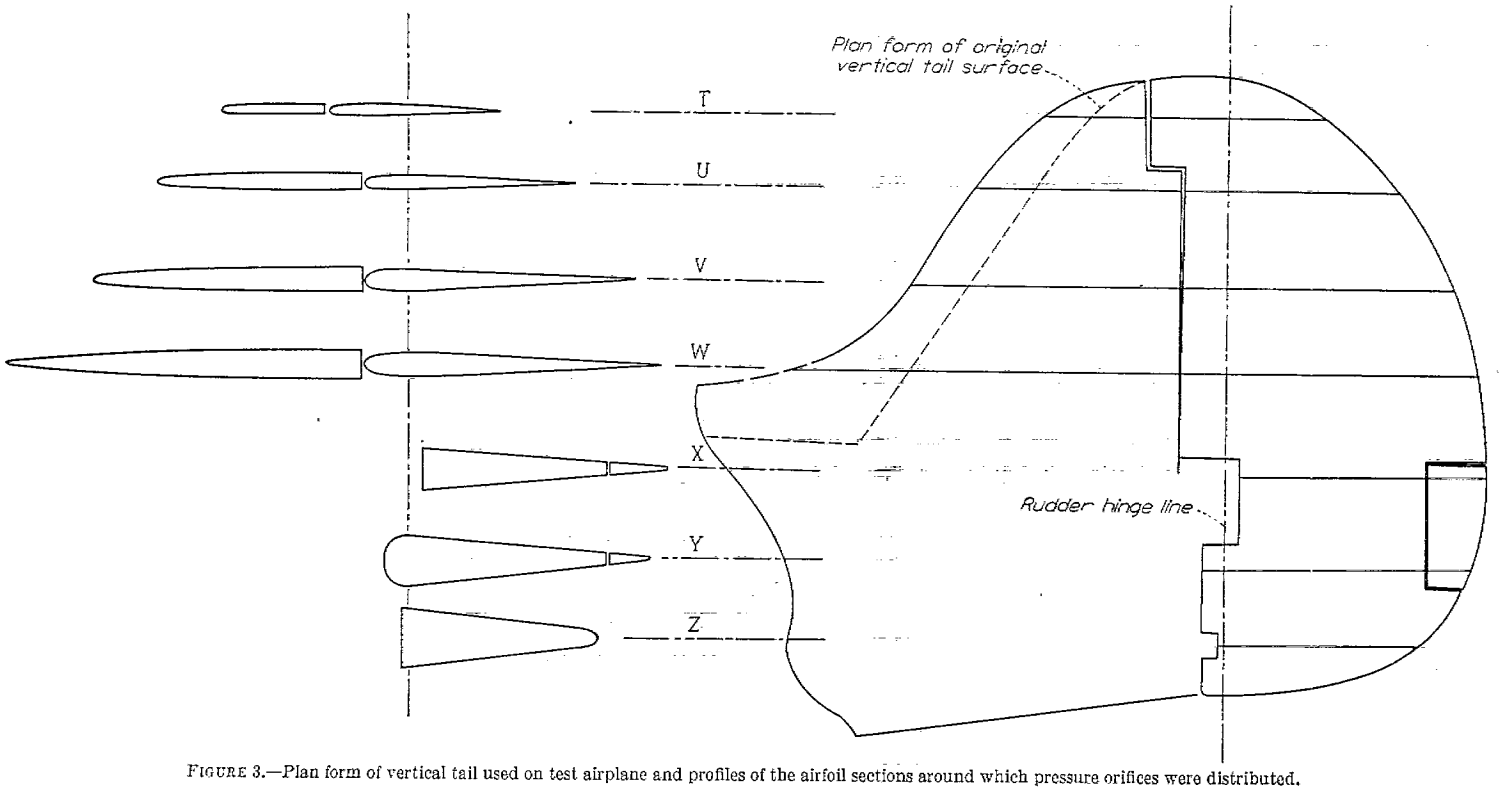

FIGURE 3.—Plan form of vertical tail used on test airplane and profiles of the airfoil sections around which pressure orifices were distributed.

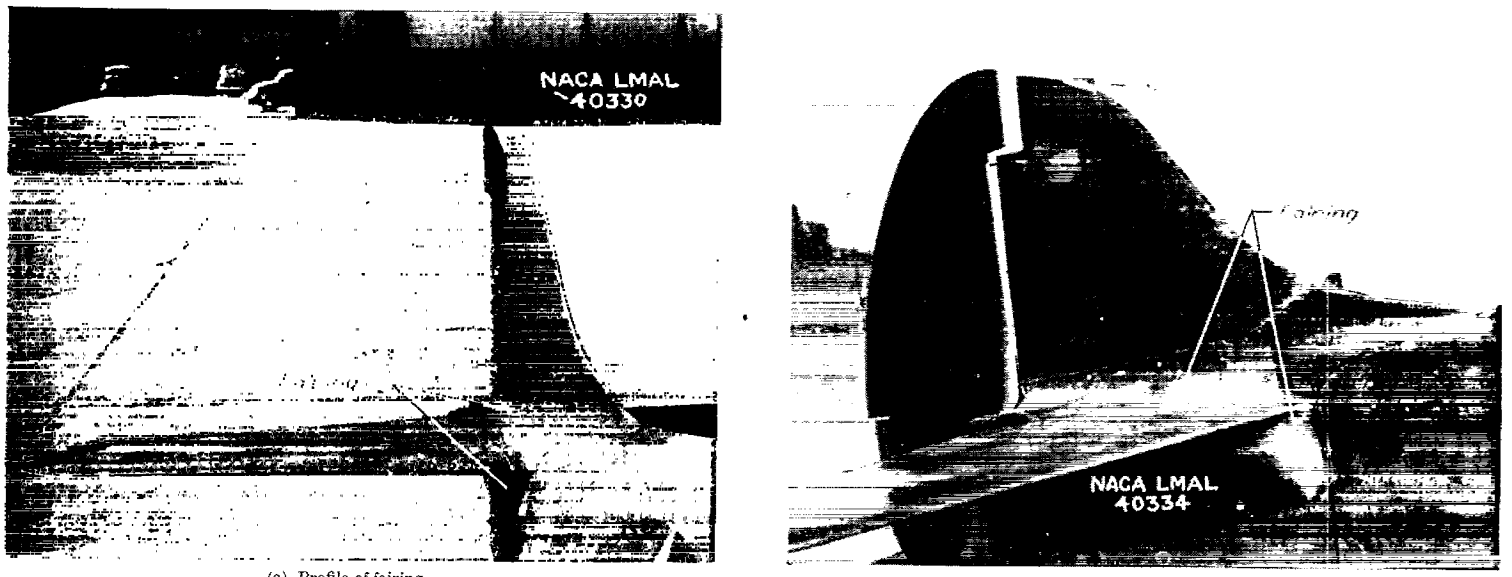

(a) Profile of fairing.

(b) Side view of fairing.

FIGURE 4.—Vertical tail showing profile and plan form of protuberance caused by fairing over pressure lines.

an initial steady sideslip. The runs were made at speeds of approximately 100, 200, and 300 miles per hour with power on and power off. The rudder kicks were performed at medium and fast rates from trimmed flight. In addition, 70 rudder kicks in which loads were not measured were found to be useful in the analysis.

Fishtail maneuvers.—Fishtail maneuvers (periodic rudder oscillations) were made with power off and power on at speeds of 150 and 200 miles per hour during which the pilot attempted to maximize the loads on the vertical tail. Also, runs were made at 150 miles per hour during which the pilot applied an abrupt rudder deflection against the swing at the time of maximum yawing velocity. A second pilot was asked to perform mild fishtail maneuvers at speeds of 200, 250, 300, and 350 miles per hour. For this series the pilot was free to use as much coordination as he wished so that information would be obtained to evaluate the maneuver under such conditions.

Rib	Chord (in.)	Orifice location, percent chord from leading edge											
		1	2	3	4	5	6	7	8	9	10	11	12
T	34.0	11.3	23.1	29.4	52.6	65.9	76.2	89.4					
U	49.2	4.1	10.2	35.6	45.8	52.9	58.9	73.2	90.4				
V	63.2	3.8	13.3	26.4	37.8	44.8	52.8	57.6	68.7	82.1	93.4		
W	75.0	3.1	6.0	10.4	16.3	27.8	41.1	51.7	56.4	60.4	69.7	81.1	95.7
X	28.6	7.4	37.1	63.3	86.0								
Y	31.2	10.9	41.4	71.8	89.4								
Z	22.8	7.5	40.4	77.6									

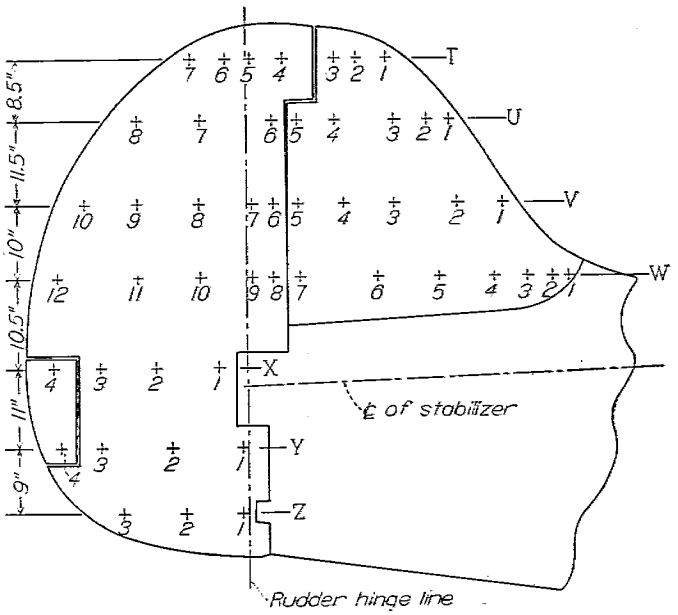

FIGURE 5.—Location of orifices at which pressures were measured.

METHODS

Pressure distributions.—The records used in evaluating the pressure distributions were read at time values which would permit an accurate time history to be represented. The chordwise integrations were performed in two parts so that the chordwise and spanwise loads could be obtained separately for the fin and rudder. A numerical method of obtaining the spanwise center of load on the fin was used.

Other records.—The angle of sideslip for the steady-sideslip results was corrected for the effect of inflow as determined from the results of a calibration flight in which similar sideslip-angle recorders were installed on each wing tip. This correction was not made for the sideslip-angle records in the time histories since only incremental values were used in the analysis and the angle of inflow correction was nearly constant throughout the maneuver.

The only other corrections made were the compressibility correction to the airspeed and the correction to the rudder and elevator angles for the amount of trim-tab deflection required to keep the wings in level trim.

The rate of control deflection and angular accelerations were obtained by mechanically differentiating the control deflection and the angular-velocity records, respectively.

Separation of load components.—The method of separation of load components on the vertical tail was found to be accomplished most conveniently by considering the load to be made up of two components: one necessary to balance the unstable wing-fuselage yawing moment in sideslip and one due to yawing acceleration, or

$$\Delta N_v = \Delta\beta \frac{dC_n}{d\beta} qS\frac{b}{x_v} - \frac{I_Z}{x_v}\ddot{\psi} \tag{1}$$

However, some use was also made of the expression for the load in terms of effective angle of attack at the tail; that is,

$$\Delta N_v = \Delta\alpha_v \left(\frac{dC_L}{d\alpha}\right)_v qS_v \tag{2}$$

where, approximately,

$$\Delta\alpha_v = -\beta + \left(\frac{d\alpha}{d\delta_r}\right)_v \Delta\delta_r$$

The form of equation (1) is particularly useful in the present case because both the parameter $dC_n/d\beta$ and the factor I_Z/x_v were derivable from flight results as shown subsequently herein and also because the maximum loads could be defined when only the value of maximum yawing acceleration $\ddot{\psi}$ and the maximum angle of sideslip $\Delta\beta$ were known.

RESULTS AND DISCUSSION—STEADY FLIGHT

Wings level.—The pertinent data obtained from tests with wings level are shown plotted in figures 6 and 7. Figure 6 shows the variation with speed of the amount of rudder, elevator, and sideslip angle required to maintain wings level for power on and power off. Figure 7 shows the variation of the normal-force coefficients over the fin, rudder, and total vertical tail, and the spanwise variation of center of load on the fin with speed. These curves are typical for a single-engine airplane. The variations shown in figures 6 and 7 are caused by the effects of propeller rotation in producing a twisting slipstream and by a direct asymmetric thrust due to the inclined propeller. With power off the variations are probably the result of a windmilling propeller, particularly at speeds lower than 200 miles per hour where the amount of blade adjustment possible is insufficient to maintain the rotation of the constant-speed propeller. The spanwise center of load on the fin moves outboard with decreasing speed but, from consideration of the loads, this movement with wings level is not very significant because of the small bending moments involved.

Steady sideslip.—Steady-sideslip data are presented in table II and in figures 8 to 12. The data are shown as incremental values measured from the condition with wings level.

Figure 8 presents the changes in rudder deflection, rudder pedal force, and elevator deflection required for changes in sideslip measured from the wings-level trim value. The increments in pedal force are shown as pedal-force factors, which are obtained by dividing the pedal force by the dynamic pressure so that the data from all speeds may be combined.

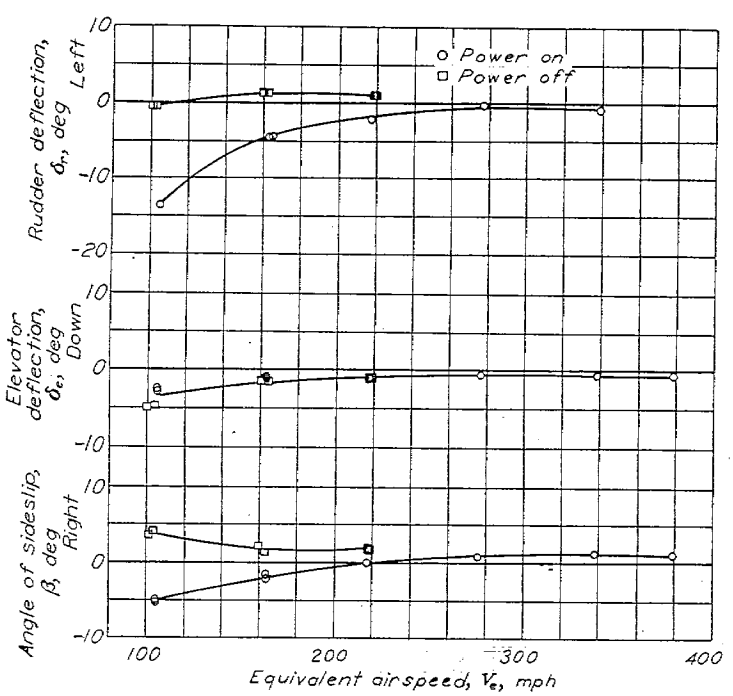

FIGURE 6.—Variation with equivalent airspeed of rudder and elevator control deflections (for tab at zero) and angle of sideslip (corrected for inflow) required to maintain wings level with power on and power off.

The change in elevator angle required with a change in sideslip results from a change in the pitching moment of the airplane with sideslip. The variation of rudder angle with angle of sideslip is seen to be approximately linear throughout the speed range. Figure 9 presents the variation of the normal-force coefficient with sideslip for the rudder, fin, and total vertical tail surface. The variations shown are consistent with the trends of figure 8. The rate of change of normal-force coefficient on the vertical tail with angle of sideslip $\left(\frac{dC_N}{d\beta}\right)_v$ is used to define the load required on the vertical tail to balance the unstable yawing moment of the wing-fuselage configuration. From this value the parameter $dC_n/d\beta$ may be obtained as

$$\frac{dC_n}{d\beta}=\left(\frac{dC_N}{d\beta}\right)_v\frac{x_v}{b}\frac{S_v}{S}$$

Figure 10 presents isometric views of the pressure distribution over the vertical tail at various incremental values of sideslip for power on at an airspeed of 220 miles per hour. The spanwise load distributions on the fin and rudder corresponding to the isometric diagrams of figure 10 are shown in figure 11.

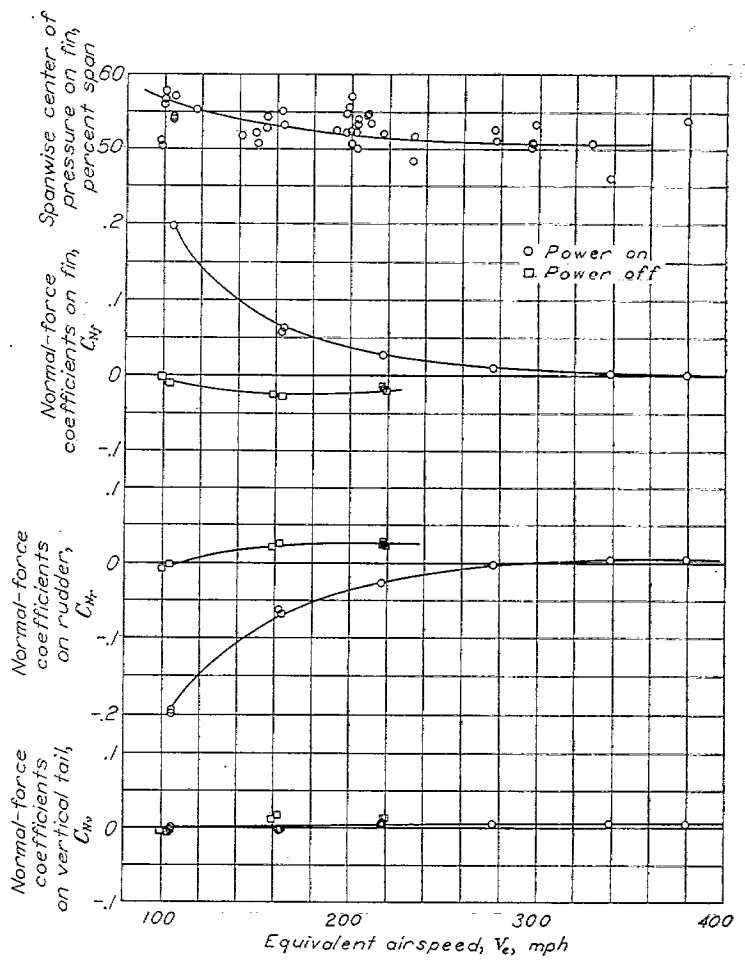

FIGURE 7.—Variation with equivalent airspeed of normal-force coefficients on surfaces of vertical tail for wings in level flight with power on and power off and variation of spanwise center of pressure on fin.

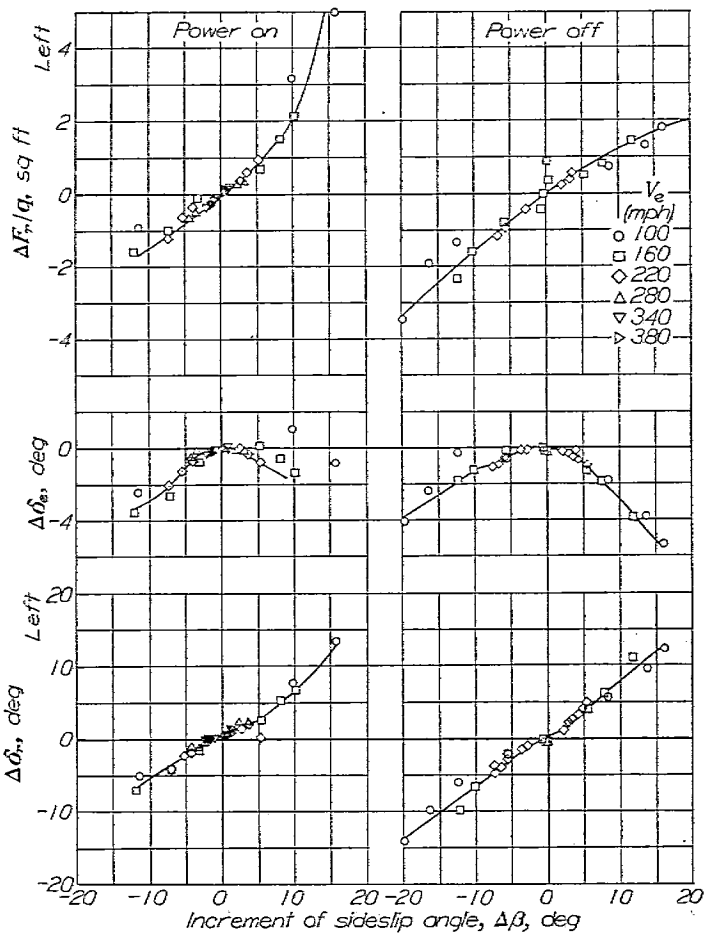

FIGURE 8.—Variation of increments of rudder and elevator control deflections and pedal-force factor with incremental change in sideslip measured from wings in level flight with power on and power off.

Figure 12 shows the variation of spanwise center of load on the fin with change in sideslip from the wings-level trim value at airspeeds of 100, 160, and 220 miles per hour. With change in sideslip from the wings-level condition, according to figure 12, an inboard movement of the spanwise center of load occurs which is probably a result of the displacement of the tail from the region of greatest fuselage boundary layer.

RESULTS AND DISCUSSION—RUDDER KICKS

TIME HISTORIES

Data pertaining to the rudder kicks are plotted in figures 13 to 41. The data for all the rudder kicks are shown in tables III and IV. Before a detailed analysis of the loads is made, it would be of value to note the general nature of the airplane motion and the sequence of events. For this purpose typical time histories of the measurements are shown in figures 13 to 18.

Figures 13 and 15 present the time histories of right and left rudder kicks, respectively, made at airspeeds of 100, 200, and 300 miles per hour with power on. The normal load on the fin, rudder, and total vertical tail surfaces associated with these measurements are shown in figures 14 and 16. Time histories for two rudder kicks applied against initial steady sideslips to the left and right made at airspeeds of 200 miles per hour are shown in figure 17 and corresponding normal loads on the vertical tail surfaces, in figure 18.

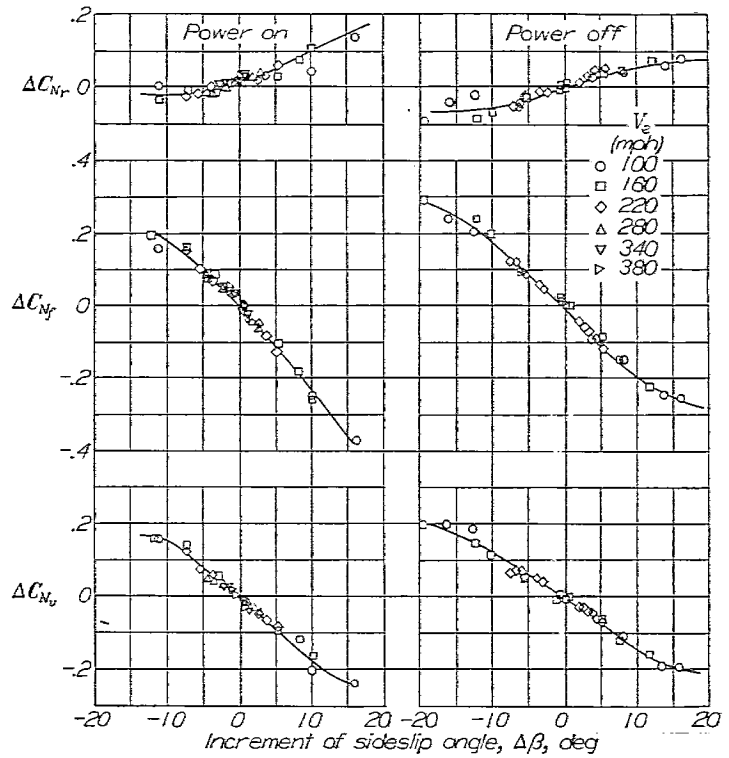

FIGURE 9.—Change of vertical tail, fin, and rudder normal-force coefficients with change in sideslip angle measured from wings-level condition with power on and power off.

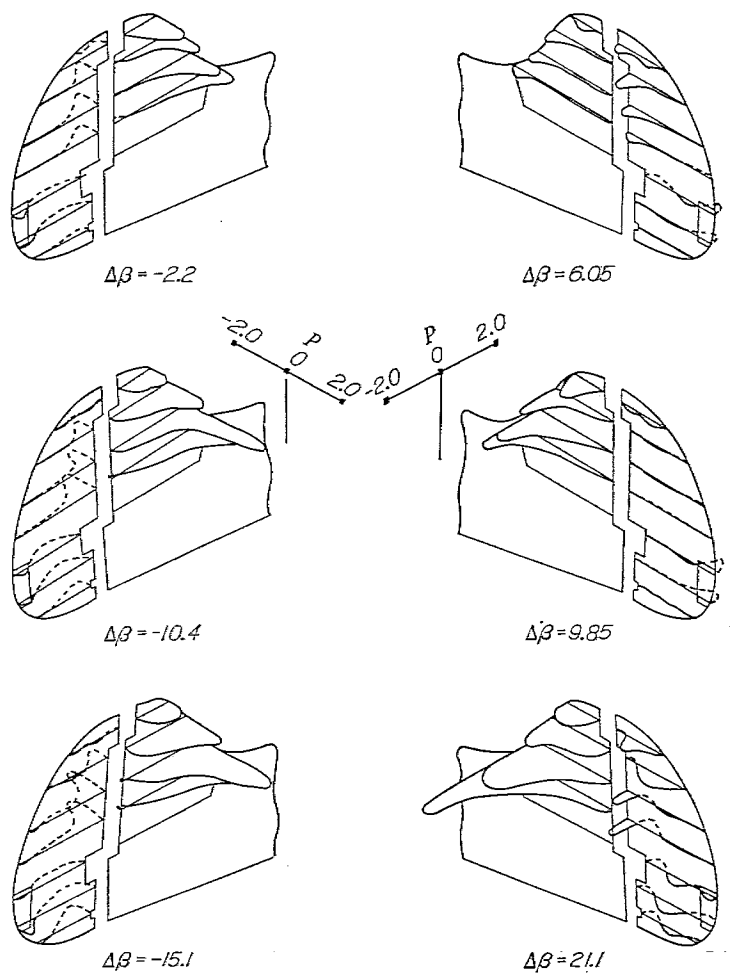

FIGURE 10.—Isometric views of pressure distribution over vertical tail surface at various increments of sideslip for wings in level flight at 220 miles per hour and with power on. Airplane lift coefficient, 0.28; T_c=0.03; Q_c=0.004.

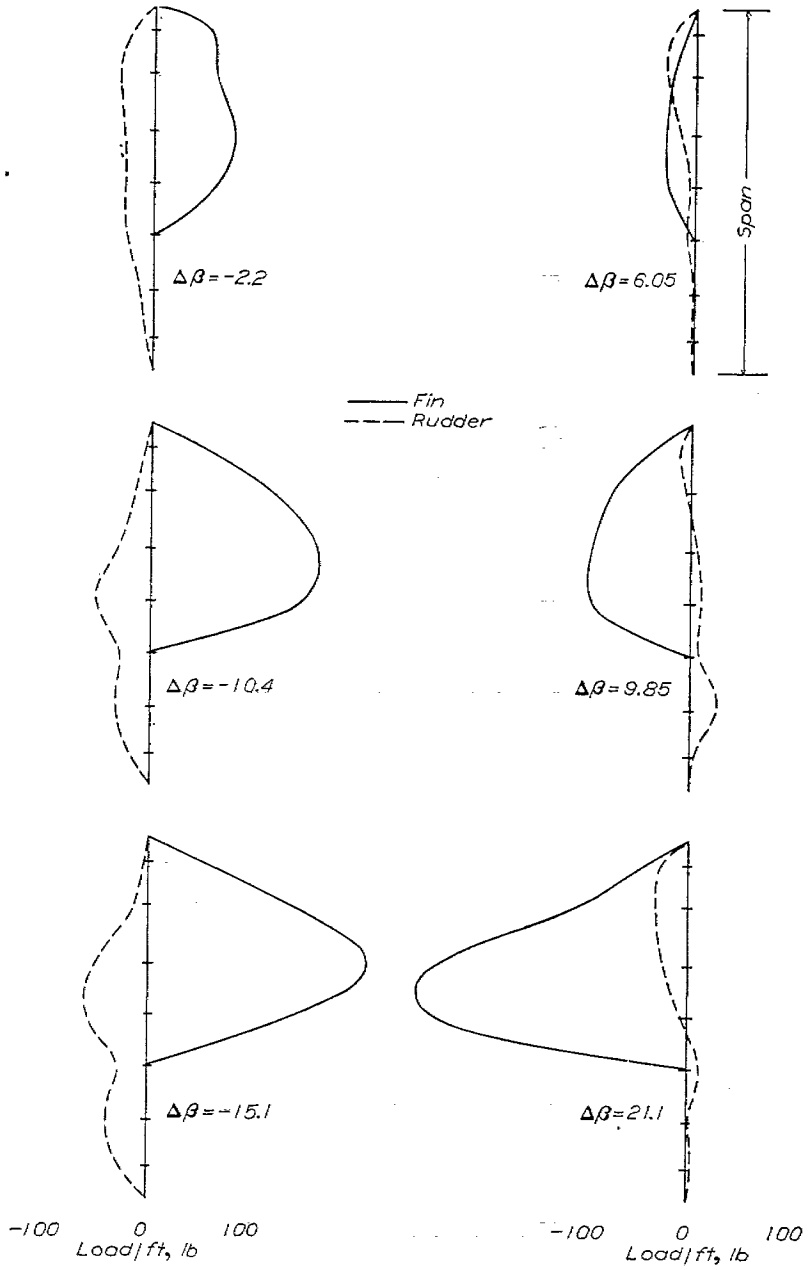

FIGURE 11.—Spanwise load distributions on fin and rudder corresponding to the isometrics of figure 10.

From a study of the time histories the following sequence of events and items of interest may be observed:

(1) Before the maneuver is started, the airplane is in steady trim flight as indicated by the constant initial values of the variables.

(2) After the application of an abrupt pedal force a lag of the order of a fraction of a second occurs before the rudder begins to respond because of flexibility in the control system.

(3) The airplane begins to yaw as soon as the rudder is deflected.

(4) The greatest rate of change of yawing velocity (the maximum yawing acceleration) following the rudder deflection occurs before the value of sideslip has changed from the trim condition.

(5) The time interval from the start of the maneuver to the time the maximum yawing velocity is reached is, roughly, inversely proportional to the airspeed.

The time histories show that an appreciable amount of pitching is induced during the maneuver. With right rudder deflection the pitching is nose-down and with left rudder deflection it is nose-up. The pitching is caused primarily by two effects; namely, the precessional moment which results from yawing the propeller disk and the change in airplane pitching moment with sideslip. The precessional effect

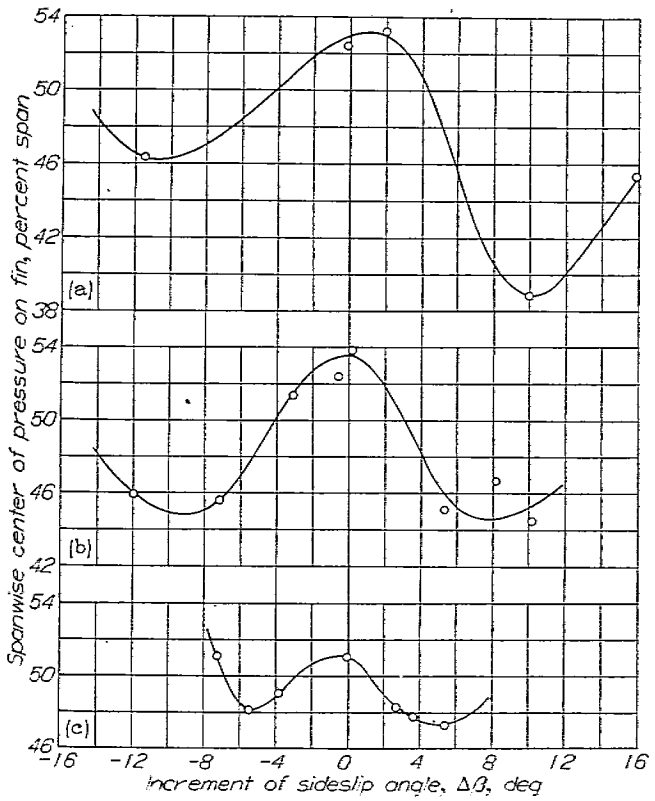

(a) V_e=100 miles per hour.
(b) V_e=160 miles per hour.
(c) V_e=220 miles per hour.

FIGURE 12.—Variation of spanwise center of pressure on fin with change in sideslip from wings-level condition at V_e=100, 160, and 220 miles per hour with power on.

leads the effect of sideslip by a phase relation of approximately 90° since it depends upon the yawing velocity rather than the angle of yaw. Also, the sign of the precessional pitching moment depends upon the direction of yawing; whereas the sign of the airplane pitching moment due to sideslip is negative regardless of sideslip direction, as is shown by the variation of elevator required with sideslip (fig. 8). The net effects are additive for right rudder kicks and canceling for left rudder kicks. This result explains the phase difference between the yawing-velocity curve and the pitching-velocity curve for left and right rudder kicks. The combined effects for right rudder kicks produce a decrement in vertical acceleration as high as approximately 1.7g at the center of gravity, as is indicated by figure 13 (c).

The time histories of the loads on the vertical tail surfaces (figs. 14, 16, and 18) exhibit the same general characteristics as the load variation on the horizontal tail following an abrupt elevator deflection. The first significant feature is the load peak due to the abrupt deflection of the rudder. This first load-peak increment is termed the "deflection load" herein. The second feature indicated by the load time histories is the build-up of load in the opposite direction as the airplane responds to the unbalance created by the control deflection. In seeking to assume a new static equilibrium position a transient "overshoot" occurs, the magnitude of which is a function of the dynamic lateral stability of the airplane. The maximum balance load thus consists of a static-balance trim value and a transient load. This second load-peak increment is referred to as the "dynamic load."

The load variation with time on the rudder and fin shows that the rudder carries most of the deflection load; whereas the fin carries most of the dynamic load.

The deflection load and dynamic load will be discussed separately, use being made of the breakdown of the load into the component necessary to balance the unstable yawing moment of the wing-fuselage combination and that associated with the yawing acceleration. (See section entitled "Methods.") A time history of the component of load due to each factor and a comparison of the combined effects with the measured vertical-tail loads is shown in figure 19 for flight 11a, run 1. As expected, the agreement is particularly good since the parameter $dC_n/d\beta$ (already shown) and the factor I_Z/x_v were determined with the aid of experimental results. The details of determining I_Z/x_v will be given in the following section.

In the subsequent discussion the definitions illustrated in figure 20 may be helpful.

DEFLECTION LOAD

General relations.—In the deflection load, as shown in figure 19, the component of load necessary to balance the unstable wing-fuselage moments in sideslip is absent and the deflection load is defined by the angular-acceleration component only; therefore, when the values of the first yawing acceleration $\ddot{\psi}_1$, the moment of inertia of the airplane I_Z, and the tail length x_v are known, the load may be determined by the relation

$$\Delta N_{v_1}=\frac{I_Z}{x_v}\ddot{\psi}_1$$

This relation is shown in figure 21 in which the maximum yawing acceleration $\ddot{\psi}_1$ is seen to be linearly related to the experimentally determined deflection load. This curve, then, is an experimental determination of the factor I_Z/x_v. Inasmuch as figure 21 shows that such a definite relationship exists, it will be used in the subsequent analysis to determine the deflection load from the value of yawing acceleration only. This relationship permits determination of tail loads by use of the rudder-kick data presented in table IV for which direct tail-load measurements were not available.

As an introduction to the factors which affect the magnitude of the deflection load, it is convenient to consider two extremes of control manipulation—zero and infinite rates of rudder deflection. When the rate of rudder deflection is zero or very slow, the airplane will adjust itself to a new static equilibrium position as each infinitesimal increment of unbalance is impressed and the deflection load will be zero

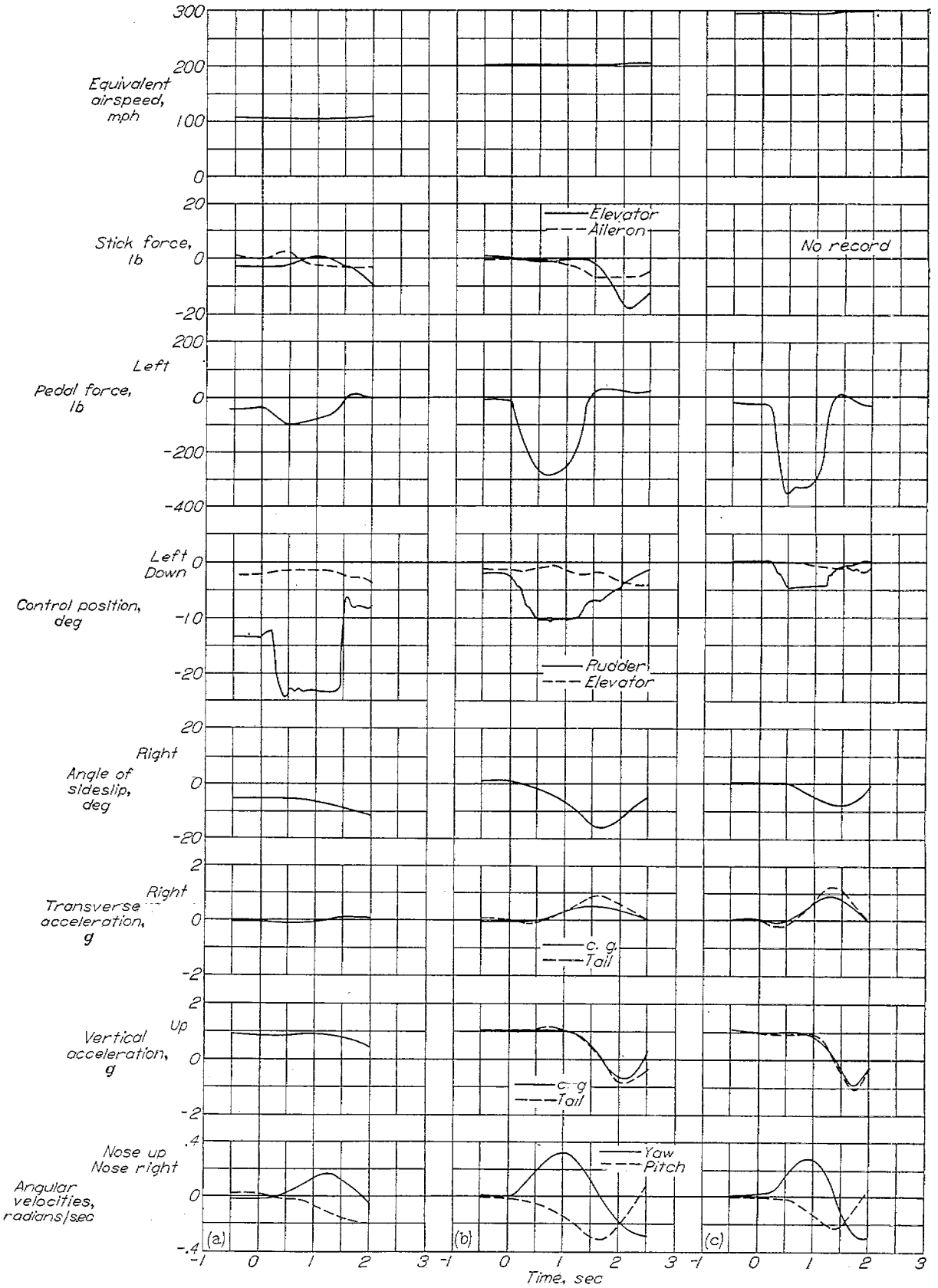

(a) Flight 6, run 6; V_e=100 miles per hour. (b) Flight 8b, run 3; V_e=200 miles per hour. (c) Flight 11a, run 1; V_e=300 miles per hour.

FIGURE 13.—Time histories of three abrupt rudder kicks to the right made at V_e=100, 200, and 300 miles per hour with power on.

regardless of the amount of control deflection or the airplane stability or mass characteristics. When the rate of rudder deflection is infinite, however, because of the inertia about the Z-axis, the lift is experienced before the airplane can respond and the deflection load becomes approximately equal to that on an isolated tail with a value corresponding to the amount of control deflection attained, that is,

$$\Delta N_{v_1}=\left(\frac{dC_L}{d\delta_r}\right)_v \Delta\delta_r q S_v$$

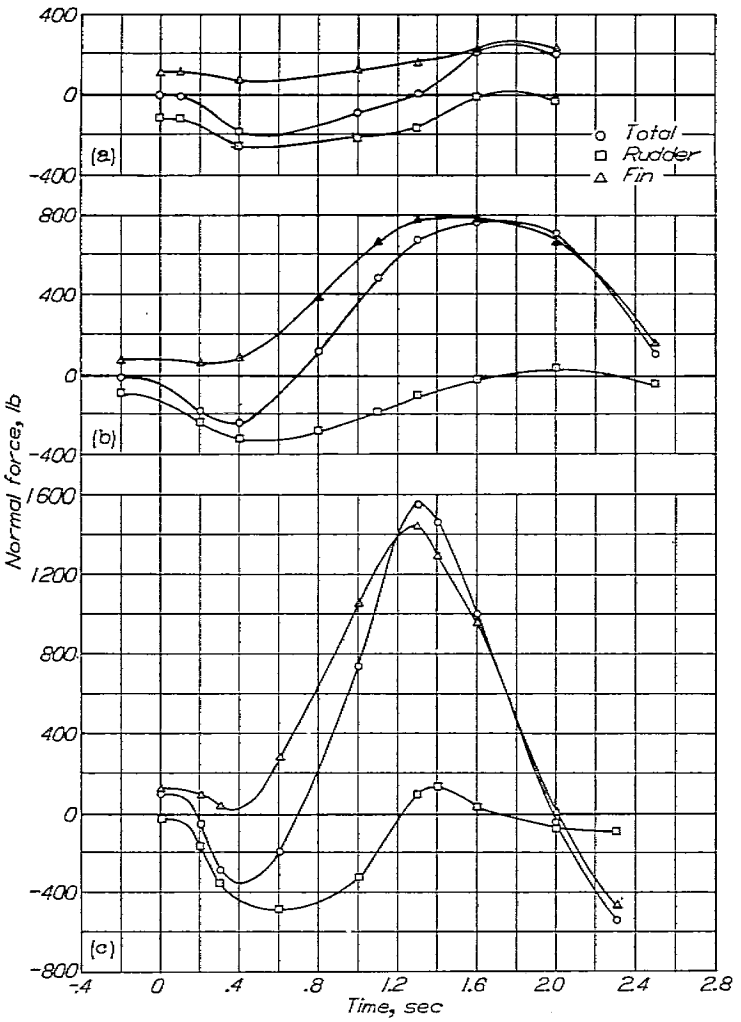

(a) V_e=100 miles per hour; flight 6, run 6.
(b) V_e=200 miles per hour; flight 8b, run 3.
(c) V_e=300 miles per hour; flight 11a, run 1.

FIGURE 14.—Time histories of normal forces on vertical tail surfaces for right rudder kicks of figure 13.

For actual cases where the rate of deflection is between zero and infinity, the deflection load is dependent upon the rate of deflection, amount of deflection, and the response characteristics of the airplane.

For an airplane of given characteristics the amount of control deflection that can be applied and the response characteristics of the airplane are, in general, fixed so that it becomes convenient to consider the rate of control deflection as the prime determinant of the deflection load. The deflection load thus involves a determination of (1) the maximum rate of control deflection the pilot employs and (2) the load corresponding to this maximum rate.

Rate of control deflection.—From the many rudder kicks performed in this investigation some information was obtained which pertained to the rate at which the controls were deflected. It is to be emphasized that these are the rates that the pilot actually used, which may or may not be those of which he is physically capable.

Data pertaining to the maximum rate at which the pilot deflects the rudder is shown in figures 22 (a), 23 (a), and 24 (a) for kicks made from the wings-level condition and in figures 22 (b), 23 (b), and 24 (b) for kicks against an initial sideslip.

In figure 22 (a), the rates of control deflection are shown plotted against airspeed for all rudder kicks made from the wings-level condition and in figure 23 (a) the rates are plotted against the maximum incremental pedal force. The faired lines in figure 23 (a) define the envelope of the maximum rate of control deflection attained. The maximum rate of deflection is noted to decrease with increase of pedal force, or amount of resistance to deflection. This result is in agreement with the results of tests made on the ground to determine the rates of elevator deflection used by a number of pilots (reference 7). On the basis of the relation indicated in figure 23 (a), the envelope describing the maximum rate (fig. 22 (a)) can be explained by the amount of resistance encountered. For instance, the rate of control deflection is greatest for the condition of power off and low speed.

In figure 24 (a) the ratio of rate of control deflection and amount of control deflection is plotted against speed for power on and power off. This figure shows that the ratio $\dot{\delta}_r/\Delta\delta_r$ approaches an upper limit of 10; the reciprocal of this ratio signifies that the minimum time to reach the highest control deflection the pilot can attain at each flight condition is a constant equal to 0.1 second. The conclusion that the ratio $\Delta\delta_r/\dot{\delta}_r$ is a constant may be deduced from the fact that both the maximum amount of deflection the pilot can attain $\Delta\delta_r$ and the maximum rate of deflection $\dot{\delta}_r$ are proportional to the same factor (the pedal force). It should be pointed out here that the rate of control deflection $\dot{\delta}_r$ used in the ratio is the maximum measured during each rudder kick (see symbols) so that the minimum time value is derived from values of the ratio, which are themselves minimums.

Similar data obtained from the rudder kicks against an initial sideslip are presented superposed on the data obtained from kicks made from the wings-level condition in figures 22 (b), 23 (b), and 24 (b). It is shown in both figures 22 (b) and 23 (b) that the rates of deflection are higher than the maximums defined by the envelope for the data for rudder kicks from the wings-level condition. This result is obtained because the increment in pedal force is measured from the initial sideslip value, which in this case is an untrimmed value, so that a resistance to deflection is indicated that is higher than actually exists. Actually, the rudder tends to move toward the trim position of its own accord when the pilot releases it to apply opposite rudder. Figure 24 (b) shows that the time to reach the maximum rudder deflection is the same constant value as that obtained by rudder kicks from the wings-level condition. In this case, the greater rates are evidently balanced by a greater increment of control deflection.

Deflection load associated with maximum rate of control deflection.—The maximum deflection load per unit rudder deflection is shown plotted against dynamic pressure in figure 25 and is compared with the value computed from the geometric parameters of the tail for an infinite rate of deflection. The loads with power on are shown to be greater than the computed values at the lower speeds due to the fact that for the computed values the dynamic pressure at the tail was assumed to be equal to the free-stream dynamic pressure. At high speeds the actual maximum load experienced is almost 100 percent of that for an infinite rate of control deflection for this airplane.

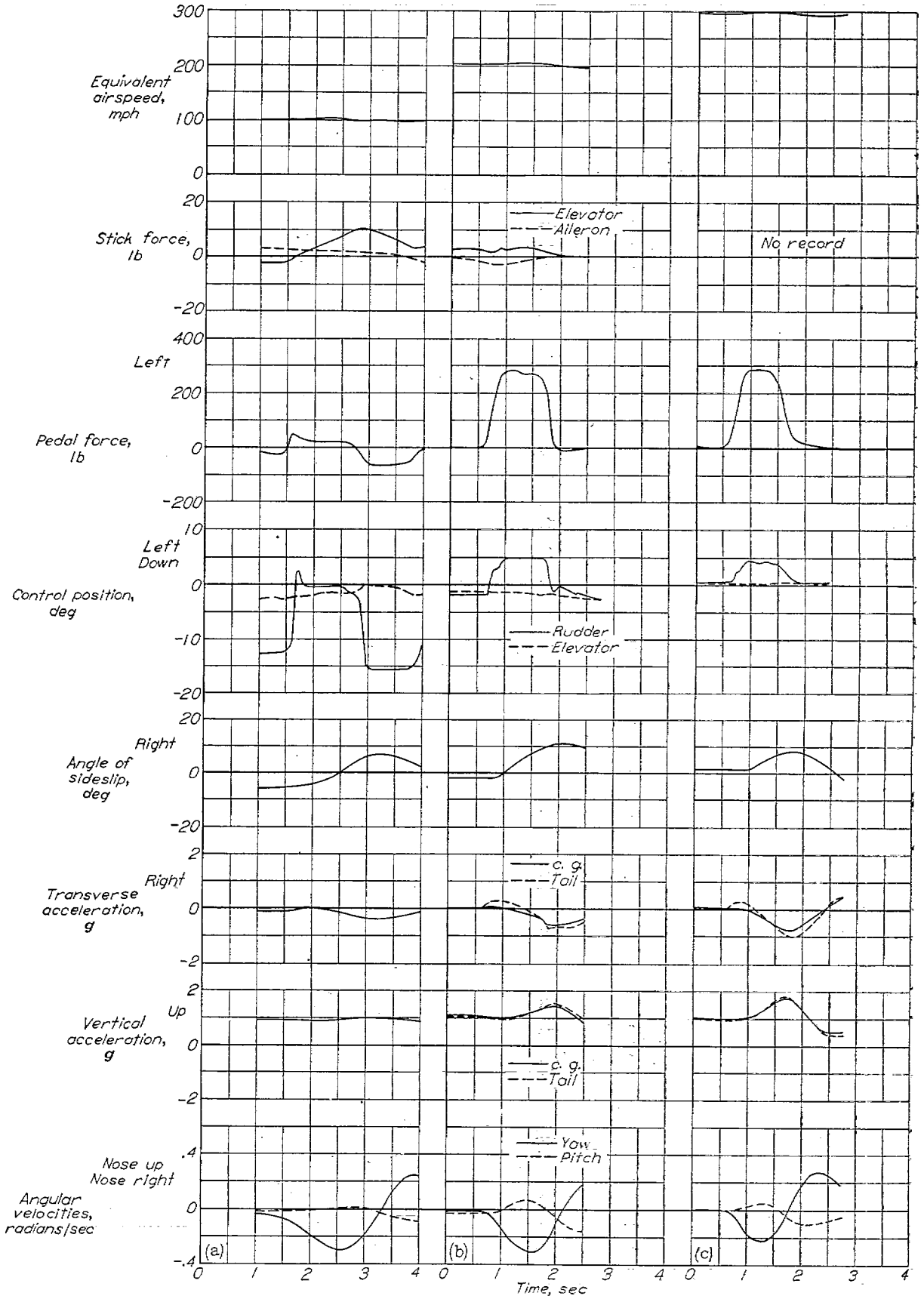

(a) Flight 6, run 9; V_e=100 miles per hour. (b) Flight 8b, run 2; V_e=200 miles per hour. (c) Flight 11a, run 3; V_e=300 miles per hour.

FIGURE 15.—Time histories of three abrupt rudder kicks to the left made at V_e=100, 200, and 300 miles per hour with power on.

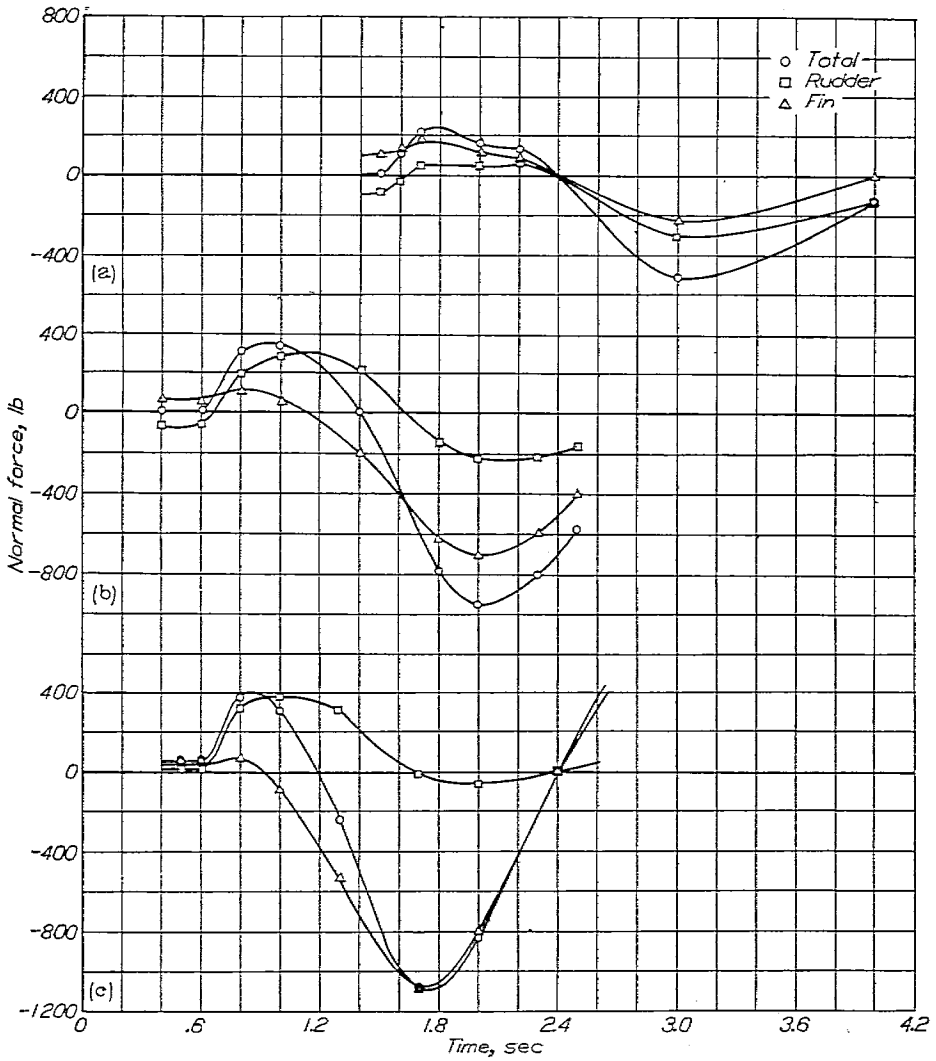

(a) V_e=100 miles per hour; flight 6, run 9.
(b) V_e=200 miles per hour; flight 8b, run 2.
(c) V_e=300 miles per hour; flight 11a, run 3.

FIGURE 16.—Time histories of normal force on vertical tail surfaces for left rudder kicks of figure 15.

As previously mentioned, the maximum rate of control deflection $\frac{\Delta\delta_r}{\dot{\delta}_r}=0.1$ is based upon the assumption of a linear-type control deflection which has a constant rate equal to the measured maximum rate. This assumed control deflection compared with a typical flight control deflection is shown in figure 26 (a). In figure 26 (b) the theoretical effect of rate of rudder movement on the deflection load is shown. The computations were made for the linear-type control deflection by the method indicated in reference 5. The figure shows the deflection load in percent of the load for an infinite rate of deflection $\frac{\Delta\delta_r}{\dot{\delta}_r}=0$ plotted against the time to reach maximum deflection $\Delta\delta_r/\dot{\delta}_r$. For the maximum rate of control deflection used by the pilot (a minimum time to reach maximum deflection of 0.1 sec) the load at 100 miles per hour is almost equal to that for a infinite rate of deflection. At higher speeds the rate becomes more critical in that the airplane responds more rapidly; however, even at a speed of 300 miles per hour the deflection load for a control deflection completed in 0.1 second is approximately 95 percent of that for an infinite rate.

DYNAMIC LOAD

General relations.—In figure 19 time histories of the component of load on the tail associated with the angular acceleration and the component due to sideslip are shown for one run, together with a comparison of the time histories of the summation of the components and the measured vertical-tail load. In figure 27 the measured dynamic loads are shown compared with the load computed from the relation

$$\Delta N_{v_2}=\frac{dC_n}{d\beta}\Delta\beta qS\frac{b}{x_v}-\frac{I_z}{x_v}\ddot{\psi}_2$$

The data for rudder kicks against sideslip (fig. 27 (b)) are noted to have a slightly different slope from those of rudder kicks from the wings-level condition (fig. 27 (a)). The difference is presumed to be a result of differences in the action of secondary effects such as damping in roll or linear

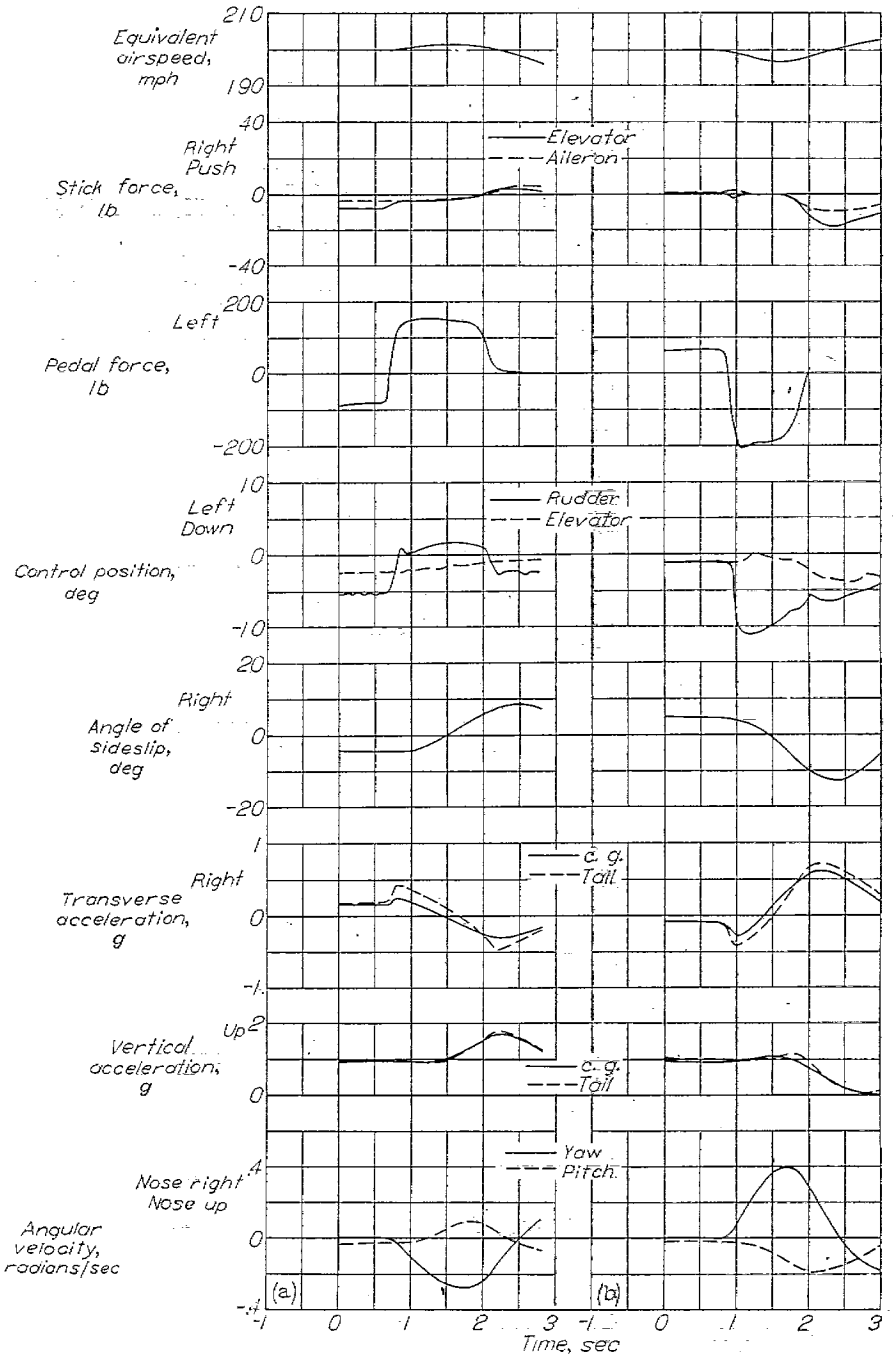

(a) Flight 12a, run 2; left sideslip. (b) Flight 12a, run 4; right sideslip.

FIGURE 17.—Time histories of left and right rudder kicks against left and right sideslips, respectively, at V_i=200 miles per hour with power on.

acceleration. The comparisons, however, indicate that for the test airplane the equation adequately represents the dynamic-loads data. Thus the dynamic load following a rudder kick may be easily determined if the maximum value of sideslip $\Delta\beta$ and yawing acceleration $\ddot{\psi}_2$ are available.

Some further discussion is needed regarding the factors which affect the angle of sideslip and the angular acceleration attained.

Angle of sideslip.—For steady sideslips the amount of sideslip attained by a given rudder angle is proportional to the factor $d\beta/d\delta_r$ (fig. 8). In abrupt rudder kicks, however, for an airplane with less than critical damping, a transitory angle of sideslip which is greater than the final steady sideslip will occur. For the case of zero directional damping and an abrupt rudder deflection, this transitory angle of sideslip would amount to twice the steady-state value of sideslip for the same rudder angle or $2(d\beta/d\delta_r)$.

The test airplane has low directional damping (as do most

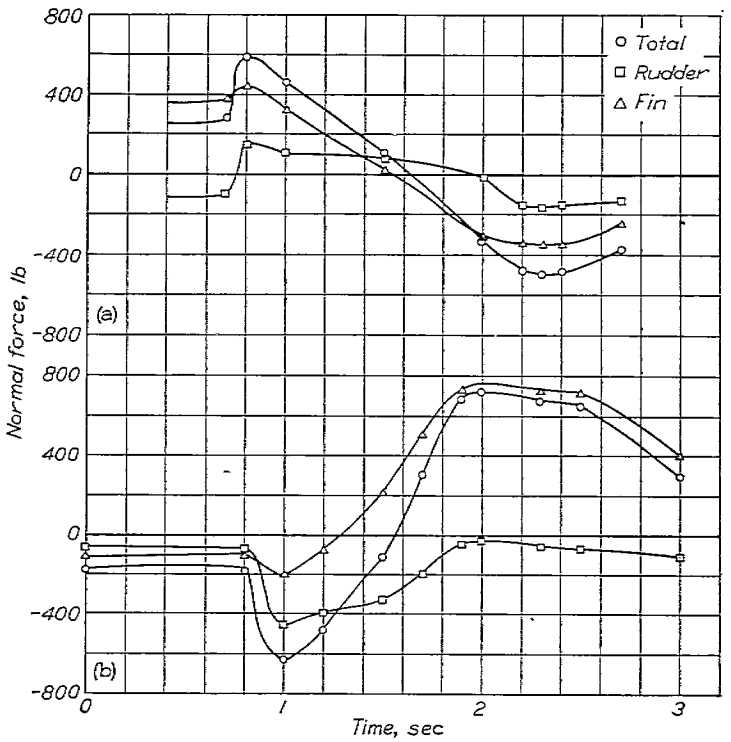

(a) Flight 12a, run 2.
(b) Flight 12a, run 4.

FIGURE 18.—Time histories of normal force on vertical tail surfaces for rudder kicks against initial sideslip of figure 17.

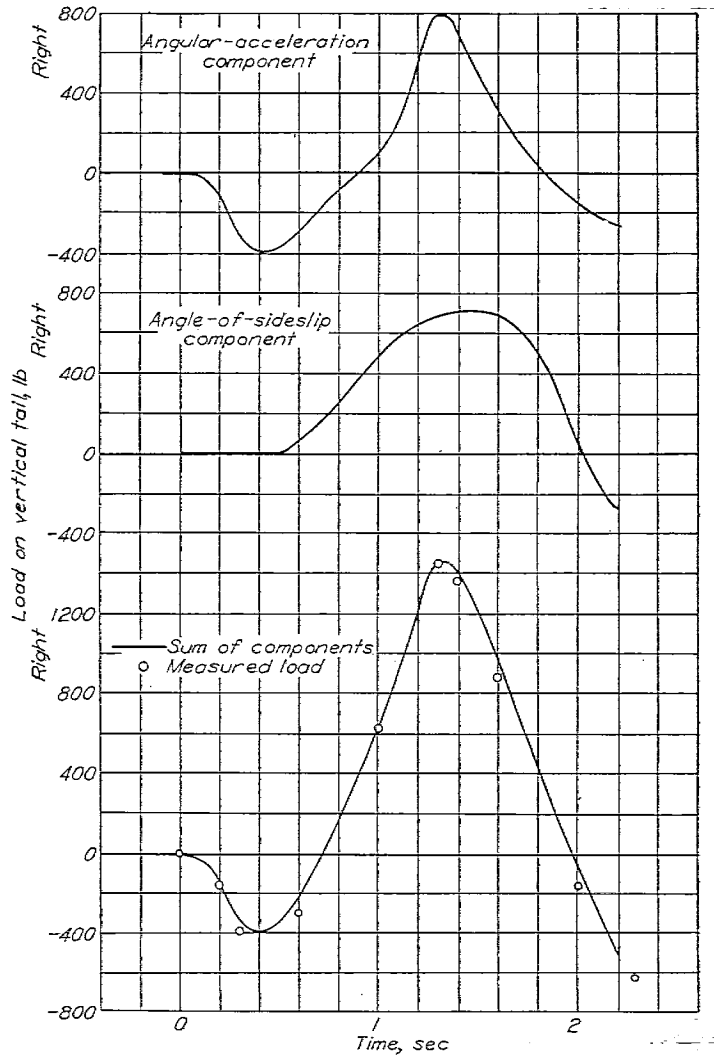

FIGURE 19.—Comparison of measured load on vertical tail with sum of component of load necessary to balance wing and fuselage moments and component associated with yawing acceleration for flight 11a, run 1 (figs. 13 and 14). V_a=300 miles per hour.

conventional airplanes) so that an overshoot resulting in a magnification factor of 1.5 to 2.0 over the steady-state value is to be expected. An approximate value of this factor for the test airplane may be obtained from figure 28 (a) which shows a plot of the ratio of angle of sideslip reached in rudder kicks to the value which would be reached in steady sideslips with the same rudder angle. At speeds of 100 and 200 miles per hour the full magnification factor is not reached because the rudder generally is reversed before the maneuver has continued long enough for the potential sideslip angle to be realized. The early rudder reversal relative to the time of maximum sideslip is shown in the time histories of the rudder kicks made at low speed (see fig. 13) and the computed effect of various times of rudder reversal on the sideslip reached is shown in figure 28 (b). At 300 miles per hour the rudder, in general, was held long enough for the full sideslip to be realized so that the magnification factor of approximately 1.5 obtained at this speed is believed to be near the true value for the test airplane.

Angular acceleration.—The maximum angular acceleration $\ddot{\psi}_2$ is made up of the superposition of a component that is proportional to the amount of overshoot and a component resulting from the reversal of the rudder. The component due to the amount of overshoot depends upon the amount of damping, being zero for the case of critical damping and equal to the deflection angular acceleration $\ddot{\psi}_1$ for zero damping. The component of angular acceleration due to rudder reversal is dependent upon the rate and amount of control deflection in the same manner as is the deflection angular acceleration. If the reversal deflection has the same rate and amount as the initial deflection (U-type rudder manipulation), the reversal component will exactly equal the deflection angular acceleration $\ddot{\psi}_1$.

The two parts making up the yawing acceleration $\ddot{\psi}_2$ are indicated in figure 29 in which the time histories of the load associated with the yawing acceleration only are shown for two rudder kicks in which the rudder was returned to zero after different time intervals. The time history for run 5 indicates the maximum angular acceleration without the reversal; whereas in run 6 the rudder was reversed at the time of maximum sideslip so that the maximum yawing acceleration includes the effect of rudder reversal. From this figure it is evident that the rudder kick in which the maneuver was stopped earlier results in higher loads because of the superposition of the two yawing-acceleration components near the time of their maximum values.

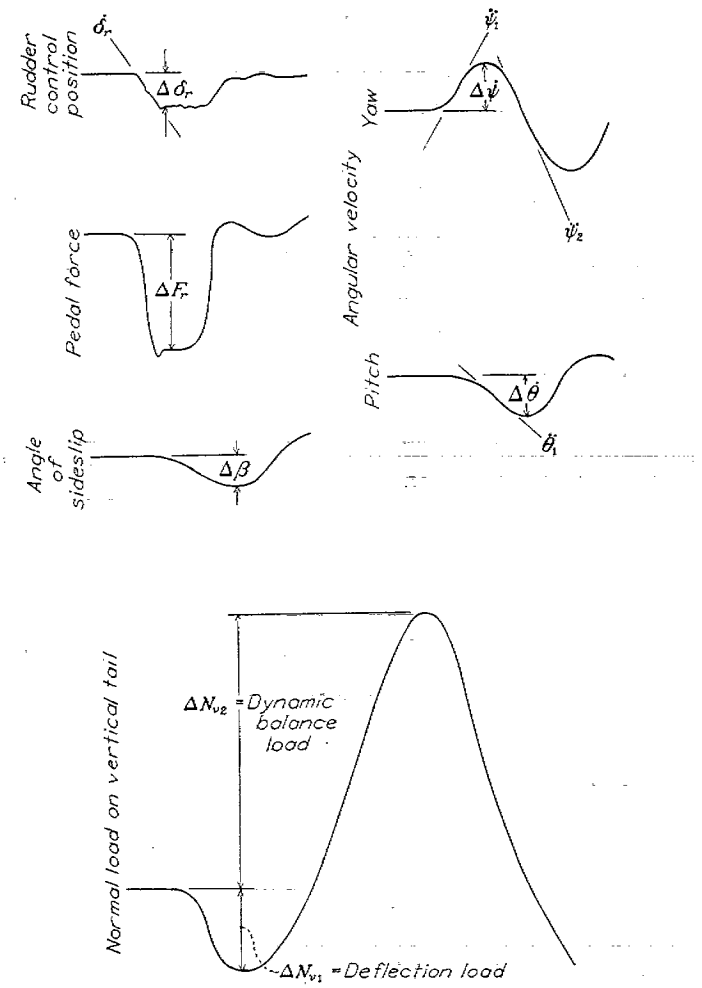

FIGURE 20.—Illustration of symbols used for slopes and incremental values.

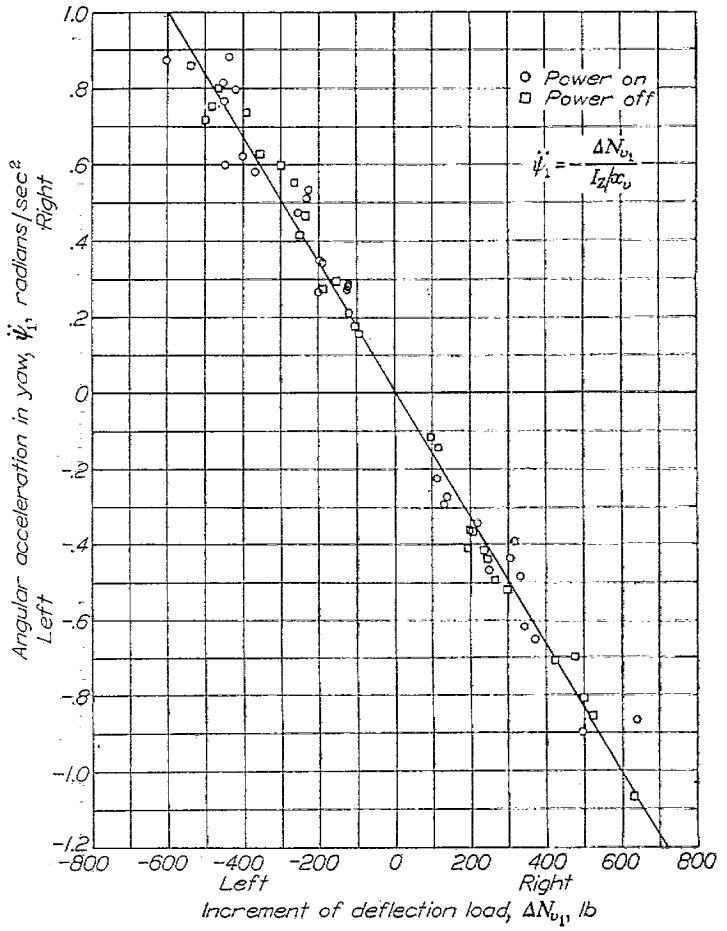

FIGURE 21.—Relation between the maximum deflection load and the maximum angular acceleration in yaw.

In order to indicate the likelihood with which the angular accelerations superpose at their maximum values, the ratio of the second peak angular acceleration to the first peak $\ddot{\psi}_2/\ddot{\psi}_1$ is shown plotted against speed in figure 30 (a). In general, an approach of the ratio to a factor of 2 would indicate that the angular acceleration components superposed at their peaks; without the reversal component the ratio would be less than 1.0 since the overshoot component of $\ddot{\psi}_2$ alone will always be less than the deflection value. Strictly speaking this value is obtained only for U-type control manipulation and, as indicated by some high values of the ratio (as high as 2.45), the rudder was returned past the trim position in some cases. The time histories (figs. 13 and 15) indicate, however, that although the rudder reversal was made at rates and amounts sometimes greater and sometimes less than the initial rudder kick the U-type manipulation represents an average type.

The computed effect of the time interval during which the rudder is held upon the manner of superposition of the angular acceleration components is shown in figure 30 (b).

The data of figure 30 (a) show that at 300 miles per hour the average of the components of angular acceleration due to overshoot and rudder reversal superpose near their maximum values and also that the U-type rudder manipulation is not an unduly conservative one as is sometimes felt in the specification of control motions.

Estimate of maximum value for dynamic load from flight data.—An approximate formula for the estimation of the order of magnitude of the dynamic load would assist in assessing the relative significance of the factors involved. For this purpose the expression for the load on the vertical tail in terms of an effective angle of attack is most convenient; that is,

$$\Delta N_{v_2} = \Delta\alpha \left(\frac{dC_L}{d\alpha}\right)_v qS_v$$

$$= \left[-\beta + \left(\frac{d\alpha}{d\delta_r}\right)_v \Delta\delta_r\right]\left(\frac{dC_L}{d\alpha}\right)_v qS_v$$

This expression is adequate when maximum values are considered inasmuch as the angular velocity is zero at the time of maximum β; also, the sidewash factor may be assumed to be zero.

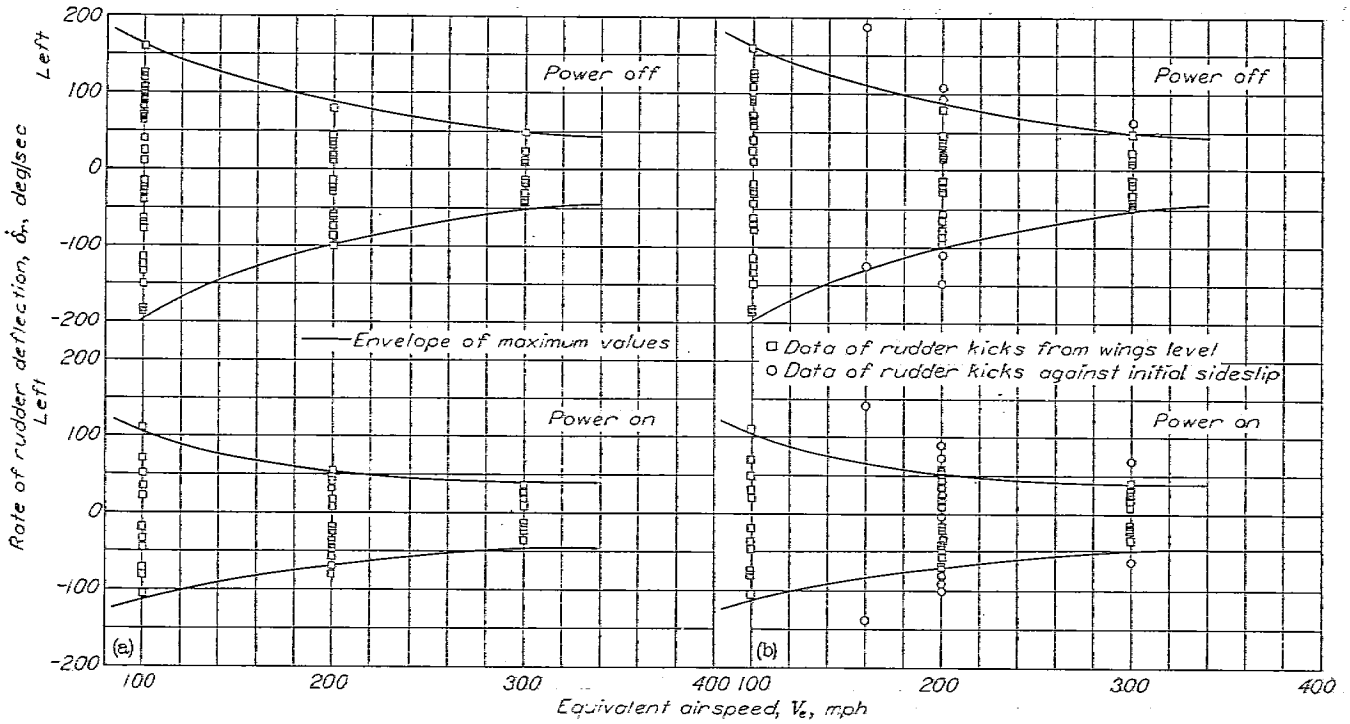

(a) Rudder kicks from wings level. (b) Rudder kicks against initial sideslip.

FIGURE 22.—Rates of rudder deflection used by pilot plotted against equivalent airspeed with power on and power off.

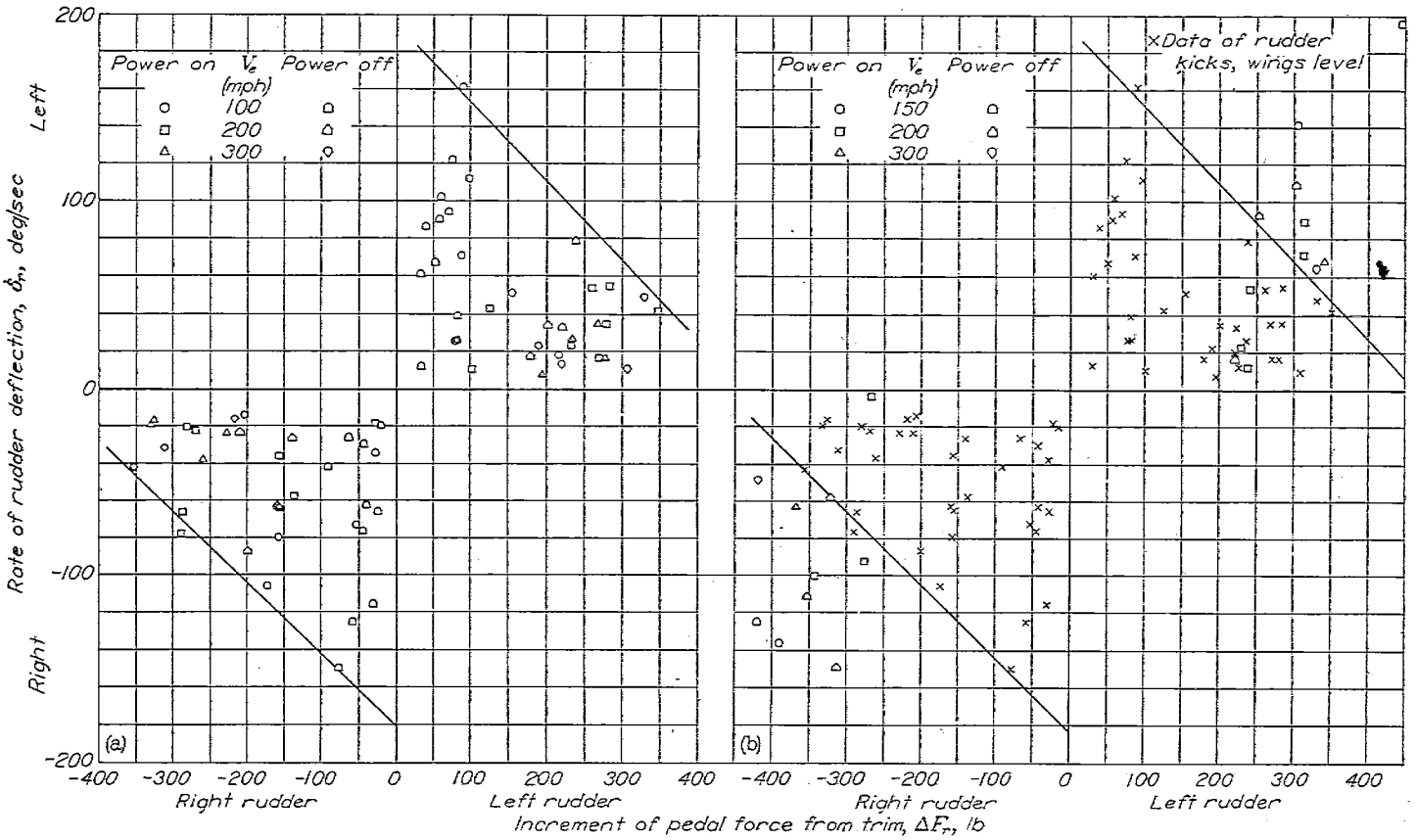

(a) Rudder kicks from wings level. (b) Rudder kicks against initial sideslip.

FIGURE 23.—Rate of rudder deflection plotted against increment of pedal force used by pilot.

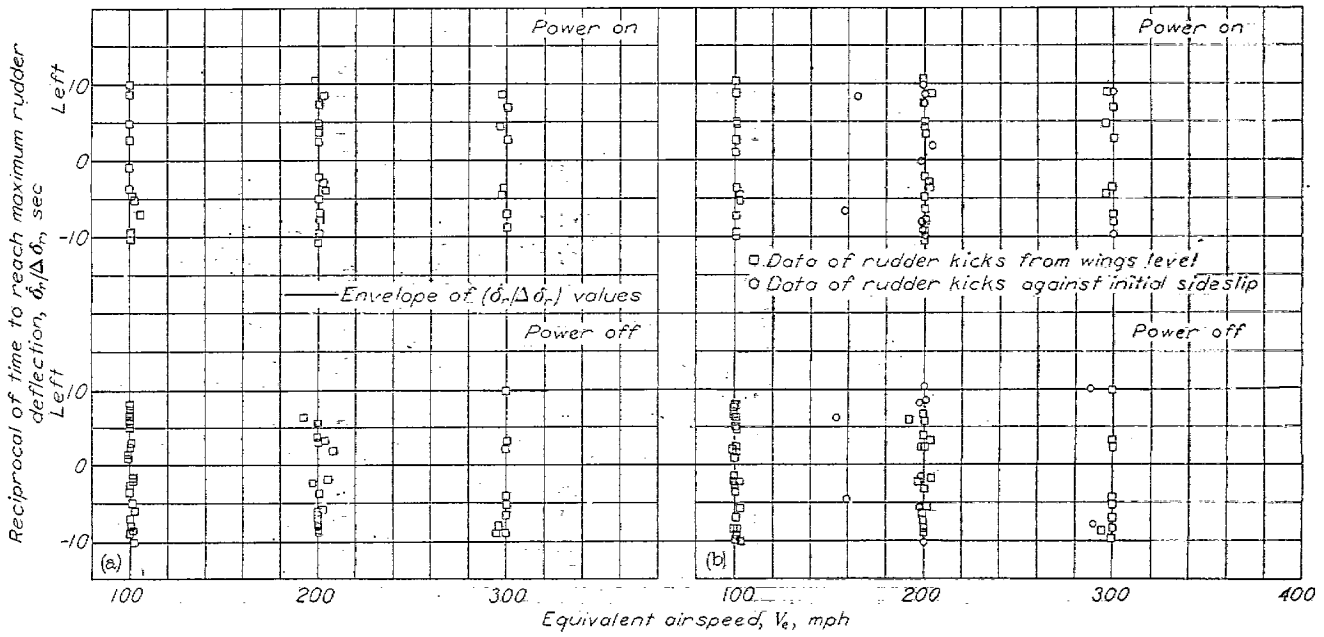

(a) Rudder kicks from wings level. (b) Rudder kicks against initial sideslip

FIGURE 24.—Reciprocal of time to reach maximum rudder deflection against equivalent airspeed with power on and power off.

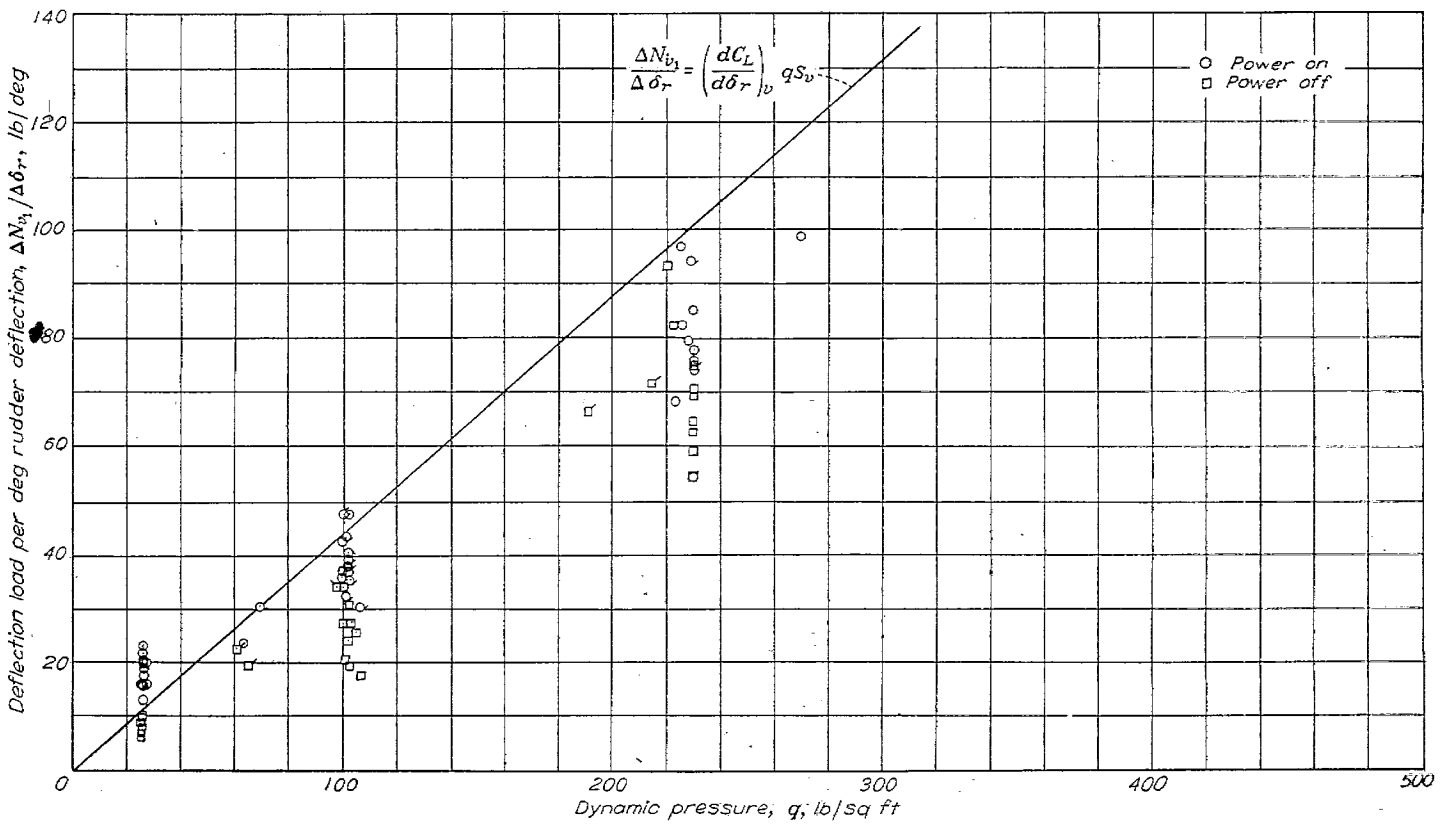

FIGURE 25.—Deflection load per degree rudder deflection plotted against dynamic pressure compared with deflection load for infinite rate of control deflection. Tailed symbols denote rudder kick against initial sideslip.

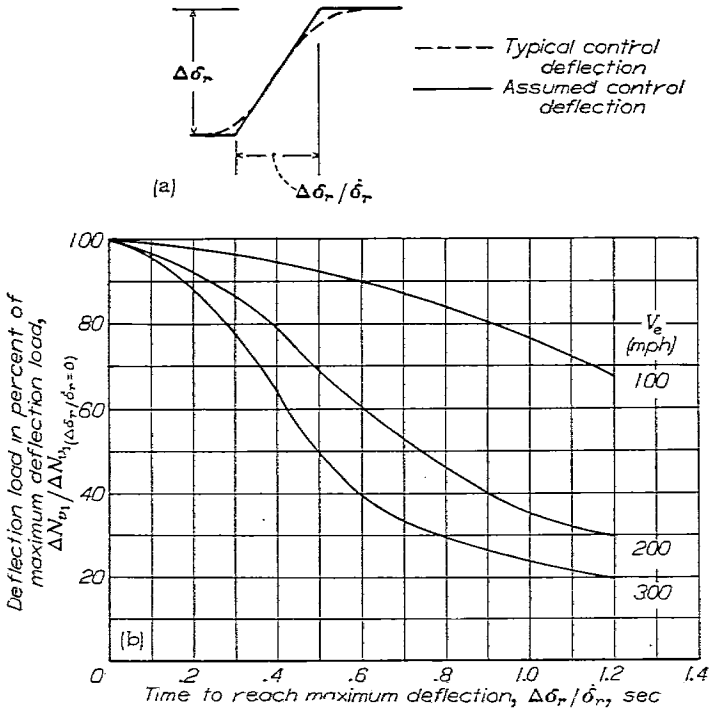

(a) Comparison of control deflection.
(b) Computed deflection load.

FIGURE 26.—Computed deflection load on vertical tail of test airplane in percent of load for infinite rate of deflection against time to reach final control deflection and comparison of typical control deflection with linear type assumed for computations.

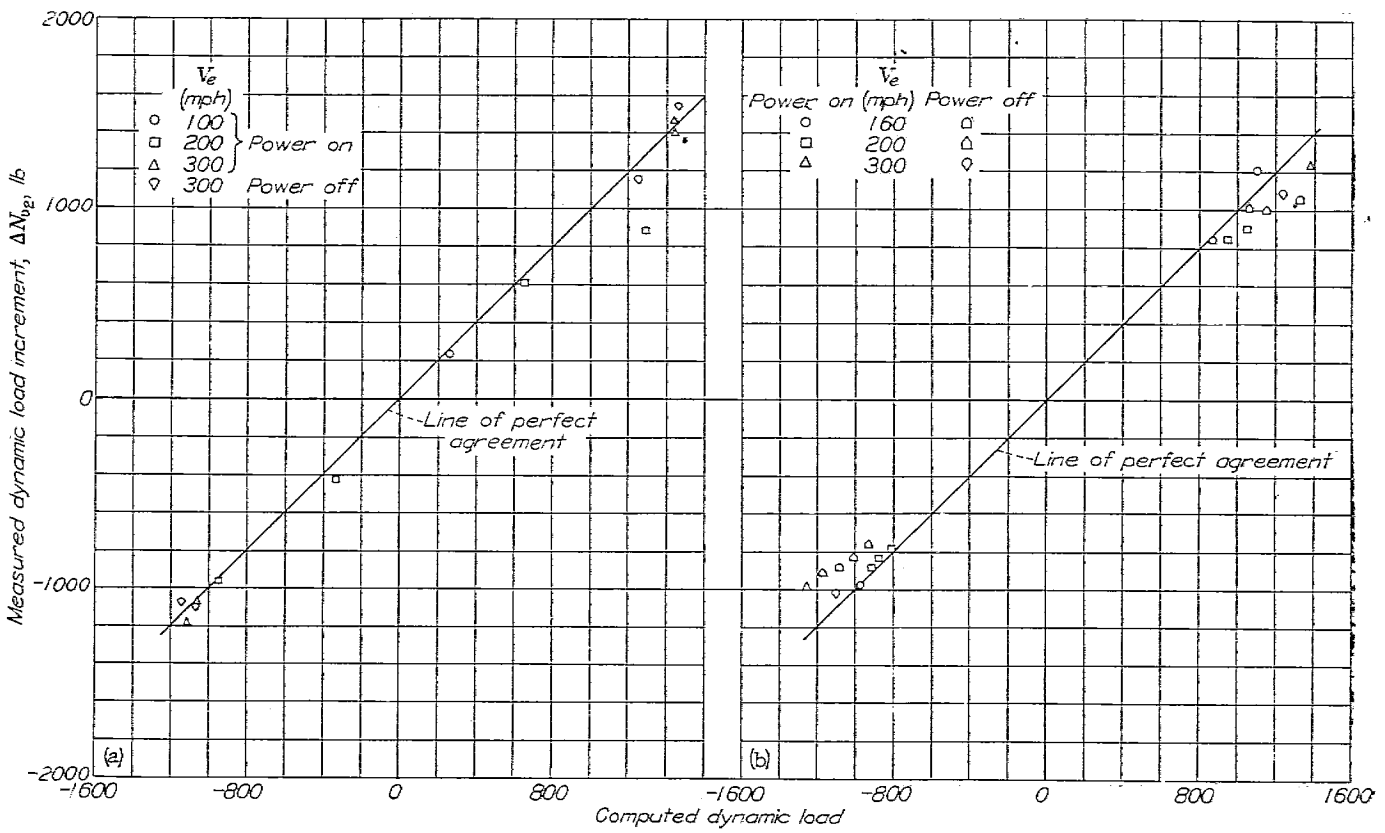

(a) Rudder kicks from wings level.
(b) Rudder kicks against initial sideslip.

FIGURE 27.—Comparison of measured dynamic load with dynamic load computed from the relation $\Delta N_{v_2}=\frac{dC_n}{d\beta}\Delta\beta qS\frac{b}{x_v}-\frac{I_z}{x_v}\ddot{\psi}_2$.

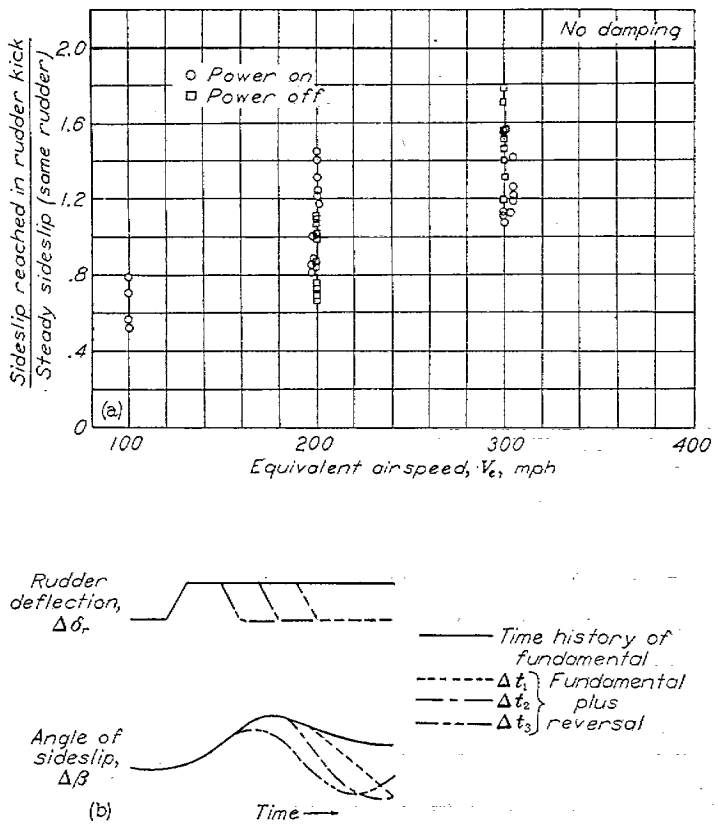

(a) Measured magnification.
(b) Computed effect of initial reversal at several time intervals.

FIGURE 28.—Ratio of angle of sideslip in rudder kicks to value in steady sideslip for corresponding amount of rudder deflection plotted against equivalent airspeed and illustration of computed effect of the time of control reversal on sideslip angle reached.

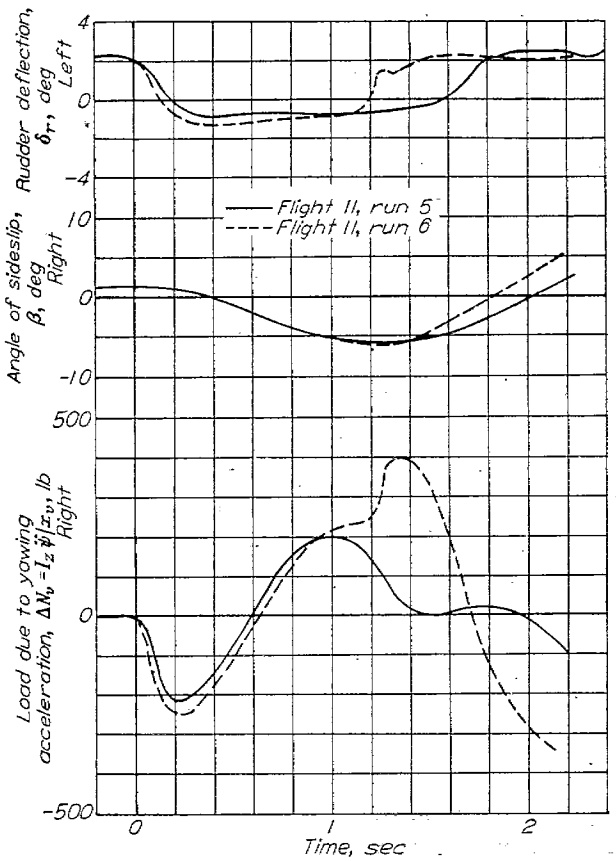

FIGURE 29.—Comparison of load due to angular acceleration in yaw for two types of rudder manipulation in otherwise similar runs.

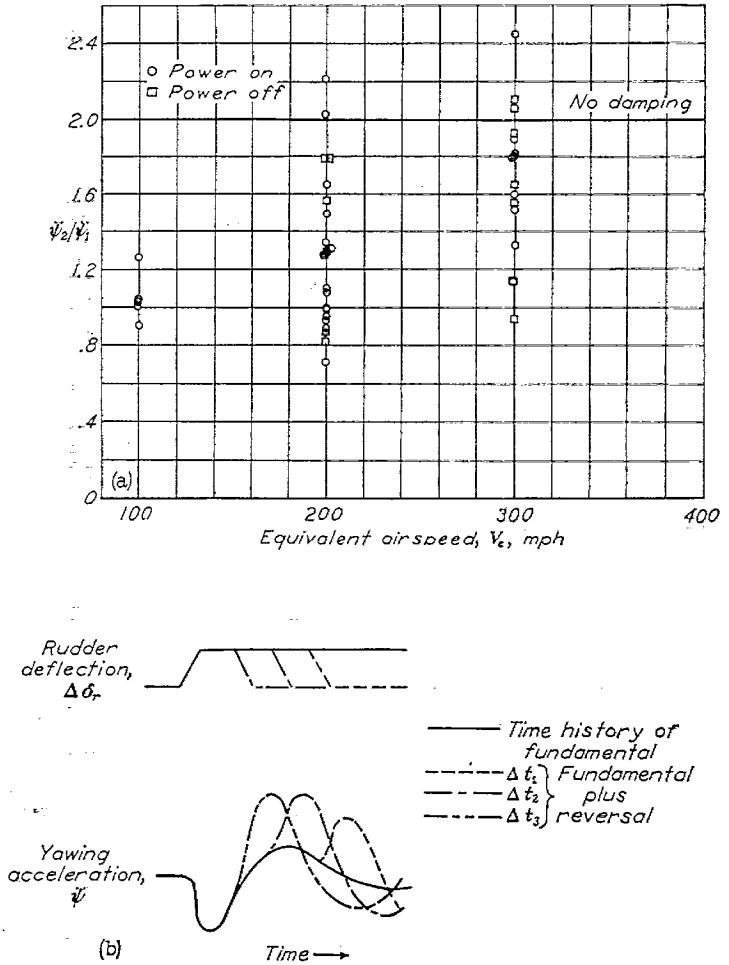

(a) Measured magnification.
(b) Computed effect of control reversal at several time intervals.

FIGURE 30.—Ratio of second and first maximum angular accelerations plotted against equivalent airspeed and illustration of computed effect of time of control reversal on angular acceleration in yaw.

The angle of sideslip attained in a rudder kick may be written as

$$\beta = k\left(\frac{d\beta}{d\delta_r}\right)\Delta\delta_r$$

where $d\beta/d\delta_r$ is the measured slope as obtained from steady sideslips and k is a magnification factor which, as noted previously, would range from a value of 1 for a critically damped airplane to a value of 2 for zero damping. Thus,

$$\Delta N_{v_2} = -k\frac{d\beta}{d\delta_r}\left(\frac{dC_L}{d\alpha}\right)_v \Delta\delta_r q S_v + \left(\frac{dC_L}{d\delta_r}\right)_v \Delta\delta_r q S_v$$

For the critical case of a rudder reversal at the time of maximum dynamic load the term $-\left(\frac{dC_L}{d\delta_r}\right)_v \Delta\delta_r q S_v$ is added to the expression. If the reversal is assumed to be made at an infinite rate and to be equal to the initial deflection, the load becomes

$$\Delta N_{v_2} = -k\frac{d\beta}{d\delta_r}\left(\frac{dC_L}{d\alpha}\right)_v \Delta\delta_r q S_v$$

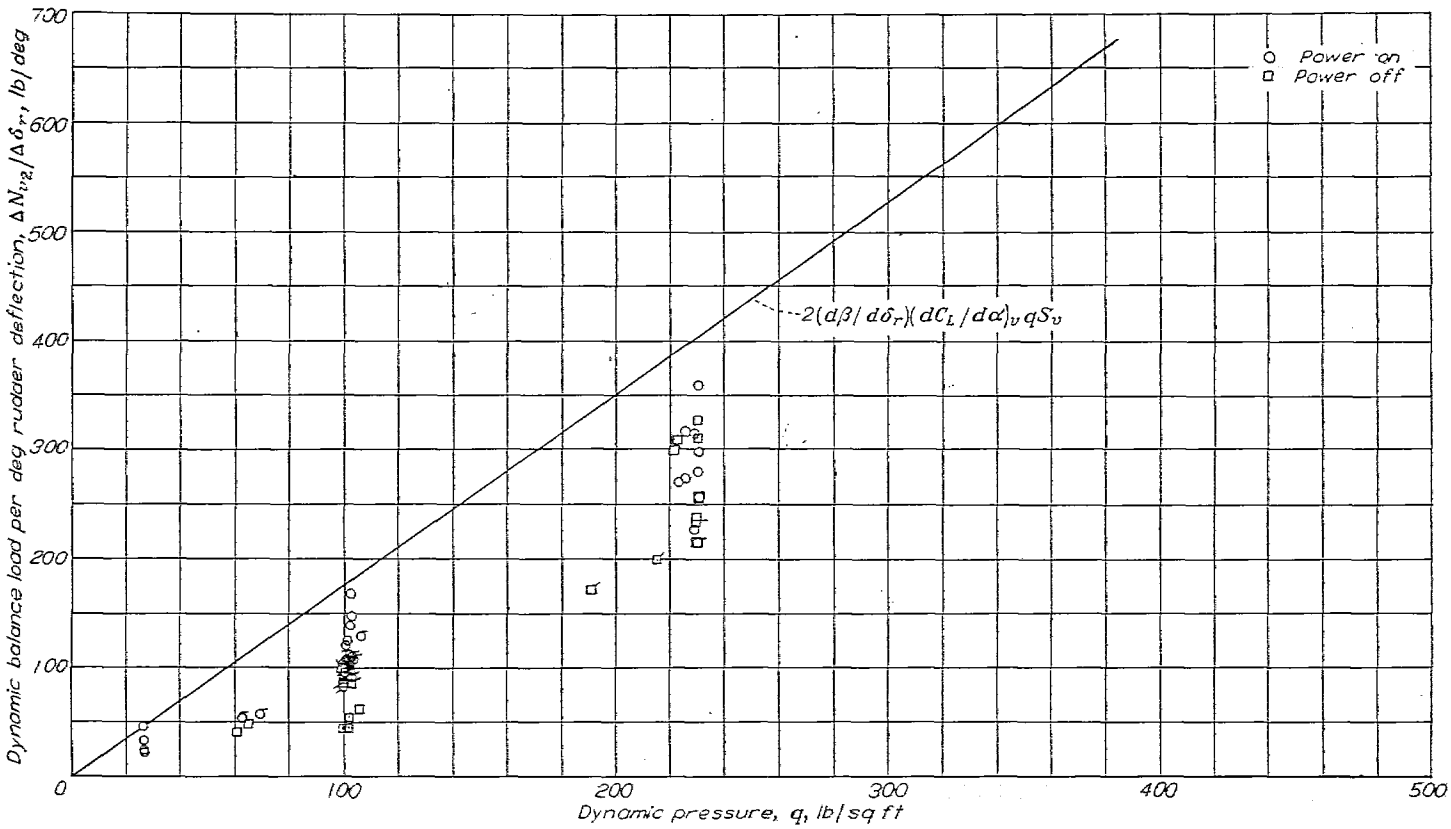

FIGURE 31.—Dynamic balance load per degree rudder deflection plotted against dynamic pressure. Tailed symbols denote rudder kick against initial sideslip.

For the test airplane $d\beta/d\delta_r$ is approximately equal to 1.5 (fig. 8) and as an upper-limit value, $k=2.0$. The comparison of the measured load with the load computed from the approximate formula is shown by the line in figure 31.

LOAD DISTRIBUTION

In order to furnish a general picture of the distribution of load during a rudder kick, isometric views of the pressure distribution over the vertical tail during right and left rudder kicks are shown in figure 32. The figure shows the distributions on the vertical tail for steady flight, the time of maximum deflection load, an intermediate point in the maneuver, and the time of maximum dynamic load. It can be seen from this figure and the time histories (figs. 14, 16, and 18) that the rudder carries most of the deflection load and that the fin carries most of the dynamic load. As regards the chordwise distribution of load, all types of distributions appear to occur during the rudder kick. The deflection load represents the zero-yaw full-rudder load; the intermediate point during the maneuver is the balance-type load; and the maximum dynamic load is a high angle-of-attack type of load with high leading-edge pressures.

Distribution of load between rudder and fin.—Further information on the distribution of the load between the rudder and fin is given in figures 33 and 34. A comparison of the magnitude of the deflection load on the rudder with that on the total vertical tail is shown in figure 33 (a) for rudder kicks from the wings-level condition and in figure 33 (b) for rudder kicks against initial sideslip. As shown by the time histories of figures 14 and 16 the maximum deflection load on the rudder occurs after the maximum on the total vertical tail so that the load values plotted in figure 33 do not necessarily occur at the same time. From figure 33, the load on the rudder is found to be approximately equal to the total deflection load. For the high loads which were attained at 300 miles per hour the rudder deflection load is actually greater than that on the total vertical tail. This condition results from a combination of the lower rate of control deflection with the more rapid airplane response, with the consequence that the airplane starts to yaw before the rudder has completed its travel. The yawing velocity imposes a load on the fin that is opposite to the rudder load and results in a lower net load on the tail. This effect is illustrated in figure 32 by the higher pressures on the rudder at an intermediate point during the maneuver rather than at the time of maximum vertical-tail deflection load.

A comparison of the dynamic load carried by the fin with that carried by the total vertical tail is shown in figure 34 (a) for rudder kicks from the wings-level condition and in figure 34 (b) for rudder kicks against steady sideslip. The fin is shown to carry approximately 90 percent of the dynamic load in rudder kicks from the wings-level condition and about 100 percent of the dyanmic load in kicks against sideslip. When the fin carries a load greater than 100 percent, the total load includes a rudder load in a direction opposite to that on the fin.

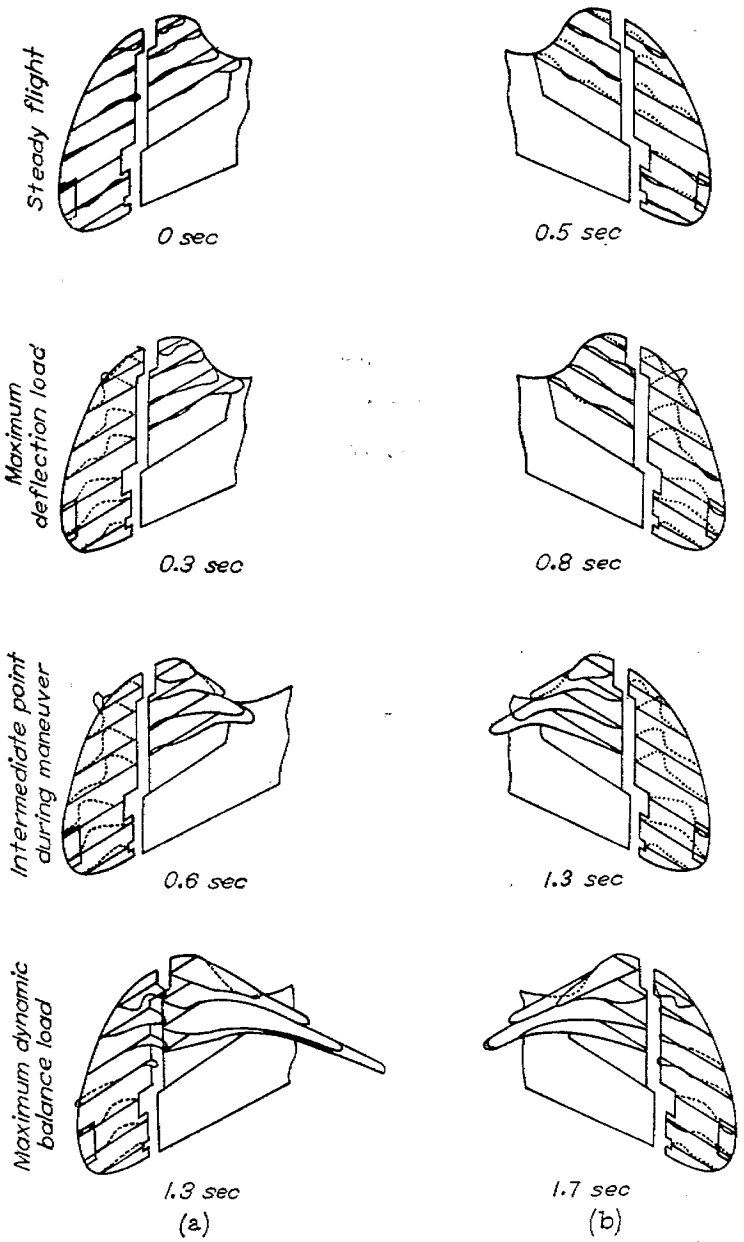

(a) Flight 11a, run 1; right rudder kick. (b) Flight 11a, run 3; left rudder kick.

FIGURE 32.—Isometric diagrams of pressure distributions over vertical tail during right and left rudder kicks.

Spanwise and chordwise load distribution.—The spanwise load distributions on the fin at the time of maximum fin load and on the rudder at the time of maximum rudder load are presented in figure 35 for power on and figure 37 for power off for the most severe rudder kicks made in each direction and at each test speed. The symbols in these figures are used to distinguish chordwise-load points of two runs having approximately the same value of load. The chordwise pressure distributions over rib V (fig. 5) obtained at times corresponding to the times for which the spanwise load distributions are shown are presented in figures 36 and 38.

Figure 39 shows that the spanwise center of load on the fin varies slightly depending upon the direction of kick as well as upon the airspeed. On an average, the spanwise center of load is 10 percent farther outboard than the airload distribution for which the surfaces were designed.

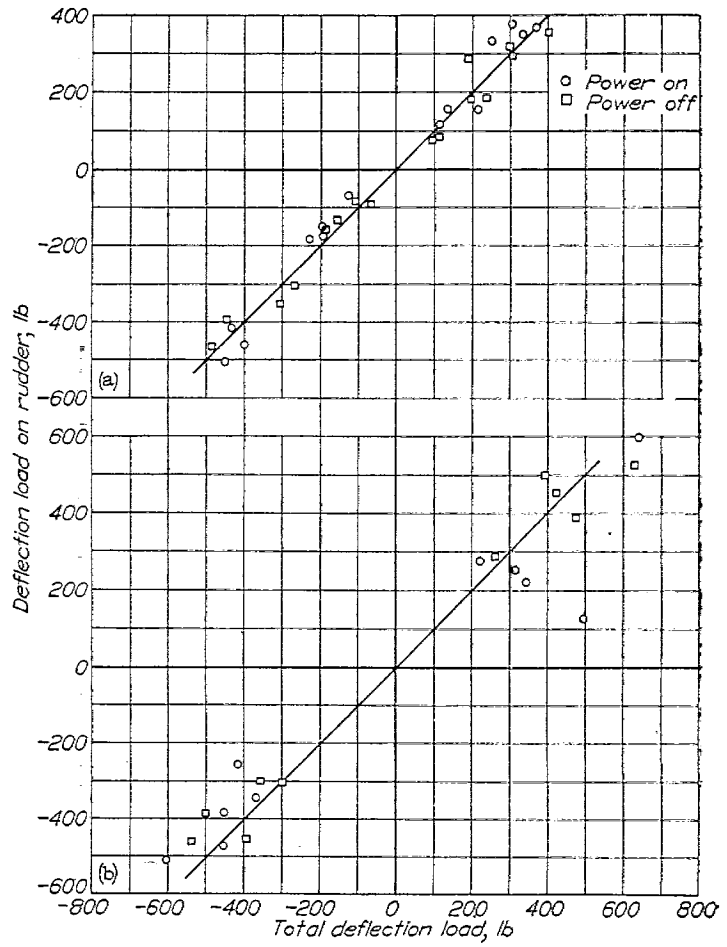

(a) Rudder kicks from wings level.

(b) Rudder kicks against initial sideslip.

FIGURE 33.—Comparison of magnitude of deflection load on rudder with total deflection load on vertical tail in rudder kicks.

The chordwise load distributions in figures 36 and 38 show that (except at an airspeed of 100 mph) the maximum fin load is, in general, associated with a small value of load on the rudder, whereas the maximum rudder load occurs during an intermediate point in the maneuver when the fin has some load due to yawing.

LOAD DIAGRAMS

The construction of load diagrams for the vertical tail surfaces may be made by the use of the foregoing results. For instance, the deflection load was shown to be critical for the rudder. At high speeds the total deflection load was less than the load for an infinite rate of control deflection (see fig. 25) but the load on the rudder was greater than 100 percent of the deflection load, and it is therefore reasonable to assume that the critical rudder load may be equal to the total deflection load at an infinite rate of control deflection. Thus,

$$\Delta N_r = \Delta\delta_r \left(\frac{dC_L}{d\delta_r}\right)_v qS_v$$

In figure 40 (a) the load computed by this equation is shown to compare well with the maximum values of measured rudder loads.

The dynamic load was found to be critical for the fin. The load on the fin may be expressed as some fraction K of

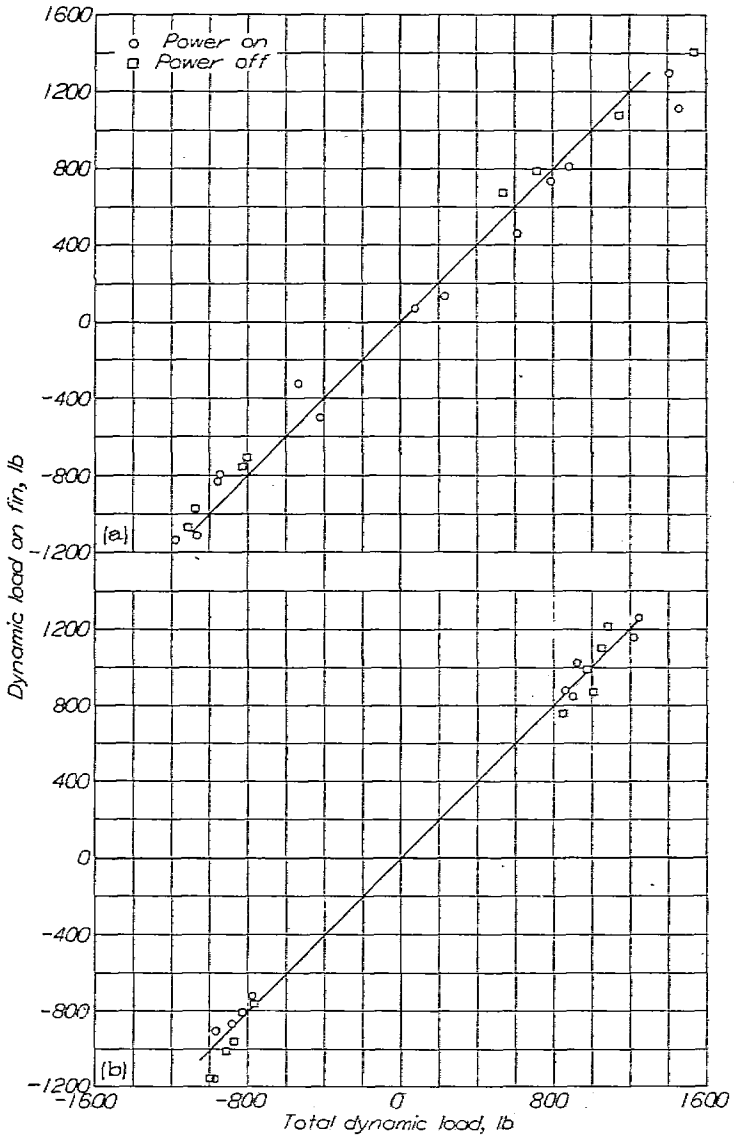

(a) Rudder kicks from wings level.
(b) Rudder kicks against initial sideslip.

FIGURE 34.—Comparison of magnitude of maximum dynamic load on fin with total dynamic load on vertical tail in rudder kicks.

the dynamic load. The factor K may be determined from the geometric characteristics of the tail for the assumption of a hypothetical control motion in which the rudder is returned to zero at the time of maximum sideslip; that is,

$$\Delta N_{f_2}=K\,\Delta N_{v_2}$$
$$=K\left[-k\,\frac{d\beta}{d\delta_r}\left(\frac{dC_L}{d\alpha}\right)_v\Delta\delta_r qS_v\right]$$

For the test airplane the factor K for this condition was shown to be 90 percent in rudder kicks from the wings-level condition (fig. 34 (a)).

In figure 40 this relation is shown on the basis of the load per degree rudder deflection against dynamic pressure along with experimental values. In the calculations the magnification factor k was assumed to be 2.0 and $\frac{d\beta}{d\delta_r}=1.5$.

The load diagram in figure 41 was constructed from the preceding formulas. The dashed lines show computed loads

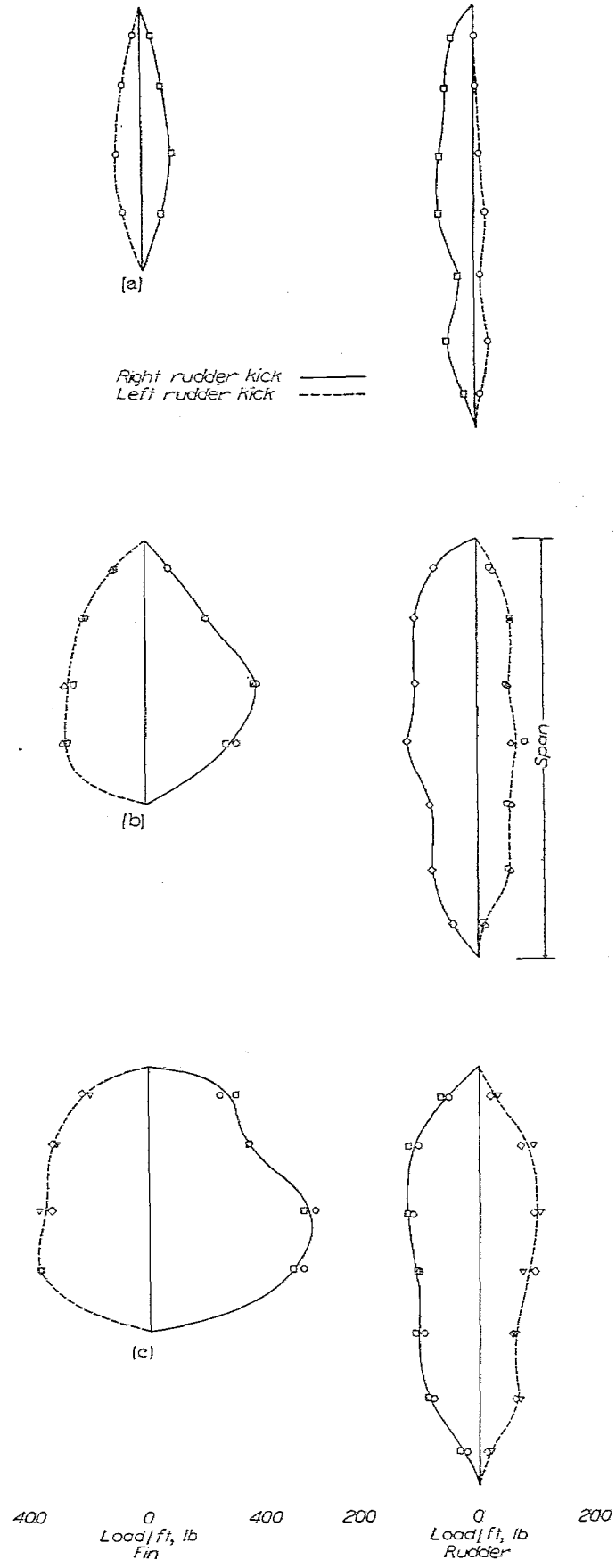

(a) V_e=100 miles per hour.
(b) V_e=200 miles per hour.
(c) V_e=300 miles per hour.

FIGURE 35.—Spanwise load distributions on the fin and rudder for the time of maximum load on each surface during rudder kicks at V_e=100, 200, and 300 miles per hour with power on. Symbols show chordwise loads.

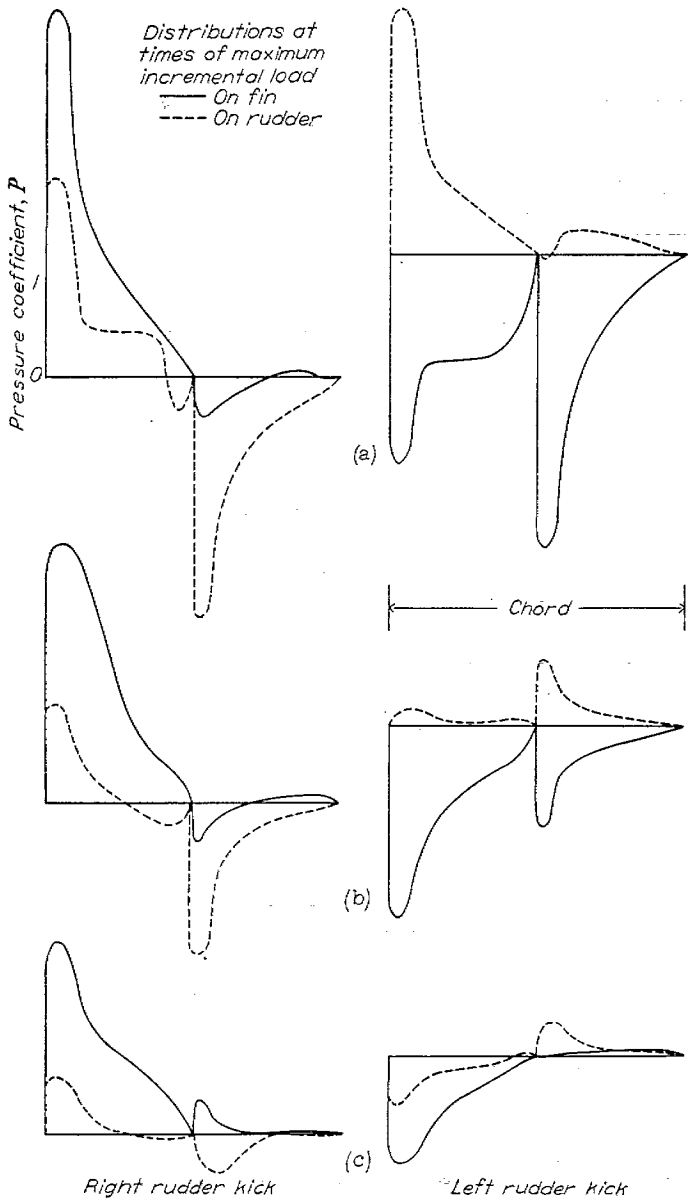

(a) V_e=100 miles per hour.
(b) V_e=200 miles per hour.
(c) V_e=300 miles per hour.

FIGURE 36.—Chordwise pressure distributions over rib V (see fig. 5) for spanwise load distributions of figure 35.

for two pedal forces and the points represent the largest experimental values obtained at equivalent airspeeds of 200 and 300 miles per hour.

RESULTS AND DISCUSSION—FISHTAIL MANEUVERS

Vertical-tail failures have occurred on military airplanes during evasive action or fishtail maneuvers. Some concern has therefore been expressed about including the fishtail maneuver as a critical design condition because the weight penalty for adequate strength was considered prohibitive. In addition, there was for a time an impression among some designers that the vertical tail could fail on any airplane if the rudder were deflected in a sinusoidal manner at the natural frequency of the airplane. Consequently, it seemed to be in order that a specification be made as to how far the maneuver was to be continued. For this purpose, an analogous system which is familiar in simple dynamics may be used to furnish useful information concerning the fishtail maneuvers.

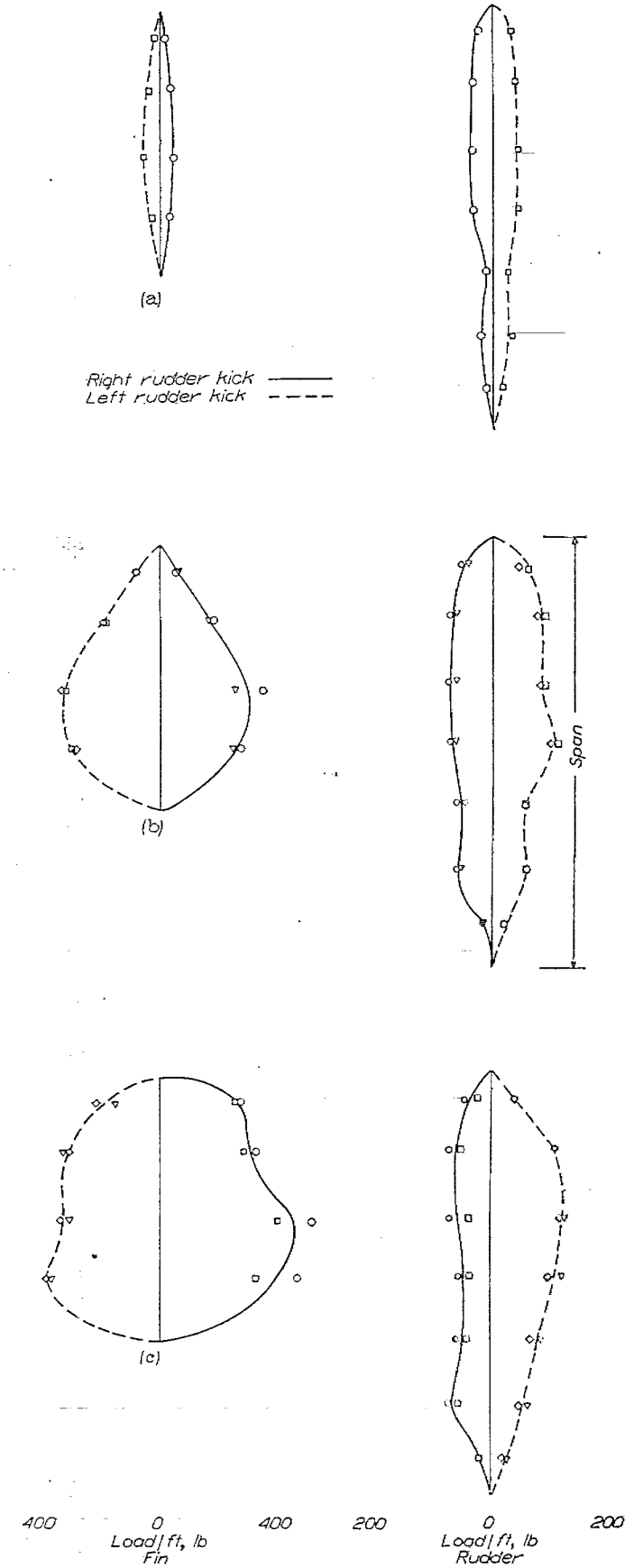

(a) V_e=100 miles per hour.
(b) V_e=200 miles per hour.
(c) V_e=300 miles per hour.

FIGURE 37.—Spanwise load distributions on the fin and rudder for the time of maximum load on each surface during rudder kicks at V_e=100, 200, and 300 miles per hour with power off. Symbols show chordwise loads.

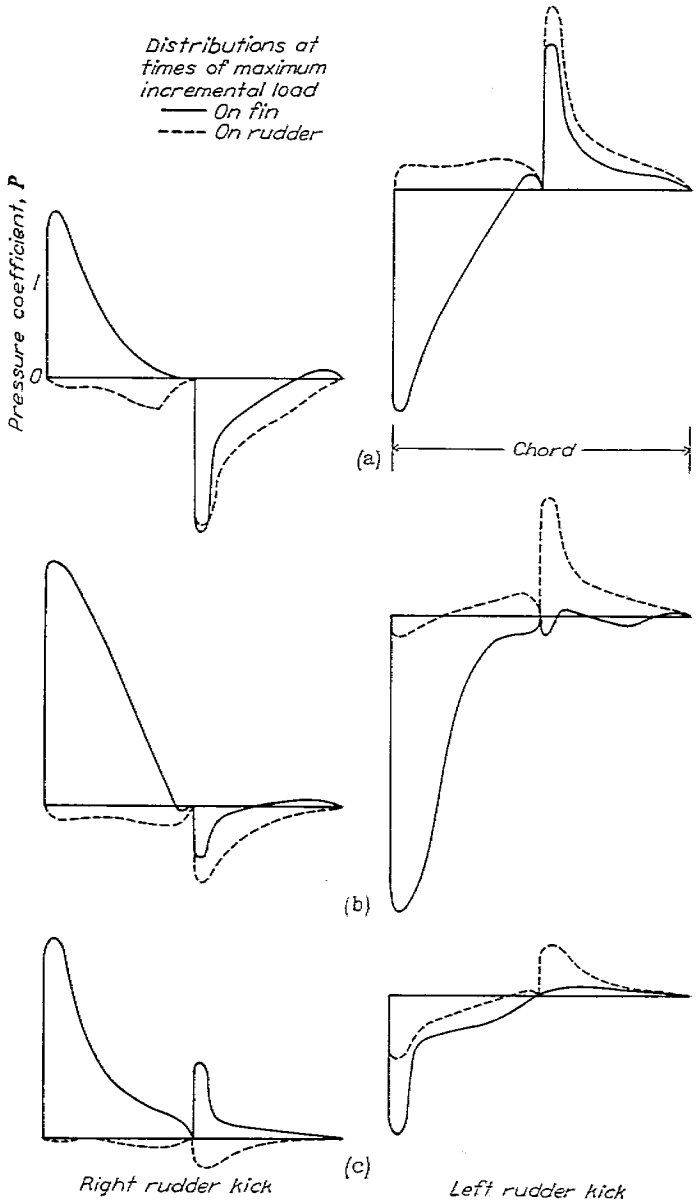

(a) V_e=100 miles per hour.
(b) V_e=200 miles per hour.
(c) V_e=300 miles per hour.

FIGURE 38.—Chordwise pressure distributions over rib V (see fig. 5) for spanwise load distributions of figure 37.

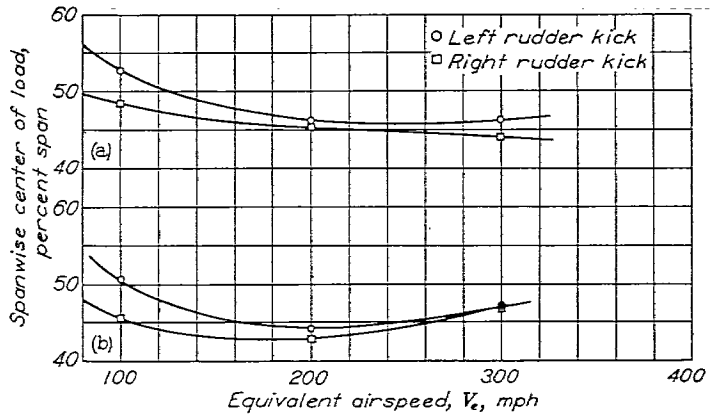

(a) Power on.
(b) Power off.

FIGURE 39.—Variation with equivalent airspeed of the spanwise center of load on the fin at the time of maximum fin load for most severe rudder kicks with power on and power off.

CONSIDERATIONS FROM SIMPLE DYNAMICS

As was pointed out in reference 5, the fishtail maneuver can be assumed to be a flat yawing maneuver so that the solution to this problem might be equivalent to that for a linear single-spring system. A brief review of well-known results of the spring system from simple dynamics will therefore furnish a useful background. The curves shown in figure 42 (taken from reference 8) apply to the case of an external sinusoidal force acting upon the spring system.

Figure 42 (a) shows the amplitude magnification factor plotted against the ratio of the frequency of the impressed force to the natural frequency of the system for systems having different ratios of damping to critical damping. In figure 42 (b) the phase relation between the impressed force and the amplitude is presented for the same conditions. In terms of what happens in the fishtail maneuvers the following observations may be made from this figure.

(1) For an airplane with some damping the sideslip (or amplitude) magnification will reach a finite equilibrim value even for the case of a rudder oscillation having the same frequency as the airplane. The amount of magnification is dependent upon the ratio of the damping to the critical damping and, of course, upon the frequency at which the rudder is deflected relative to the natural frequency of the airplane.

(2) The rudder angle (or forcing function) is out of phase with the angle of sideslip (or amplitude) by an amount depending upon the amount of relative damping. At resonance, however, the phase relation is always 90°. For resonance, therefore, for a perfect fishtail, the rudder angle will be zero at the time of maximum sideslip and maximum at the point of zero sideslip.

It should be noted at this point that these curves could have been derived in terms of loads in which case the magnifications of figure 42 (a) would then be expressed in terms of load magnification. For the case where the impressed frequency is the same as the airplane frequency, in which case the rudder deflection would be zero at the time of maximum sideslip (fig. 42 (b)), the expression for the load in a fishtail maneuver would become

$$\Delta N_{v_2} = -\beta \left(\frac{dC_L}{d\alpha}\right)_v q S_v$$

ANALYSIS OF TESTS

The results obtained during the fishtail investigation are given in table V. The first eight of these fishtails were slightly artificial since the pilot deliberately tried to obtain high tail loads, whereas the last four were made in as natural and comfortable a manner as possible.

The first set of maneuvers was intended to show how critical the maneuver could be if the pilot deliberately tried to work the rudder control at the same frequency as the airplane frequency in order to reach high angles of yaw. The time histories of these maneuvers are presented in figures 43 and 44 for the power-on and power-off maneuvers made at 150 and 200 miles per hour, respectively. In figure 45 are presented power-on and power-off fishtail maneuvers in which the pilot kicked the rudder against the swing at the point of maximum yawing velocity. All of these maneuvers (figs. 43 to 45) were very uncomfortable to the pilot because of the severe pitching which resulted.

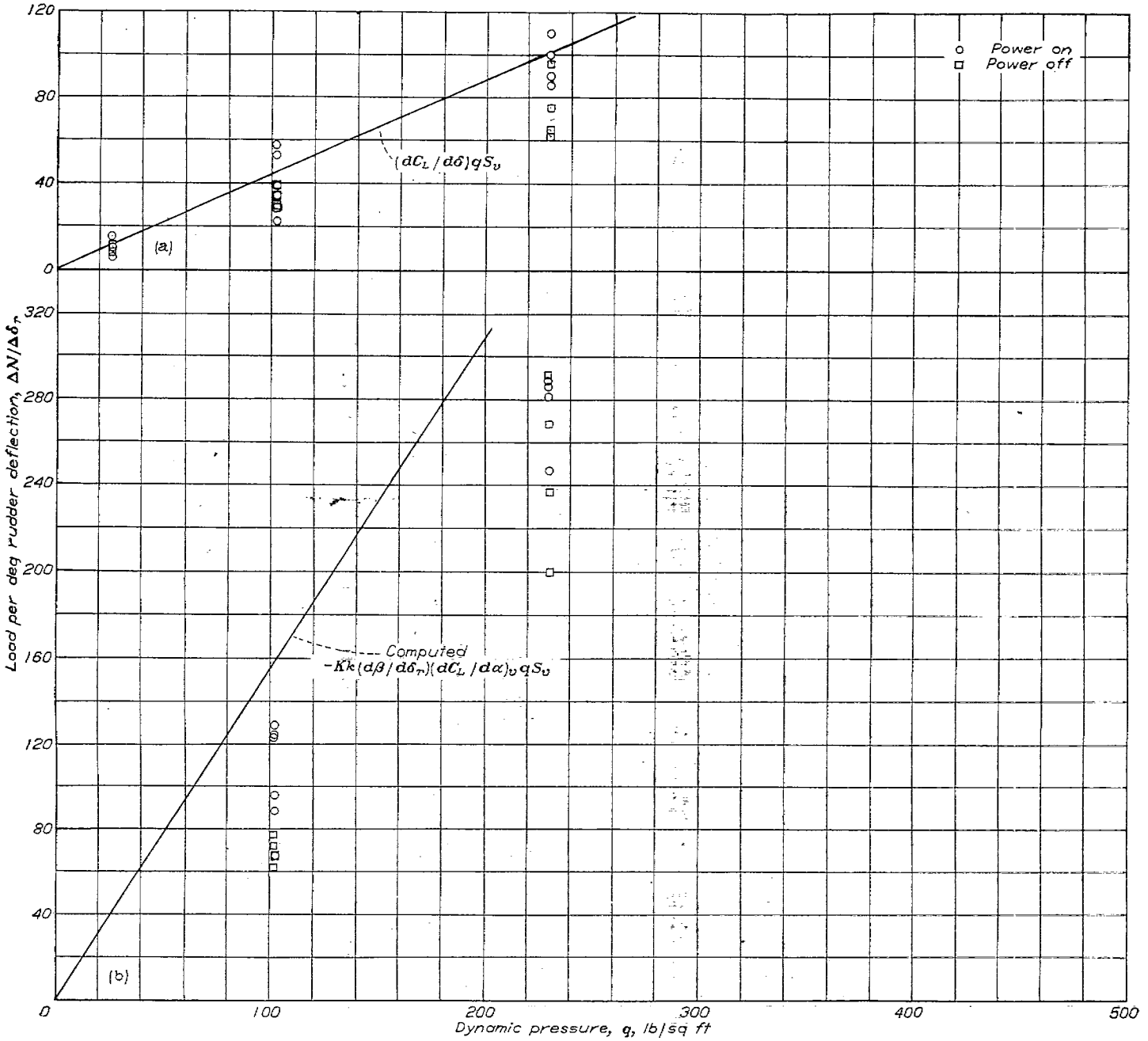

(a) Rudder.

(b) Fin.

FIGURE 40.—Variation of load per degree rudder deflection with dynamic pressure, including estimated maximum loads for load on rudder and for load on fin.

The second set of tests consisted of the fishtail maneuvers in which a different pilot performed a mild fishtail maneuver in as comfortable a manner as possible. These maneuvers are presented in figures 46 and 47 at speeds of 200 and 250 miles per hour and 300 and 350 miles per hour, respectively.

A study of the time histories of the fishtail maneuvers yields the following deductions:

(1) The maneuvers in which the pilot was free to coordinate the controls show that the pitching was very much less, with the result that the maneuver was not particularly uncomfortable.

(2) Within only one cycle of rudder motion the loads attain values close to the maximum measured during the whole maneuver.

(3) As the maneuver continues, the load on the rudder tends to bear the 90° phase relation with the load on the fin. This result is indicated in figure 42 (b) for the condition of resonance.

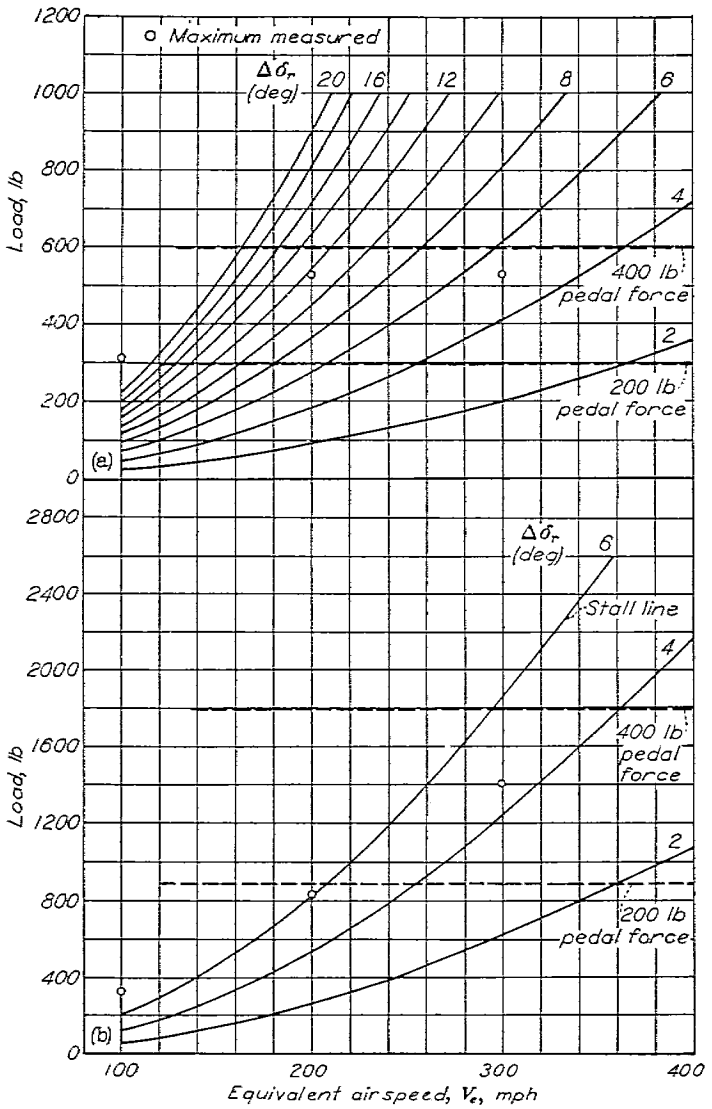

(a) Rudder.
(b) Fin.

FIGURE 41.—Diagram showing loads on rudder and fin plotted against equivalent airspeed

(4) The abrupt rudder deflection applied against the maximum velocity of swing results in high rudder loads (fig. 45). If the rudder is moved against the airplane swing, the phase relation of the rudder and fin loads is disturbed so that the loads become additive.

Frequency of rudder operation with relation to frequency of airplane.—One of the points of interest in the fishtail tests was to note whether, as might be expected, the pilot tends to move the rudder in phase with the airplane frequency. In order to obtain the average rudder frequency for each maneuver, the actual control manipulation was arbitrarily approximated by a sine function. The rudder control deflections for all 12 runs are shown in figure 48 in nondimensional form; the actual control deflection was divided by the amplitude of the sine curve used in the approximation of the

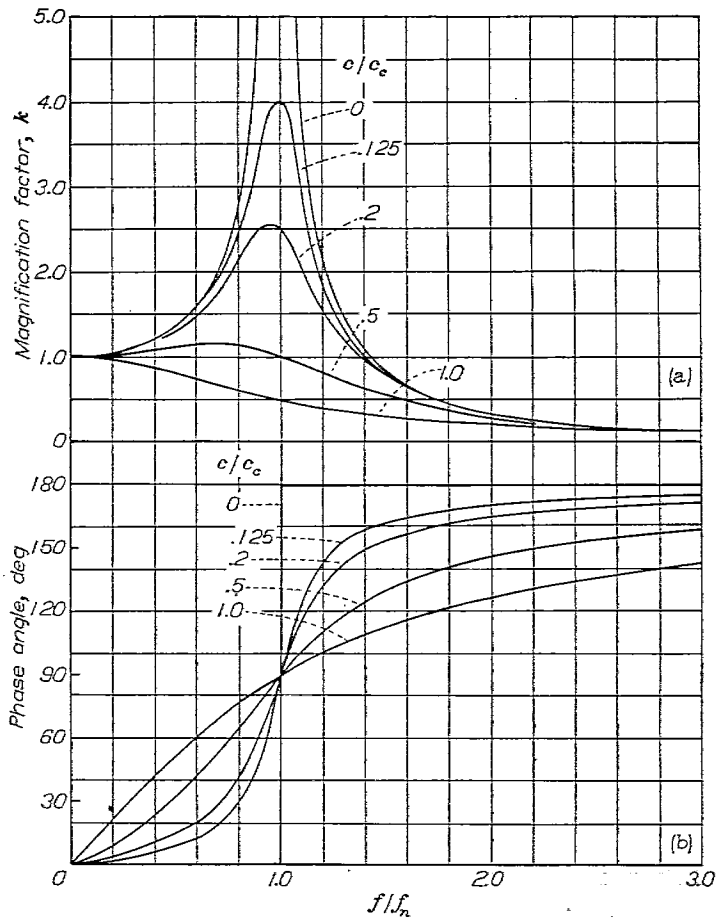

(a) Amplitude magnification.
(b) Phase relation.

FIGURE 42.—Curves from reference 8 showing magnification of amplitude for various ratios of damping to critical damping c/c_c against the ratio of frequency of impressed force to natural frequency of system f/f_n and phase lag between impressed sinusoidal force and amplitude.

motion. The assumed sine curves are also shown. The natural frequency f_n of the airplane was computed from the expression

$$f_n=\frac{1}{2\pi}\sqrt{K_2-\frac{K_1}{4}}$$

where K_1 and K_2 are determined from the aerodynamic characteristics of the airplane and are defined by equation (5) of reference 5.

Inasmuch as the period $1/f_n$ is a more usual way of plotting the airplane response, the data are shown plotted in that manner in figure 49. From this figure it is seen that the fishtail maneuvers made by the pilot when his actions were unrestricted (symbols with tails) were as close to the airplane period as those maneuvers in which he attempted to work the controls at the same period as the airplane. Although the control deflections are irregular, the results indicate that the pilot does tend to work the controls in phase with the airplane frequency in performing a fishtail.

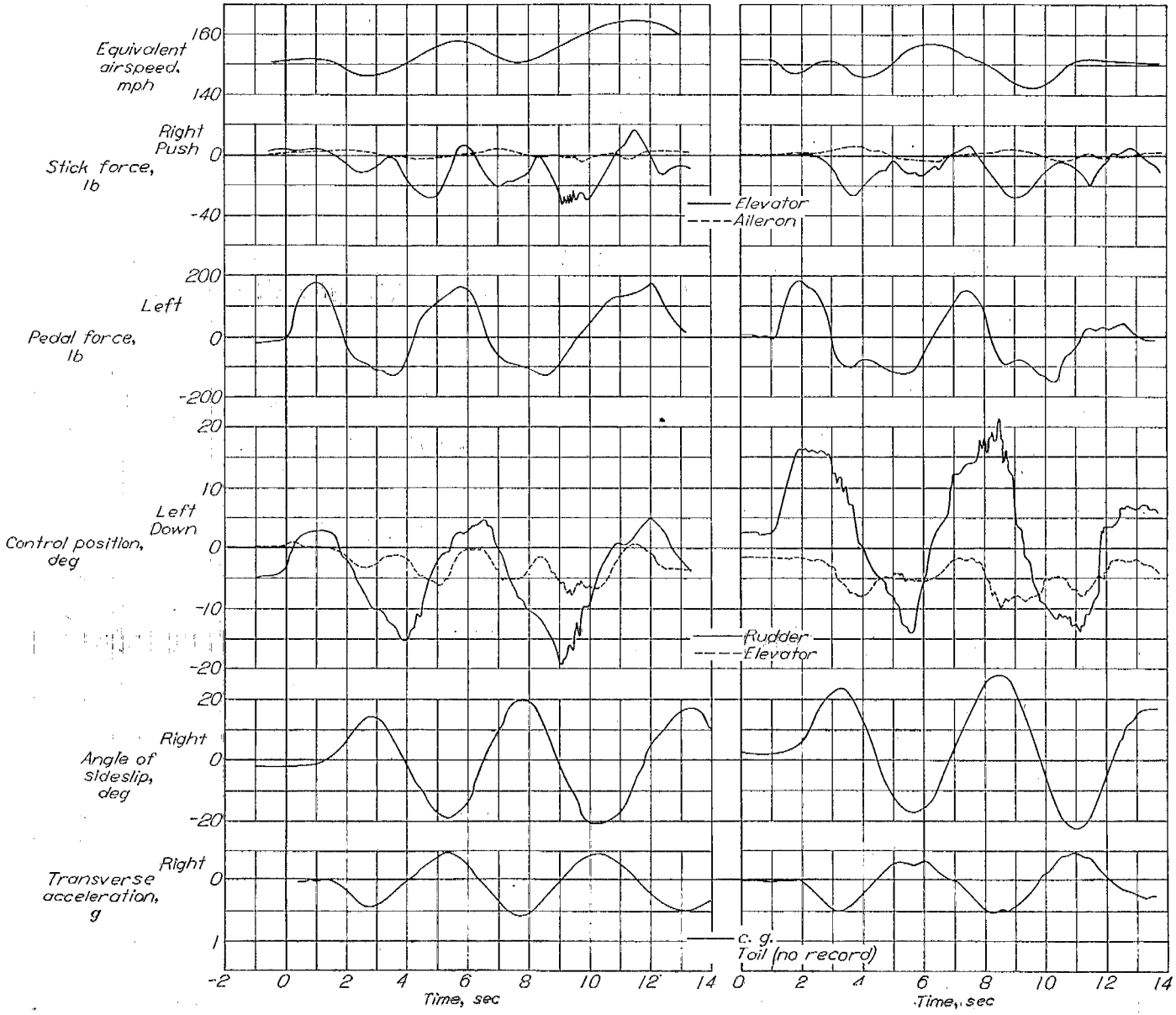
Equivalent airspeed, mph
160
140
Right
Push
Stick force, lb
0
-40
Elevator
Aileron
200
Left
Pedal force, lb
0
-200
20
10
Left
Down
Control position, deg
0
-10
Rudder
Elevator
-20
20
Right
Angle of sideslip, deg
0
-20
Right
Transverse acceleration, g
0
1
c. g.
Tail (no record)
-2
0
2
4
6
8
10
12
14
Time, sec
0
2
4
6
8
10
12
14
Time, sec

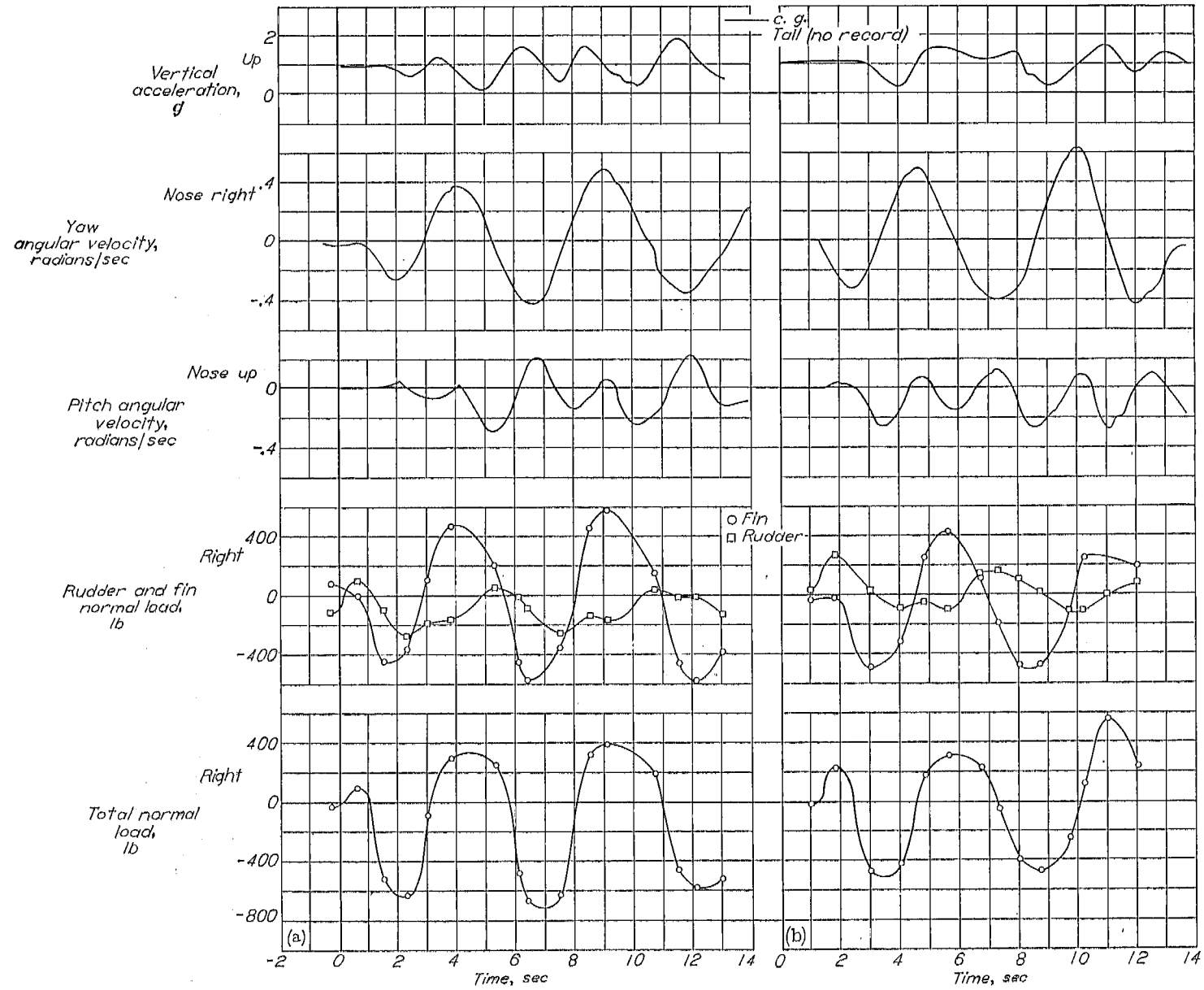

(a) Flight 16, run 1; power on.

(b) Flight 16, run 2; power off.

FIGURE 43.—Time histories of measurements recorded during power-on and power-off fishtails at 150 miles per hour.

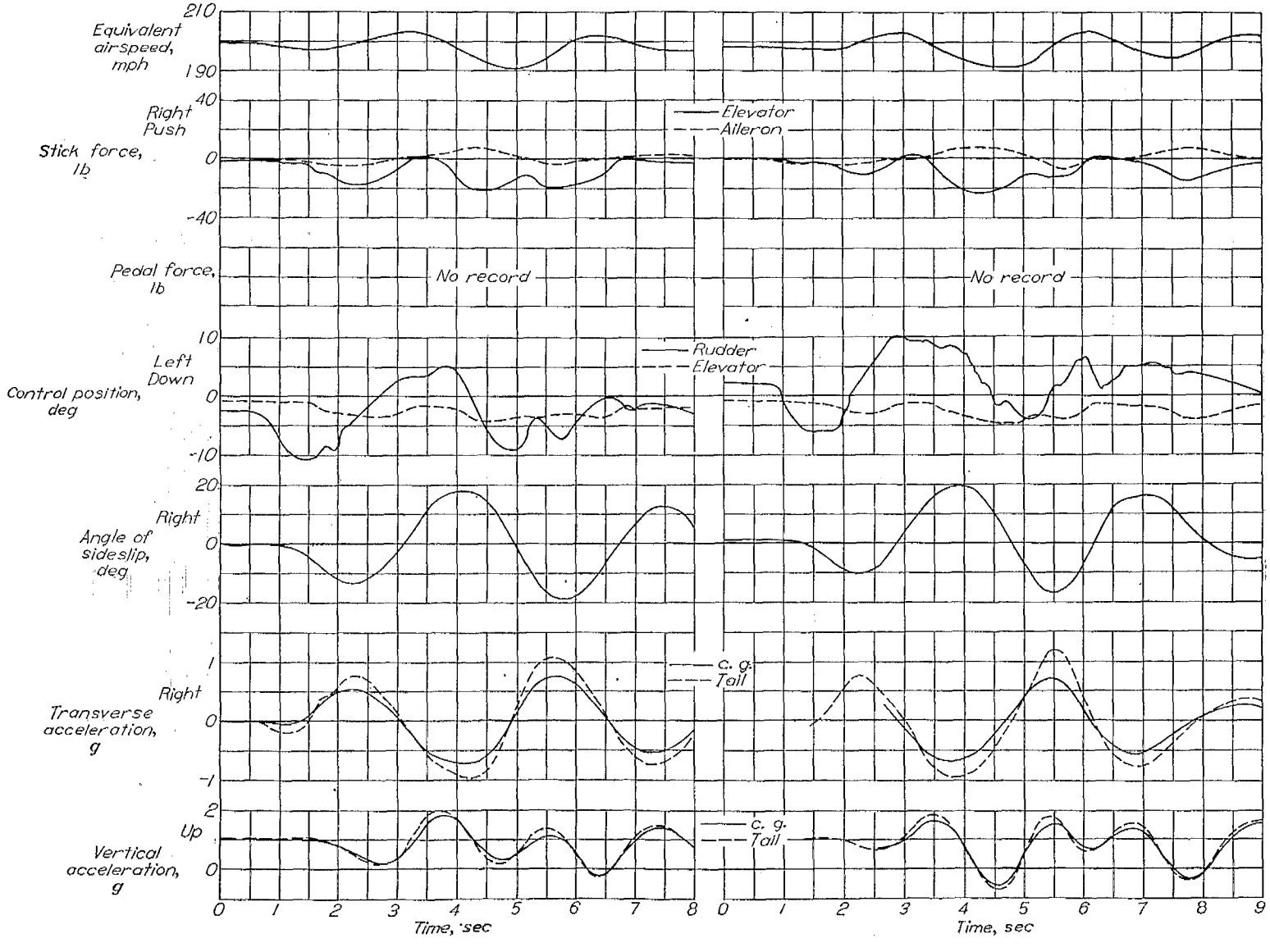
Equivalent airspeed, mph
210
190
Right
Push
Stick force, lb
40
0
-40
Elevator
Aileron
Pedal force, lb
No record
No record
Left
Down
Control position, deg
10
0
-10
Rudder
Elevator
Right
Angle of sideslip, deg
20
0
-20
Right
Transverse acceleration, g
1
0
-1
c. g.
Tail
Up
Vertical acceleration, g
2
0
c. g.
Tail
0 1 2 3 4 5 6 7 8
Time, sec
0 1 2 3 4 5 6 7 8 9
Time, sec

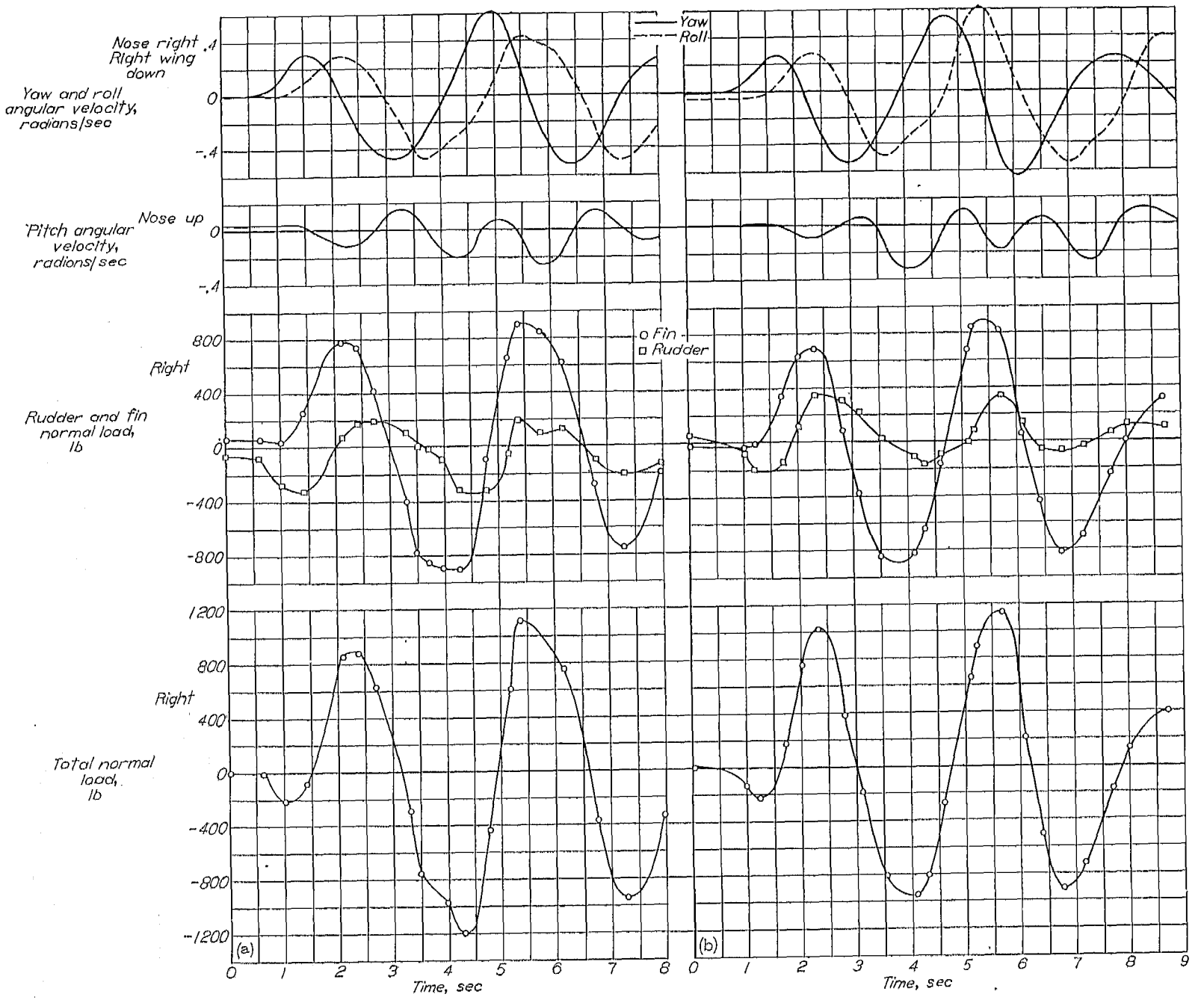

(a) Flight 25a, run 1; power on.

(b) Flight 25a, run 2; power off.

FIGURE 44.—Time histories of measurements recorded during power-on and power-off fishtails at 200 miles per hour.

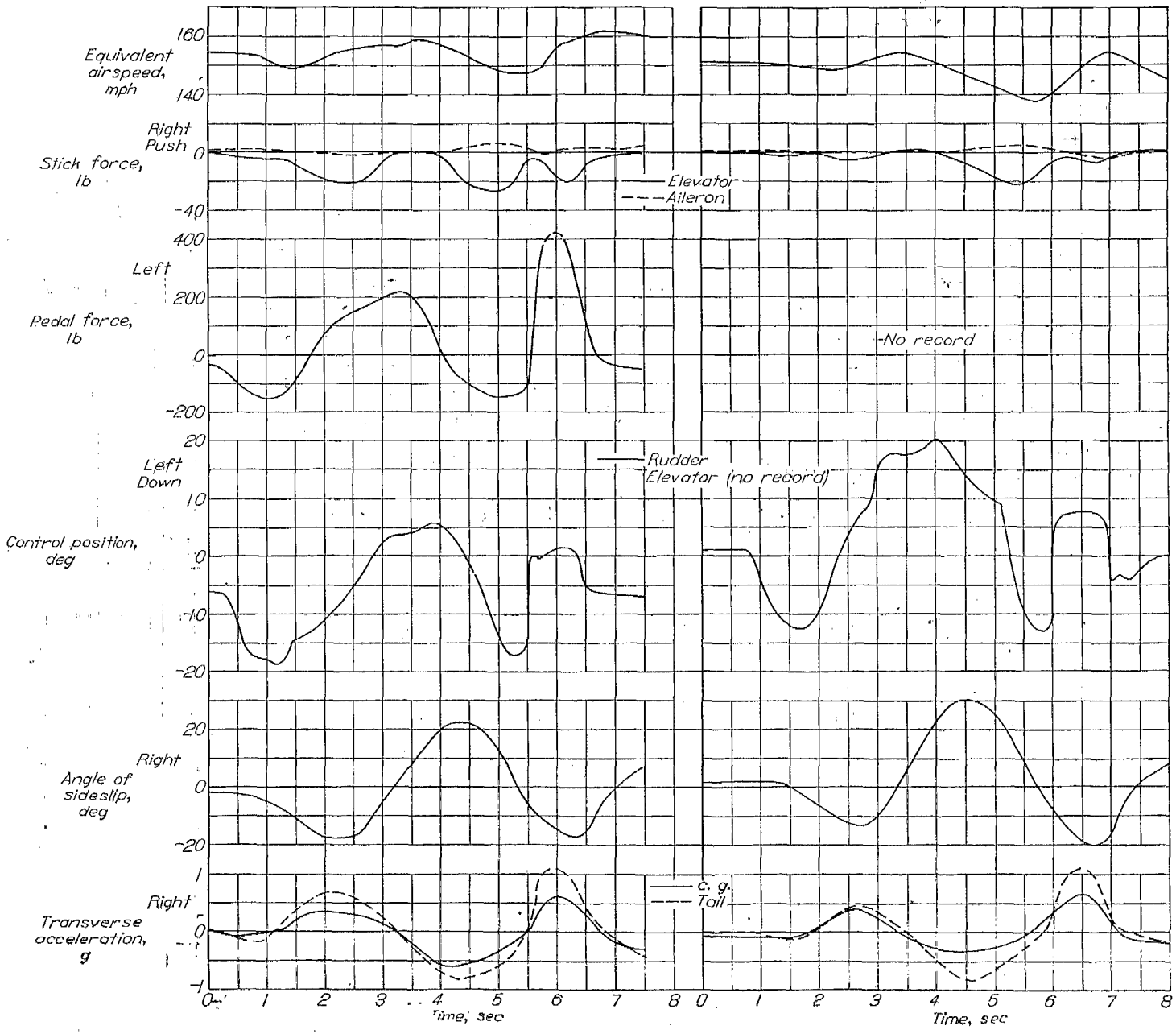
Equivalent airspeed, mph
160
140
Right
Push
Stick force, lb
0
-40
Elevator
Aileron
400
Left
200
Pedal force, lb
0
-200
No record
20
Left
Down
10
Control position, deg
0
-10
-20
Rudder
Elevator (no record)
20
Right
Angle of sideslip, deg
0
-20
1
Right
Transverse acceleration, g
0
-1
c. g.
Tail
0 1 2 3 4 5 6 7 8
Time, sec
0 1 2 3 4 5 6 7 8
Time, sec

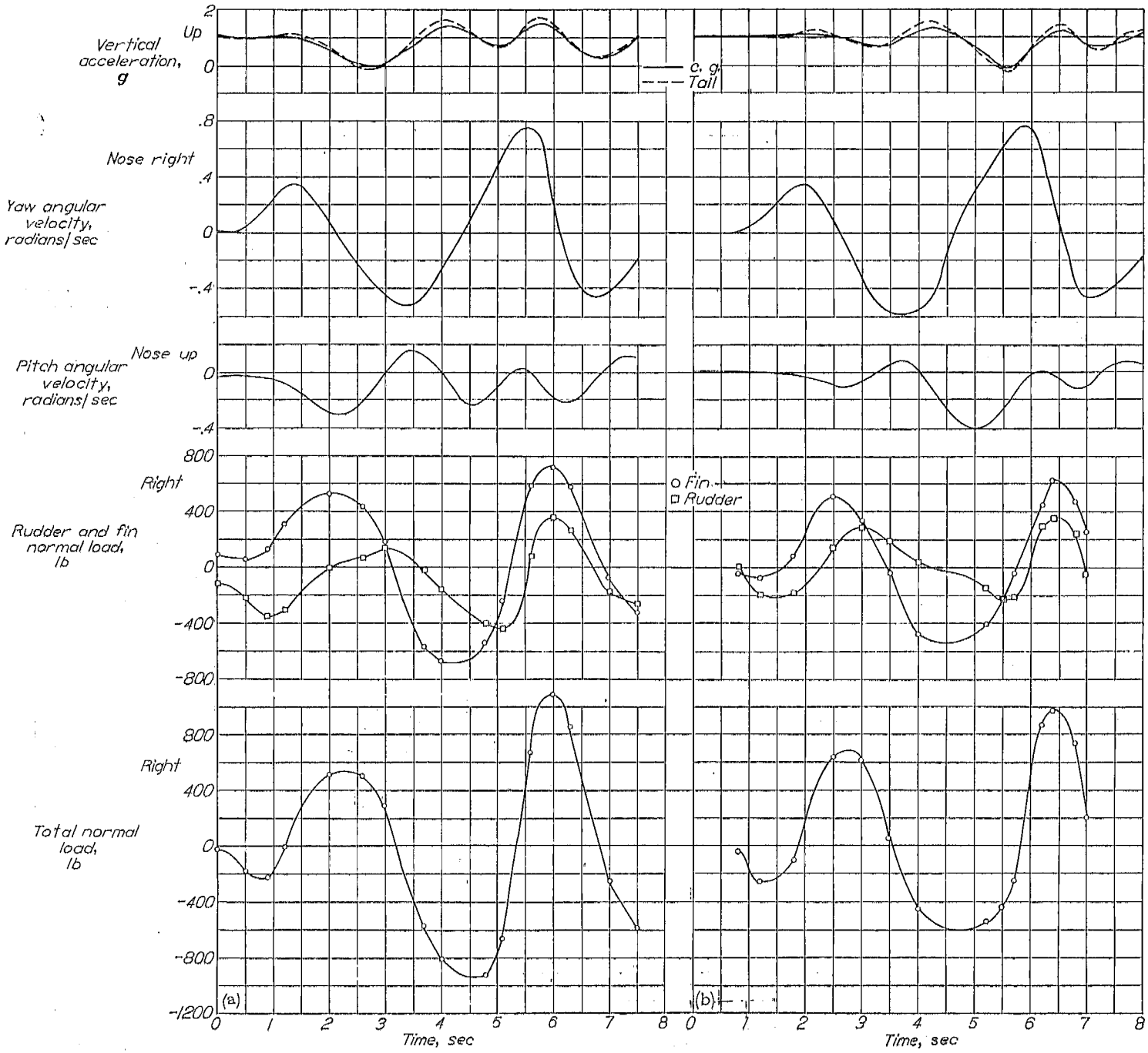

(a) Flight 18a, run 1; power on.

(b) Flight 18a, run 3; power off.

FIGURE 45.—Time histories of measurements recorded during power-on and power-off fishtails at 150 miles per hour in which pilot kicked rudder against the swing at point of maximum yawing velocity.

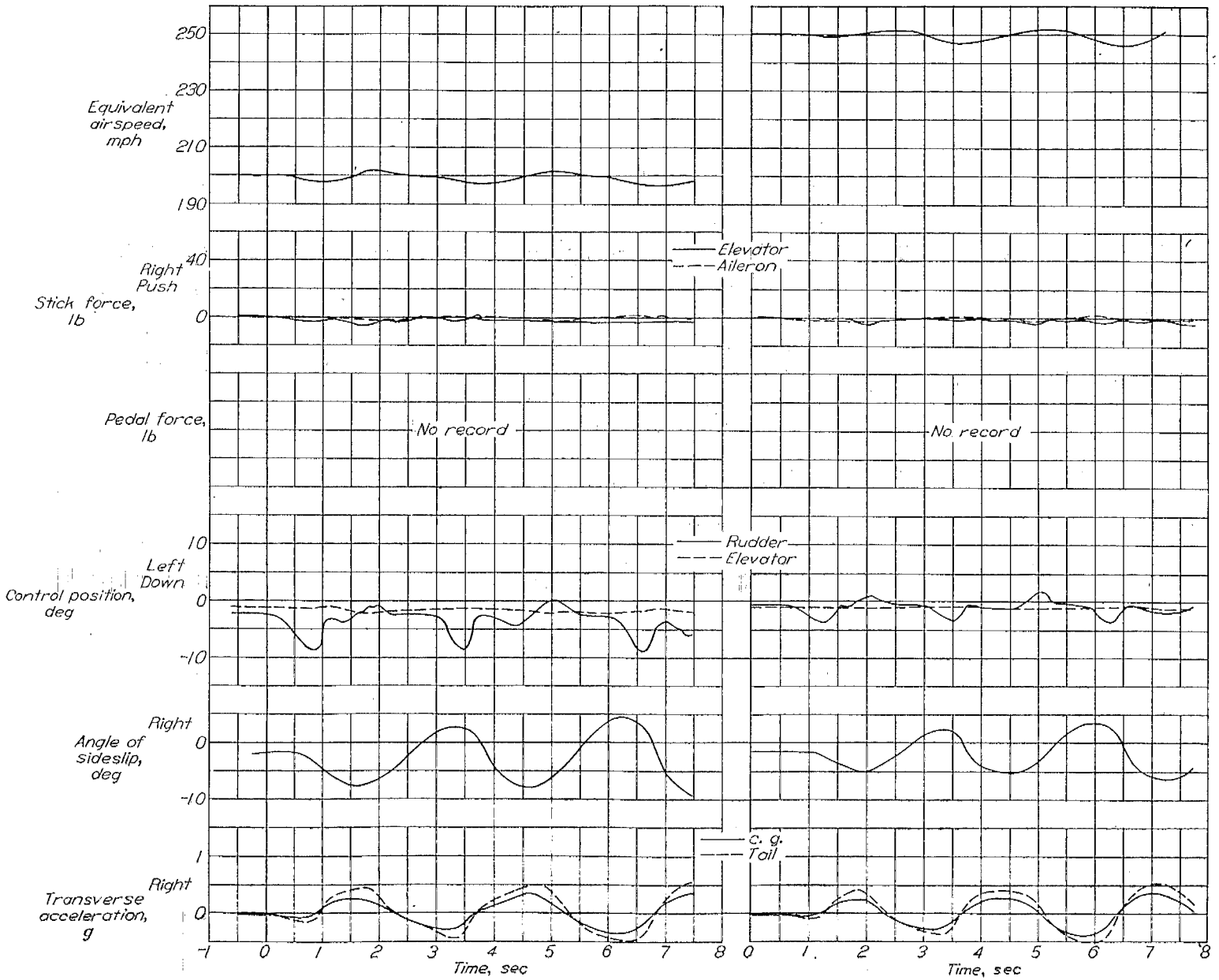
Equivalent airspeed, mph
250
230
210
190
Stick force, lb
Right Push
40
0
Elevator
Aileron
Pedal force, lb
No record
No record
Control position, deg
Left Down
10
0
-10
Rudder
Elevator
Angle of sideslip, deg
Right
0
-10
Transverse acceleration, g
Right
1
0
c. g.
Tail
-1
0
1
2
3
4
5
6
7
8
Time, sec
Time, sec

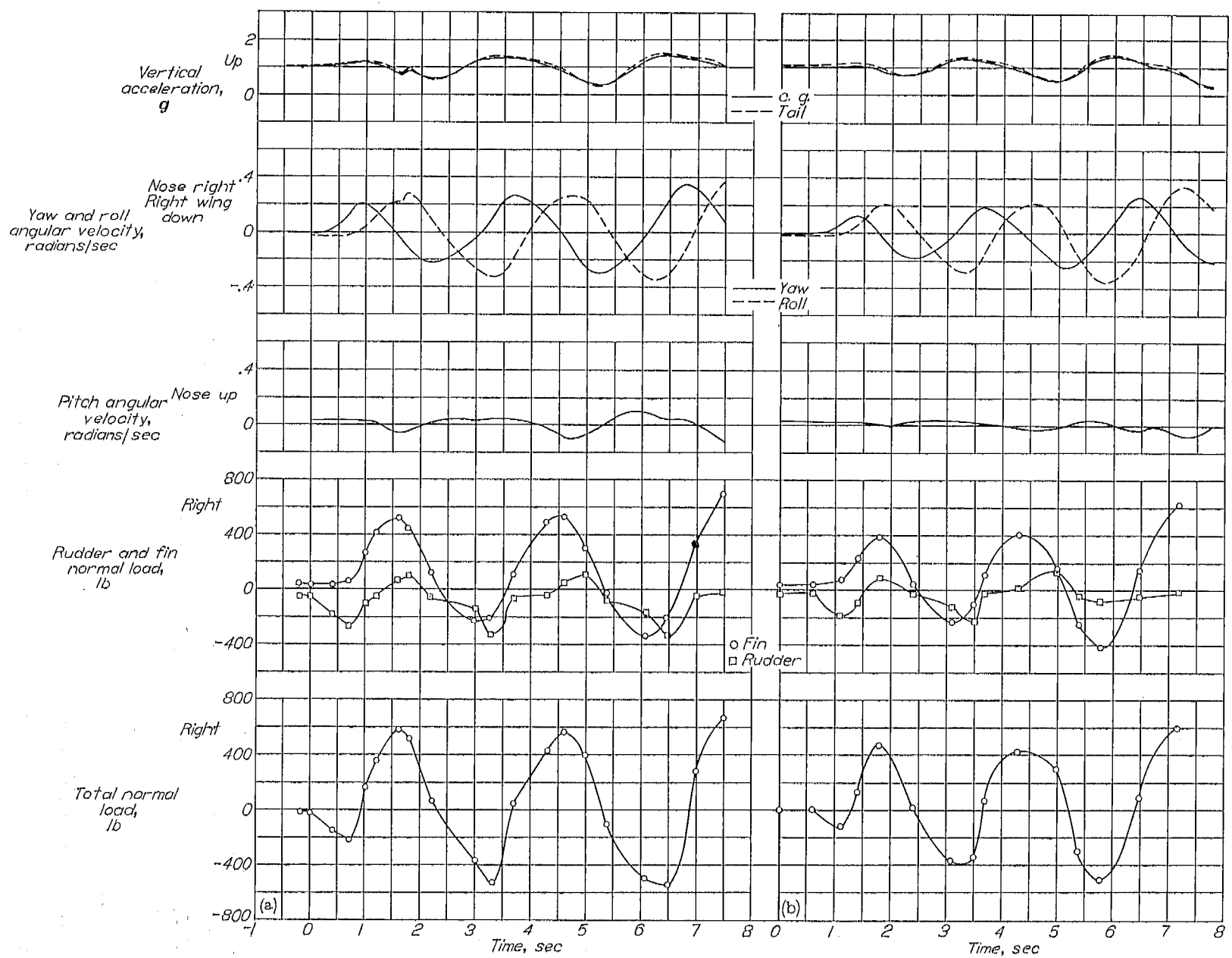

(a) Flight 26, run 1; V_e=200 miles per hour.

(b) Flight 26, run 2; V_e=250 miles per hour.

FIGURE 46.—Time histories of measurements recorded during mild fishtail maneuvers at 200 and 250 miles per hour with power on.

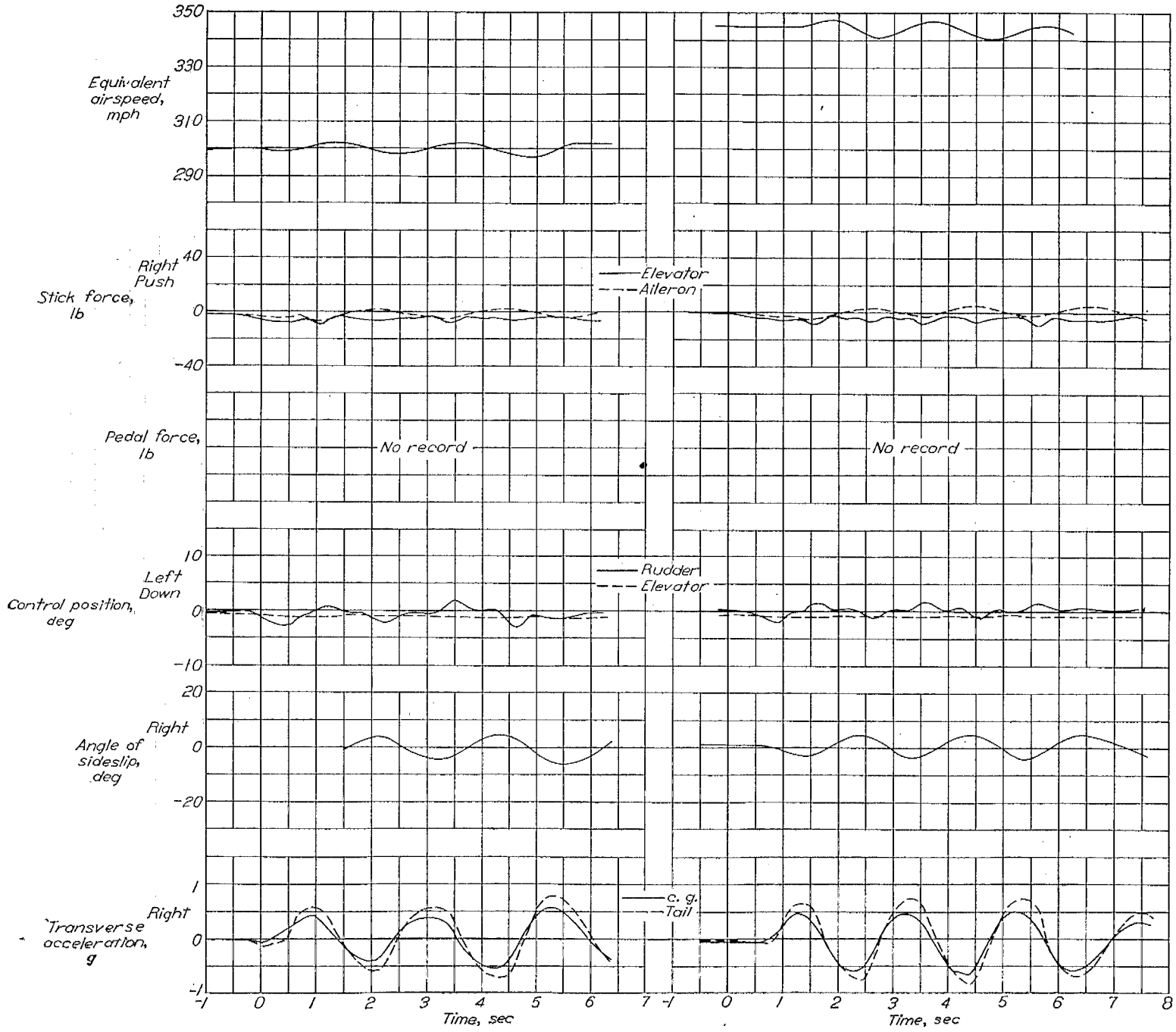
Equivalent airspeed, mph
350
330
310
290
Stick force, lb
Right Push
40
0
-40
Elevator
Aileron
Pedal force, lb
No record
No record
Control position, deg
Left Down
10
0
-10
Rudder
Elevator
Angle of sideslip, deg
Right
20
0
-20
Transverse acceleration, g
Right
1
0
-1
c. g.
Tail
-1 0 1 2 3 4 5 6 7
Time, sec
-1 0 1 2 3 4 5 6 7 8
Time, sec

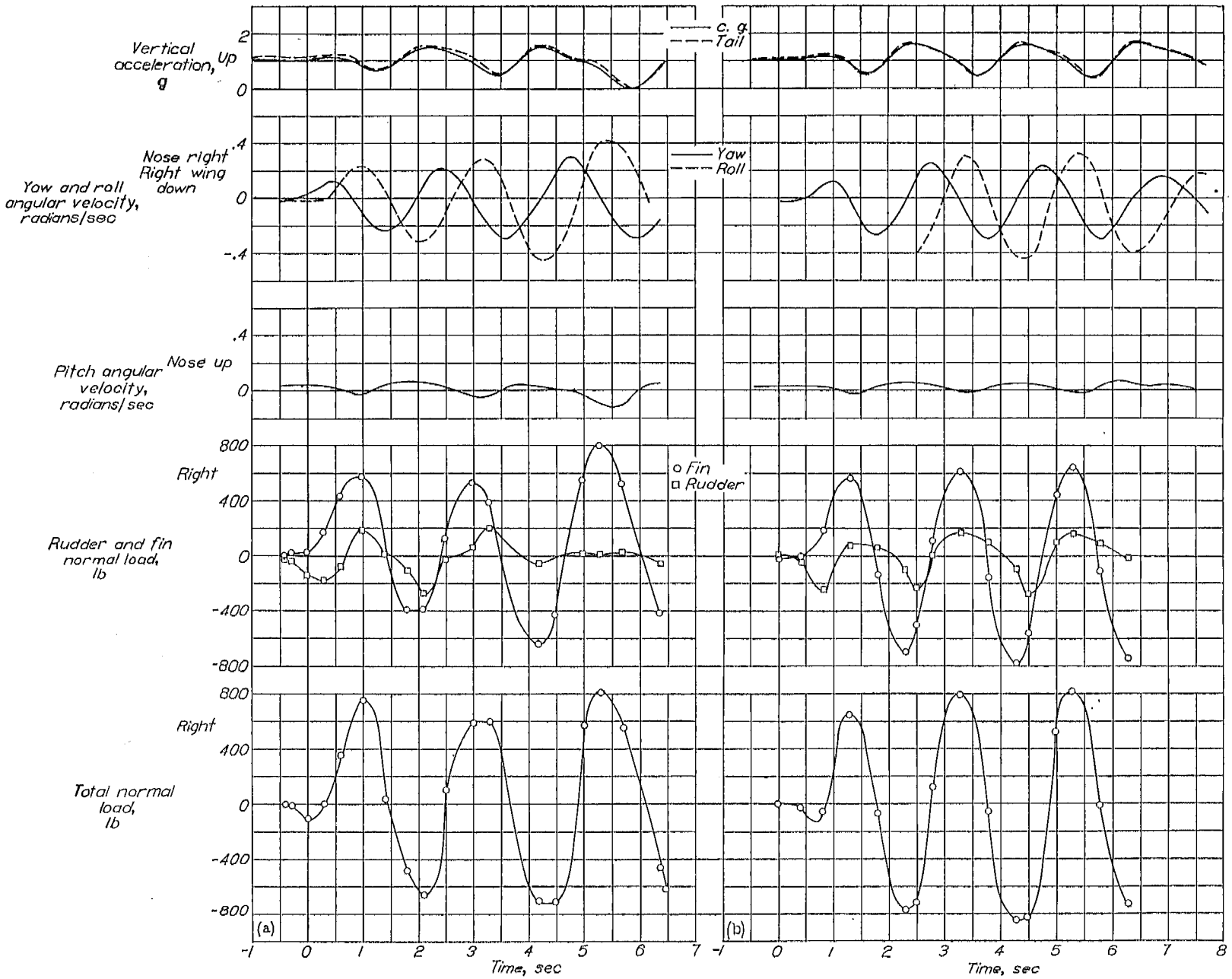

(a) Flight 26, run 3; V_e=300 miles per hour.

(b) Flight 26, run 4; V_e=350 miles per hour.

FIGURE 47.—Time histories of measurements recorded during mild fishtail maneuvers at 300 and 350 miles per hour with power on.

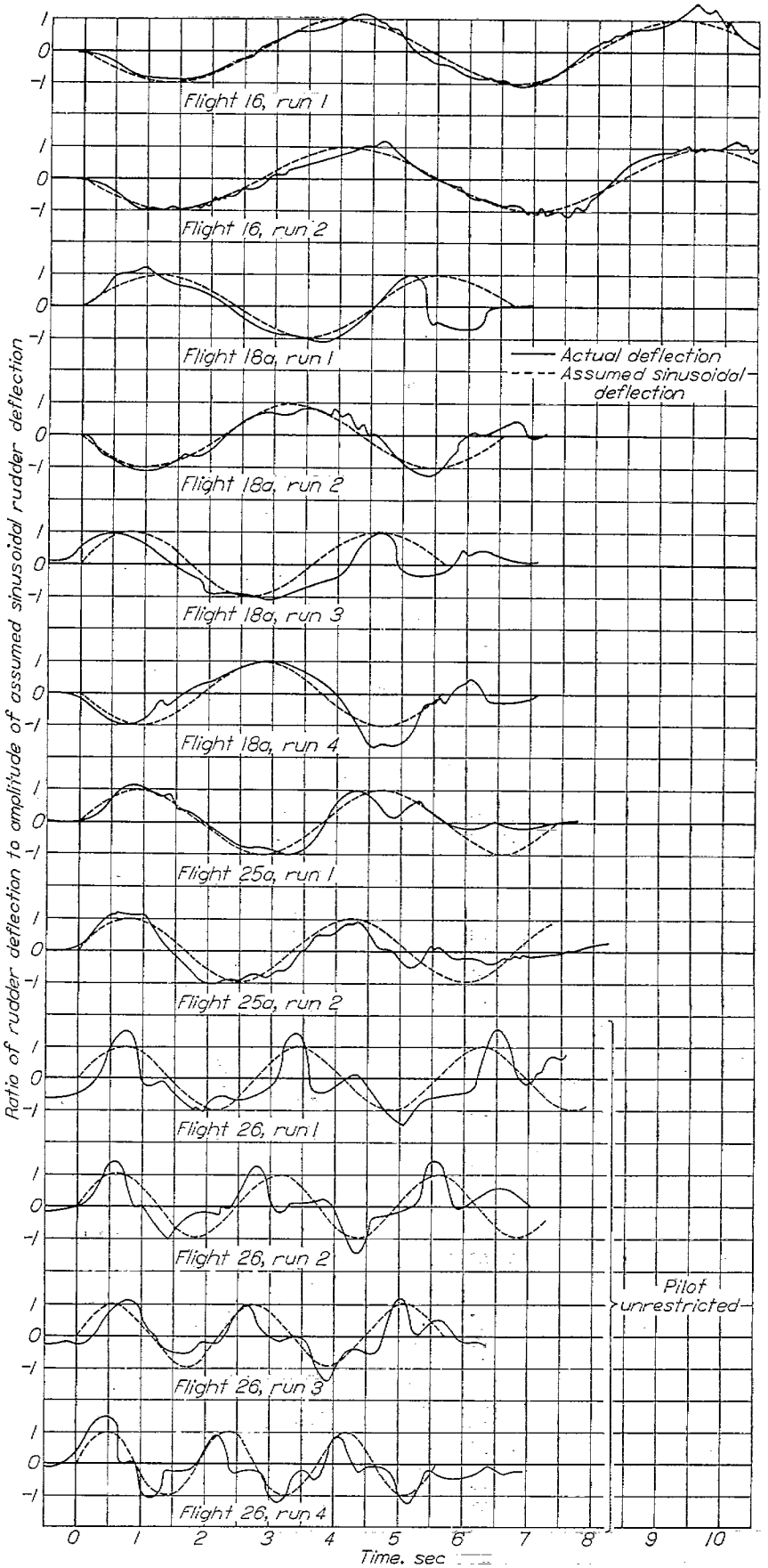

FIGURE 48.—Comparison of rudder manipulations of all fishtails with sine curves.

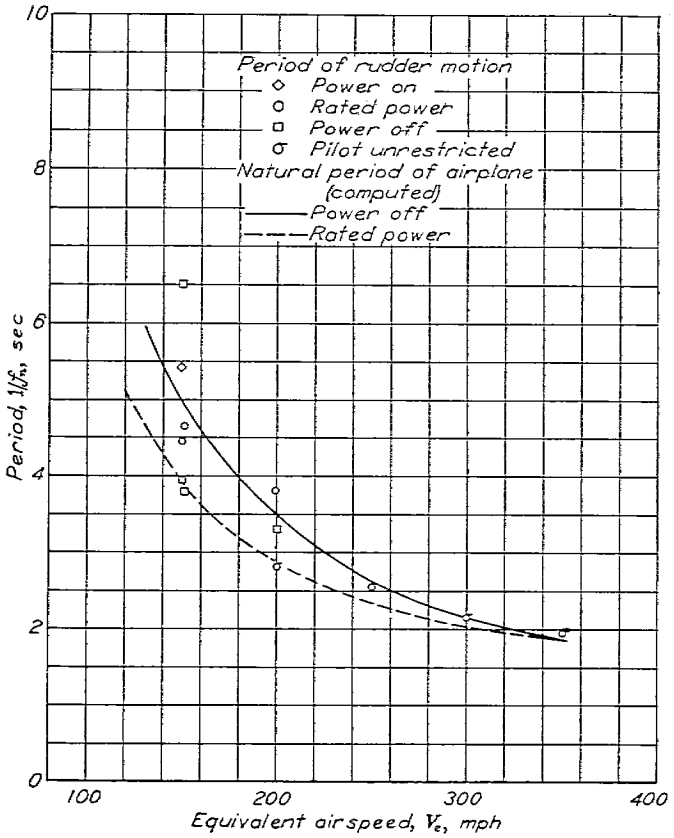

FIGURE 49.—Period of rudder motion compared with airplane period computed for rated power and power off.

Comparisons between measured and estimated load.—A comparison of the measured loads with those computed on the basis of the theory of flat yawing (reference 5) is presented in figure 50, which shows the maximum tail load measured per degree of rudder deflection during each run. Mean amplitudes of rudder deflection were used to obtain the experimental values of load per degree. Also included in figure 50 is a line corresponding to the load per degree for a control motion in which the rudder was assumed to be returned to trim at the time of maximum sideslip. Figure 50 shows that the loads measured during the fishtail did not reach the computed resonant value but were more nearly equal to the values given by the equation representing the hypothetical U-type control motion.

LOAD DISTRIBUTIONS

The fishtail maneuvers, as indicated by simple dynamics, yield an angle-of-attack load with rudder at zero deflection plus a zero-yaw full-rudder load according to the phase relations indicated by figure 42 (b).

Figure 51 presents the spanwise load distributions over the rudder and fin at various times during the power-on fishtail maneuvers of figures 43, 44, and 45. The spanwise and chordwise load distributions over fin and rudder and chordwise load distributions over rib V during the fishtails of figures 46 and 47 are presented in figures 52 and 53, respectively. Figure 54 (a) presents the center of load on the fin at the times of maximum loads on the fin during the fishtail

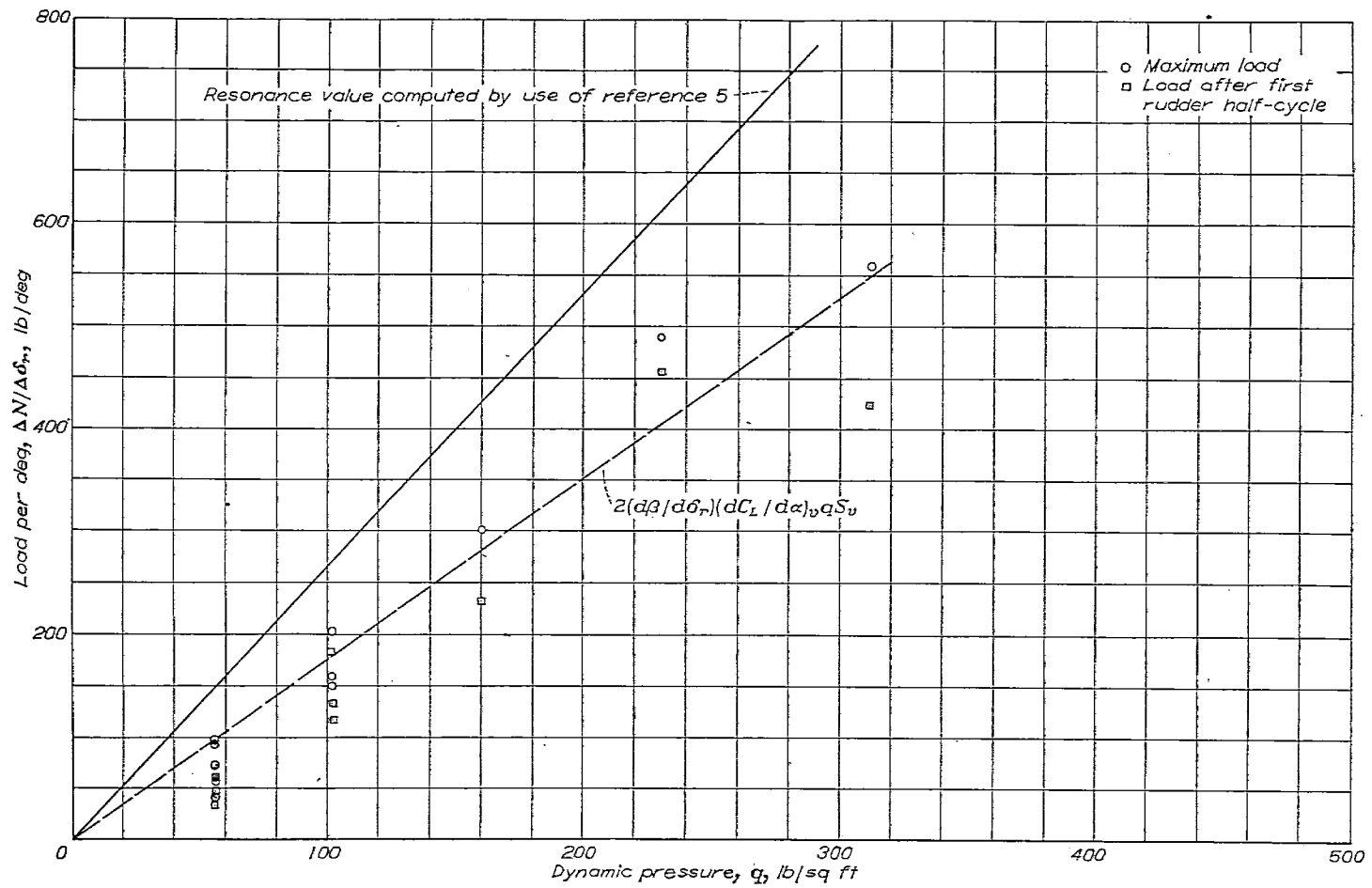

FIGURE 50.—Variation of maximum measured vertical tail load per degree with dynamic pressure as compared with computed variation for condition of resonance. Dashed line represents variation for one cycle of U-type control manipulation.

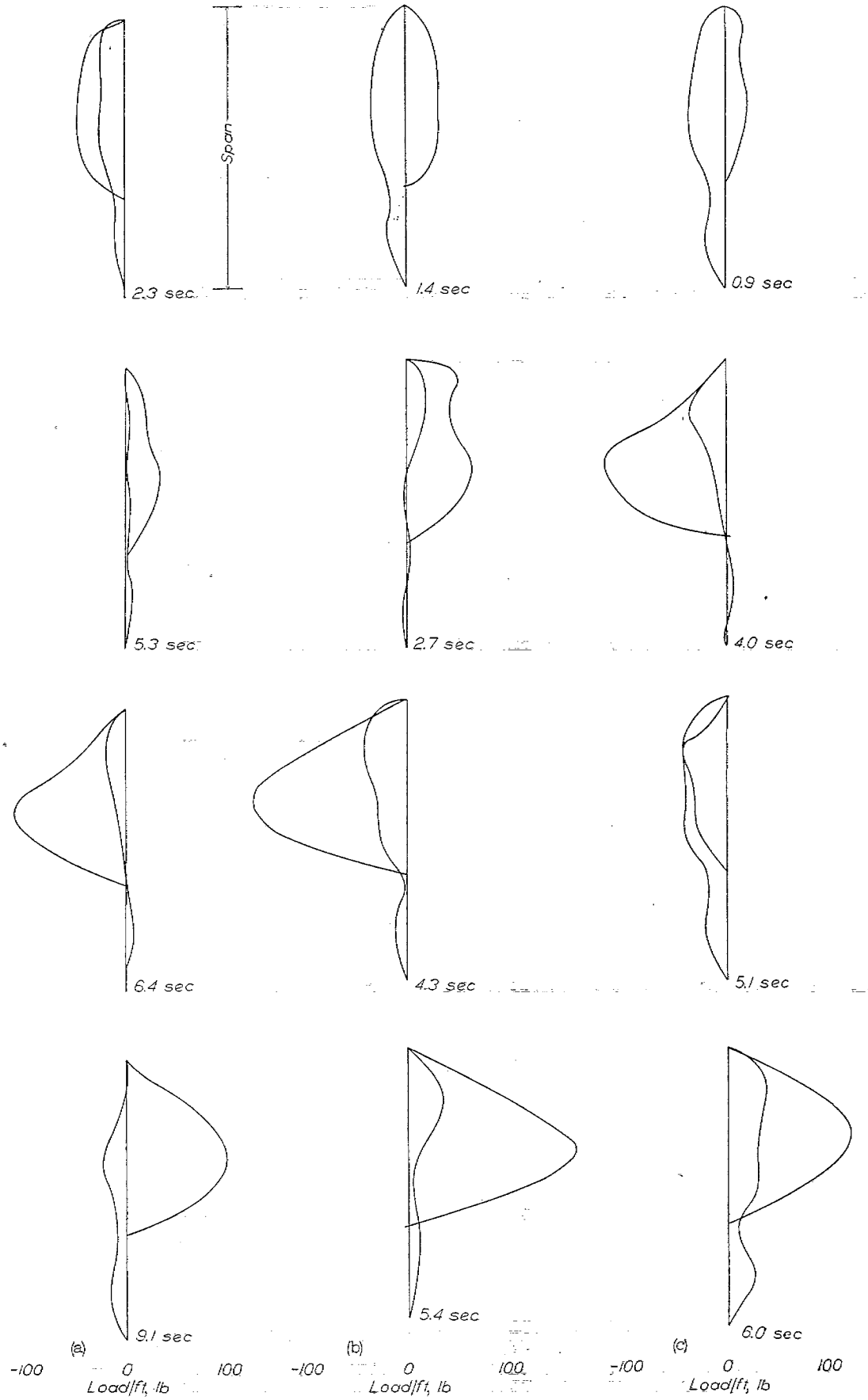

(a) Flight 16, run 1; high yaw angle; V_e=150 miles per hour. (b) Flight 25a, run 1; high yaw angle; V_e=200 miles per hour. (c) Flight 18a, run 1; kick against swing; V_e=150 miles per hour.

FIGURE 51.—Spanwise load distributions over the rudder and fin at various times during the power-on fishtails of figures 43, 44, and 45.

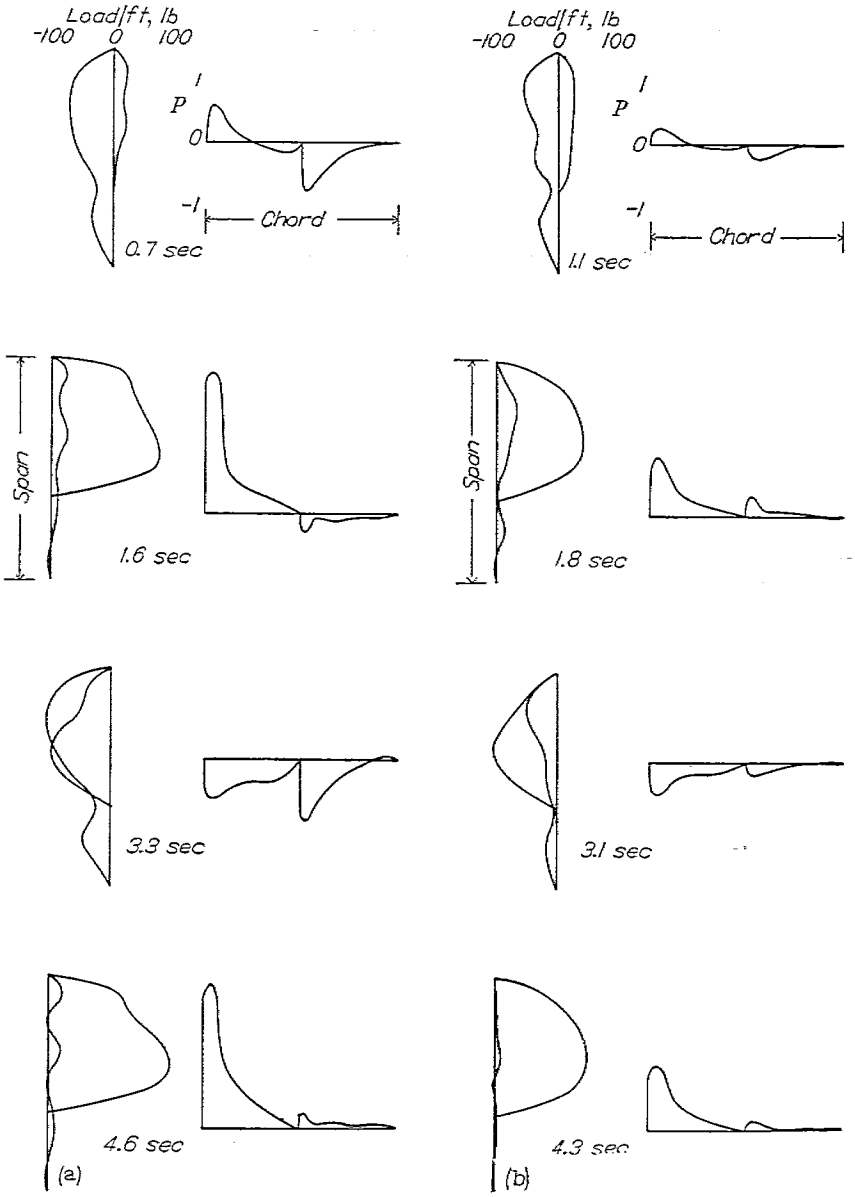

(a) Flight 26, run 1; V_e=200 miles per hour.

(b) Flight 26, run 2; V_e=250 miles per hour.

FIGURE 52.—Spanwise load distributions over fin and rudder and chordwise load distributions over rib V (see fig. 5) at times of maximum yaw for fishtails of figure 46.

Also, for illustrative purposes, time histories of the center-of-load variation during the fishtails of figures 46 and 47 are presented in figure 54 (b).

CONCLUSIONS

The conclusions are grouped under the general subject heading from which they were derived.

First load peak following a rudder kick (deflection load)

1. The deflection load can be determined with sufficient accuracy by the product of the moment of inertia and the first maximum yawing acceleration divided by the tail length.
2. The minimum time used by the pilot to attain the maximum rudder deflection at each flight condition appears to be a constant.
3. The deflection load on the vertical tail of the test airplane reaches values close to those for an infinite rate of control deflection.

Second load peak following a rudder kick (dynamic load)

1. The dynamic load can be determined with sufficient accuracy by the sum of the component of load necessary to balance the unstable yawing moment of the wing-fuselage combination in sideslip and the component of load due to angular acceleration in yaw.
2. After the initial rudder kick the return of the rudder to trim was, in general, made at the time of maximum sideslip so that the load due to abrupt reversal of the rudder was superimposed at the time of maximum overshoot load.
3. A rational approximate formula based upon a U-type control deflection satisfactorily expresses the upper limit value of the measured dynamic loads for this airplane. This formula is in terms of the sideslip-rudder ratio from steady-flight results and a magnification factor which considers the amount of directional damping in the airplane.

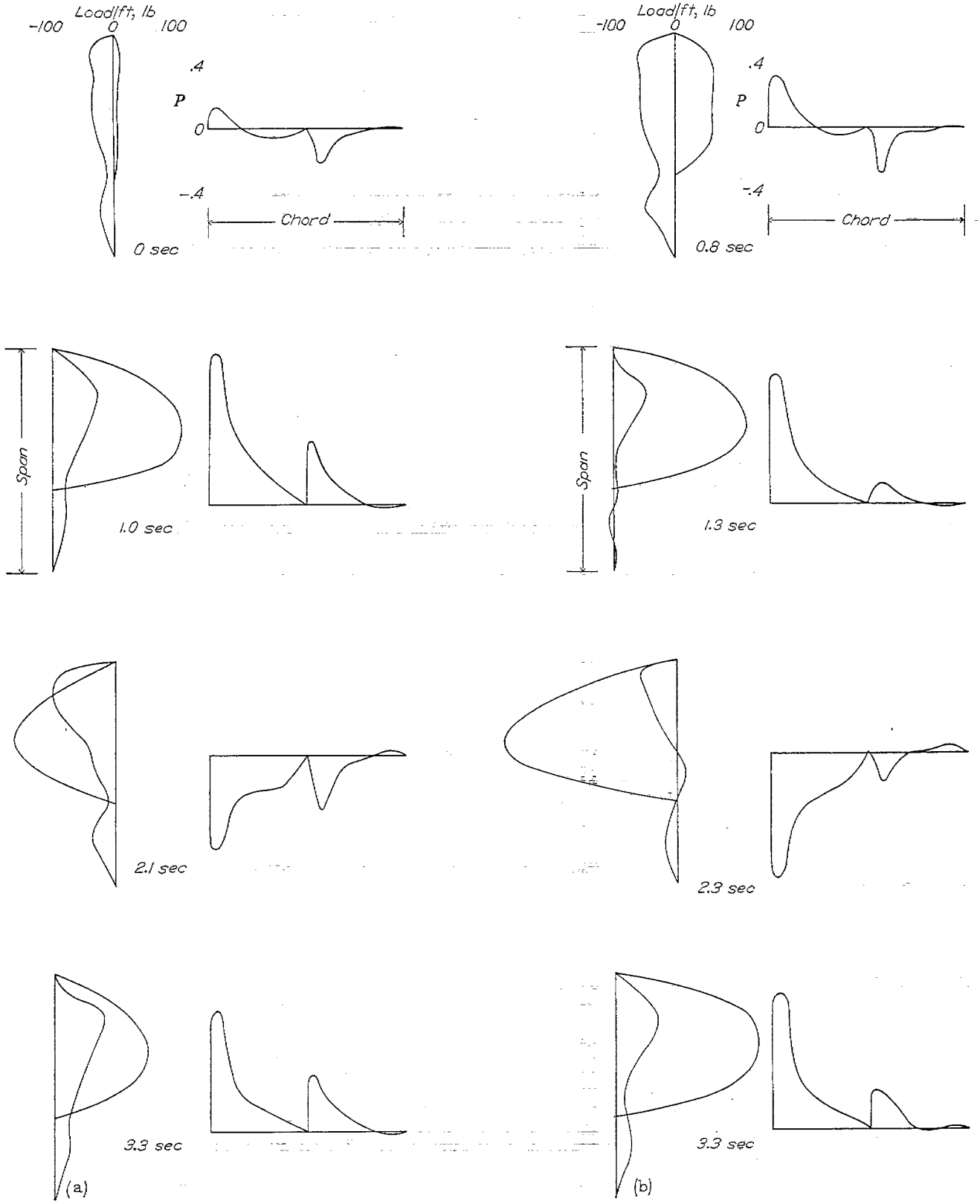

(a) Flight 26, run 3; V_e=300 miles per hour.

(b) Flight 26, run 4; V_e=350 miles per hour.

FIGURE 53.—Spanwise load distributions over fin and rudder and chordwise load distributions over rib V (see fig. 5) at times of maximum yaw for fishtails of figure 47.

Load distributions

1. The critical loads on the rudder are associated with the deflection load. The deflection load on the rudder is approximately equal to the total deflection load on the tail.

2. The critical loads on the fin are associated with the dynamic load on the tail. The upper limit of the measured dynamic loads on the fin is satisfactorily expressed as the fraction of the total dynamic load which would be carried for the rudder at zero.

3. At the time of maximum fin load the spanwise center of load on the fin is 10 percent farther outboard than the design air-load distribution.

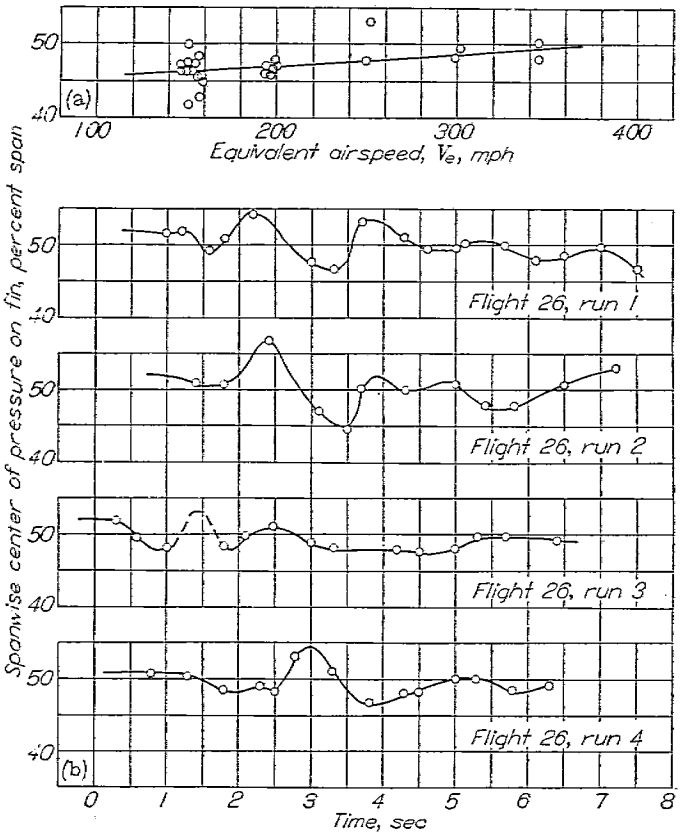

(a) Center of pressure at time of maximum load.

(b) Time history of center of pressure.

FIGURE 54.—Spanwise center of pressure on fin at time of maximum load on fin for all fishtail maneuvers against equivalent airspeed and time history of spanwise center of pressure during fishtail maneuvers of figures 46 and 47.

Fishtail maneuvers

1. The maximum loads measured during the fishtail maneuvers were no greater than those which would result from a hypothetical U-type rudder kick in which the rudder is returned to zero at the time of maximum sideslip.

2. As might be expected, the pilot tends to work the rudder in phase with the natural frequency of the airplane.

3. At resonance the rudder angle and sideslip angle are 90° out of phase so that at maximum sideslip the rudder deflection is zero and the load is proportional to the sideslip angle.

4. An abrupt stopping action in which the rudder is kicked against the swing results in high rudder loads. If the control is worked against the airplane swing, the phase relation between the rudder and fin loads is disturbed so that the loads become additive.

LANGLEY MEMORIAL AERONAUTICAL LABORATORY,
NATIONAL ADVISORY COMMITTEE FOR AERONAUTICS,
LANGLEY FIELD, VA., *April 9, 1947.*

REFERENCES

1. Pearson, Henry A.: Derivation of Charts for Determining the Horizontal Tail Load Variation with Any Elevator Motion. NACA Rep. No. 759, 1943.
2. Perkins, Courtland D.: Non-Dimensional Chart Method for Computing the Maneuver Loads on the Horizontal Tail Surfaces of Airplanes. AAF TR No. 4925, Materiel Command, Army Air Forces, May 13, 1943.
3. Kelley, Joseph, Jr., and Missall, John W.: Maneuvering Horizontal Tail Loads. AAF TR No. 5185, Air Technical Service Command, Army Air Forces, Jan. 25, 1945.
4. Gilruth, Robert R.: Analysis of Vertical-Tail Loads in Rolling Pull-Out Maneuvers. NACA CB No. L4H14, 1944.
5. Boshar, John, and Davis, Philip: Consideration of Dynamic Loads on the Vertical Tail by the Theory of Flat Yawing Maneuvers. NACA Rep. No. 838, 1946.
6. Johnson, Harold I., and Vensel, Joseph R.: Flight Measurements of the Rudder Control and Sideslip Characteristics of Four Vertical Tail Arrangements on the P-40 Series Airplanes. NACA MR, Oct. 9, 1942.
7. Beeler, De E.: Maximum Rates of Control Motion Obtained from Ground Tests. NACA RB No. L4E31, 1944.
8. Den Hartog, J. P.: Mechanical Vibrations. McGraw-Hill Book Co., Inc., 1934, p. 64.

TABLE I.—GEOMETRIC CHARACTERISTICS

Wing:	
Area, sq ft	236
Span, ft	37.29
Mean aerodynamic chord, ft	6.8
Root chord, ft	9
Section at root	NACA 2215
Section at tip	NACA 2209
Angle to thrust line, deg	1
Dihedral, deg	6
Aspect ratio	5.9
Engine:	
Type	Allison V-1710-F4R
Normal power at 10,800 ft, hp	1000
Propeller gear ratio	2:1
Propeller diameter, ft	11
Flight operation:	
Average weight in flight, lb	8200
Average position, percent M. A. C.	29.5
Vertical tail surface:	
Total area, sq ft	22.9
Height above fuselage, ft	5.67
Fin area (less fairing area), sq ft	9.18
Rudder area (including 1.94 sq ft of balance and 0.55 sq ft of tab), sq ft	13.74
Distance from c. g. to rudder hinge line, ft	20.13
Fin offset, deg	0
Horizontal tail surface:	
Total area, sq ft	48.3
Span, ft	12.79
Stabilizer area (including 3.54 sq ft of fuselage), sq ft	30.86
Elevator area (including 3.8 sq ft of balance and 1.68 sq ft of tab), sq ft	17.44
Distance from wing root L. E. to elevator hinge line, ft	20.0
Stabilizer set above thrust line, deg	2
Horizontal tail above fuselage center line, ft	1.50
Maximum elevator deflection (up), deg	31.5

TABLE II.—STEADY-SIDESLIP TESTS

Run	V_c (mph)	$\Delta\beta$ (deg) (a)	T_c	Q_c	$\Delta\delta_r$ (deg)	$\Delta\delta_a$ (deg)	ΔN_f (lb)	ΔN_r (lb)	ΔN_v (lb)	ΔC_{N_f}	ΔC_{N_r}	ΔC_{N_v}
Power on												
3	105.0	−11.40	0.109	0.007	−5.25	−2.50	102	−1	101	0.156	−0.002	0.155
4	105.0	9.95	.109	.007	7.55	1.10	−162	26	−136	−.248	.040	−.208
5	103.0	15.90	.108	.007	13.30	−.90	−235	86	−149	−.373	.137	−.237
7	162.0	−3.05	.045	.004	−1.75	−.69	120	−28	87	.077	−.018	.056
8	162.5	−7.15	.044	.004	−4.30	−2.69	246	−23	221	.159	−.015	.143
9	164.0	−12.00	.044	.004	−7.05	−3.59	307	−57	249	.193	−.036	.156
11	165.0	5.30	.043	.004	2.50	.11	−186	38	−149	−.116	.024	−.093
12	161.0	8.15	.045	.004	5.10	−.59	−286	107	−178	−.188	.070	−.117
13	159.5	10.15	.046	.004	6.85	−1.37	−388	150	−241	−.261	.101	−.162
15	217.5	−3.80	.030	.004	−1.24	−.72	176	−19	157	.064	−.007	.057
16	218.5	−5.45	.030	.004	−2.29	−1.32	275	−54	221	.098	−.019	.078
17	219.5	−7.25	.030	.004	−4.44	−2.12	418	−68	350	.147	−.024	.123
18	217.0	2.70	.030	.004	1.41	−.12	−157	42	−115	−.057	.015	−.042
19	218.0	3.65	.030	.004	2.01	−.32	−267	82	−185	−.095	.029	−.066
20	218.5	5.35	.030	.004	.34	−.82	−377	143	−234	−.134	.051	−.083
79	277.5	−2.05	.022	.004	−.60	−.17	171	−39	140	.038	−.009	.031
80	275.5	−3.50	.023	.004	−1.05	−.17	267	−78	197	.060	−.017	.044
81	275.5	−4.35	.023	.004	−1.05	−.47	331	−114	225	.074	−.025	.050
82	277.0	1.15	.023	.004	.55	.03	−100	39	−53	−.022	.009	−.012
83	277.5	2.20	.022	.004	.99	−.07	−239	80	−151	−.053	.018	−.033
84	276.5	3.20	.023	.004	2.20	−.17	−342	122	−212	−.076	.027	−.047
86	339.5	−1.00	.012	.002	.03	−.02	150	−34	113	.022	−.005	.017
87	334.5	−1.65	.013	.003	−.17	−.12	209	−61	148	.032	−.009	.023
88	337.0	−2.10	.013	.003	−.17	−.22	252	−68	185	.038	−.010	.028
89	337.0	.50	.013	.003	.54	−.02	−154	46	−107	−.023	.007	−.016
90	335.5	.90	.013	.003	.83	.10	−250	74	−176	−.038	.011	−.027
91	334.5	1.10	.013	.003	1.33	−.02	−315	94	−221	−.048	.014	−.034
93	379.5	−.80	.009	.002	−.02	−.12	124	−49	76	.014	−.006	.009
94	378.0	−1.10	.009	.002	−.12	−.02	164	−59	106	.020	−.007	.013
95	372.5	.75	.009	.002	.18	.08	−169	36	−132	−.021	.004	−.016
96	374.0	.75	.009	.002	.48	.08	−224	44	−175	−.027	.005	−.021
Power off												
36	100.0	−12.45	-------	-------	−6.08	−0.30	118	−13	109	0.201	−0.022	0.186
37	104.0	−16.32	-------	-------	−9.78	−2.35	153	−28	124	.239	−.044	.197
38	105.0	−19.82	-------	-------	−14.03	−4.05	189	−62	125	.260	−.095	.192
40	105.0	8.28	-------	-------	5.67	−1.85	−96	26	−73	−.147	.040	−.112
41	105.0	13.68	-------	-------	9.47	−3.85	−160	39	−124	−.245	.060	−.190
42	108.0	16.13	-------	-------	12.22	−5.35	−174	54	−126	−.253	.079	−.197
44	158.5	−5.60	-------	-------	−2.28	−.22	137	−39	74	.093	−.026	.050
45	159.5	−10.22	-------	-------	−6.73	−1.34	292	−101	167	.196	−.068	.112
46	161.0	−12.28	-------	-------	−9.80	−1.86	367	−128	217	.241	−.084	.142
48	164.0	5.35	-------	-------	4.09	−1.34	−138	51	−109	−.087	.032	−.068
49	161.0	7.77	-------	-------	6.05	−1.95	−230	68	−184	−.151	.045	−.121
50	161.0	11.87	-------	-------	10.80	−3.95	−338	112	−248	−.222	.074	−.163
52	218.0	−3.47	-------	-------	−1.57	−.17	175	−49	118	.062	−.017	.042
53	218.0	−5.82	-------	-------	−3.22	−.47	266	−92	169	.095	−.033	.060
54	218.5	−7.52	-------	-------	−4.67	−1.08	352	−163	192	.125	−.058	.068
56	218.5	2.83	-------	-------	2.33	−.28	−170	62	−113	−.060	.022	−.040
57	218.0	4.18	-------	-------	3.48	−.57	−245	96	−154	−.087	.034	−.055
58	218.5	5.43	-------	-------	5.03	−1.08	−345	138	−212	−.122	.049	−.075
60	219.5	−2.82	-------	-------	−1.07	−.12	140	−48	86	.049	−.017	.030
61	219.0	−5.62	-------	-------	−2.67	−.51	259	−93	160	.092	−.033	.056
62	218.5	−6.67	-------	-------	−3.97	−.96	343	−145	193	.122	−.051	.069
64	219.5	2.08	-------	-------	1.18	−.22	−113	37	−82	−.040	.013	−.029
65	219.5	3.38	-------	-------	2.48	−.52	−195	73	−128	−.069	.026	−.045
66	216.5	3.89	-------	-------	3.73	−.18	−246	108	−143	−.090	.039	−.052
67	159.5	−.37	-------	-------	−.03	−.18	22	−2	−4	.015	−.001	−.003
68	159.5	−.17	-------	-------	−.18	−.23	7	5	−12	.005	.003	−.008
69	159.5	−.37	-------	-------	−.25	−.23	11	−1	−14	.007	−.001	−.009
70	159.5	−.77	-------	-------	.05	−.13	40	−9	−13	.027	−.006	−.009

a Initial steady-flight value (increment from wings-level trim).

TABLE III.—RUDDER KICKS

Flight	Run	V_e (mph)	Power	$\Delta\beta$ (deg) [a]	T_c	Q_s	Altitude (ft)	ΔP_r (lb)	$\Delta\delta_r$ (deg)	δ_r (deg/sec)	$\ddot{\psi}_1$ (rad/sec²)	$\dot{\psi}$ (rad/sec)	$\dot{\theta}$ (rad/sec)	$\ddot{\theta}_1$ (rad/sec²)	$\Delta\beta$ (deg)	$\ddot{\psi}_2$ (rad/sec²)	ΔN_{f_1} (lb)	ΔN_{r_1} (lb)	ΔN_{v_1} (lb)	ΔN_{f_2} (lb)	ΔN_{r_2} (lb)	ΔN_{v_2} (lb)	Δt (sec)
6	4	100.0	On	0	---	---	10,000	75	10.08	26.08	−0.224	−0.200	0.082	0.186	8.56	------	30.0	115	112	-----	-----	-----	0.90
	6	106.0	On	0	---	---	10,000	−55	−10.08	−73.13	.347	.194	−.179	−.240	−4.97	−0.345	−51.0	−150	−196	130	138	229	.80
	7	101.0	On	0	---	---	10,000	---	−9.59	−45.05	.285	.178	------	−.157	-----	------	−43.0	−70	−123	72	3	75	.95
	9	100.0	On	0	---	---	10,000	---	-----	93.00	------	−.266	.046	.056	-----	------	64.0	155	216	−322	−216	−535	1.10
8	2	198.7	Rated	0	0.061	0.007	6,000	−138	−5.30	−57.04	.341	.220	−.203	−.238	−9.94	−.456	−55.0	−187	−193	459	53	613	1.55
	4	198.2	Rated	0	.062	.007	6,000	125	4.05	43.48	−.274	−.187	.054	.145	5.52	.204	15.0	159	138	−498	46	−426	2.10
8a	4	203.0	Rated	0	.057	.007	6,000	---	−11.91	−43.43	.883	.440	−.364	−.372	−19.33	−.871	−35.0	−418	−485	810	60	880	.70
8b	1	199.5	On	0	.032	.004	6,000	271	6.44	16.55	−.435	−.298	.075	.155	13.53	.725	10.0	373	305	−830	−188	−963	.90
	2	203.0	On	0	.032	.004	6,000	285	6.44	55.29	−.487	−.319	.107	.186	-----	.736	42.0	350	332	−798	−160	−955	.80
	3	202.0	On	0	.032	.004	6,000	−271	−7.73	−22.40	.514	.308	−.268	−.295	-----	−.659	−20.0	−182	−230	735	188	790	1.00
11a	1	296.5	On	0	.018	.003	6,000	−332	−4.51	−20.17	.624	.246	−.228	−.292	−8.84	−1.137	−80.0	−460	−400	1115	155	1458	.80
	2	298.5	On	0	.018	.003	6,000	−328	−4.51	−16.15	.600	.269	−.228	−.306	−9.11	−1.082	124.0	−504	−450	1297	72	1400	.75
	3	297.0	On	0	.018	.003	6,000	269	4.03	35.30	−.052	−.134	.057	.127	6.90	.877	10.0	368	370	−1135	−83	−1185	.55
	4	296.0	On	0	.018	.003	6,000	280	3.86	17.22	−.441	−.224	.057	.154	6.90	.798	−15.0	332	250	−1115	−80	−1067	.70
4b	1	100.0	Off	0	---	---	7,000	−26	−8.62	−66.48	.158	.167	−.020	−.009	−6.91	------	−30.0	−68	−95	-----	-----	-----	>2.90
	2	100.0	Off	0	---	---	5,000	32	7.81	60.85	−.112	−.133	.031	.034	5.39	------	17.0	79	95	-----	-----	-----	>3.00
	3	102.5	Off	0	---	---	7,000	−32	−11.50	−116.23	.178	.194	−.010	−.018	−8.29	------	−24.5	−82	−107	-----	-----	-----	2.80
	4	101.0	Off	0	---	---	6,000	38	10.86	86.42	−.145	−.178	.031	.046	6.63	------	36.5	85	117	-----	-----	-----	2.40
5[2]	2	101.0	Off	0	---	---	6,000	---	25.53	124.60	−.417	−.377	.092	.110	−6.91	------	61.0	184	239	-----	-----	-----	>1.00
	3	101.0	Off	0	---	---	6,000	−93	−20.81	−41.99	.296	.366	0	−.012	−11.60	------	−30.0	−131	−153	-----	-----	-----	>1.20
	4	100.0	Off	0	---	---	6,000	---	26.02	70.94	−.366	−.422	.056	.109	12.49	------	27.0	180	199	-----	-----	-----	>1.30
	5	101.0	Off	0	---	---	6,000	---	−21.46	−184.74	.274	.333	------	.017	−8.01	------	−46.0	−154	−189	-----	-----	-----	1.30
7b	2	200.0	Off	0	---	---	6,000	−200	−10.30	−86.72	------	------	−.214	−.201	−10.78	------	−53.0	−398	−445	792	−50	720	.85
	3	192.0	Off	0	---	---	6,000	238	12.08	79.03	------	------	.096	.283	15.74	------	90.0	352	405	−750	−98	−833	1.00
	4	197.0	Off	0	---	---	6,000	−212	−9.98	−22.61	------	------	−.182	.173	−10.50	------	−25.0	−351	−305	669	−135	540	>1.20
	5	203.0	Off	0	---	---	6,000	223	9.66	32.65	------	------	.075	.140	12.71	------	32.0	293	308	−708	−101	−807	.90
11a	6	294.5	Off	0	---	---	6,000	−354	−4.83	−42.44	.751	.269	−.171	−.220	−9.11	−1.170	−15.0	−468	−485	1405	173	1539	.95
	7	295.5	Off	0	---	---	6,000	−313	−4.03	−31.88	.551	.224	−.114	−.199	−8.29	−.918	27.0	−305	−265	1083	217	1150	.80
	8	299.5	Off	0	---	---	6,000	332	4.90	48.10	−.521	−.235	.057	.177	7.60	.813	30.0	318	300	−975	−59	−1077	.80
	9	299.8	Off	0	---	---	6,000	309	4.51	10.10	−.411	−.224	.057	.132	6.49	.848	−10.0	284	190	−1070	−86	−1111	.45
24	5	157.5	On	21.00	.047	.004	6,000	−391	−20.15	−137.35	.799	.588	.224	−.297	−27.08	−.728	−142.0	−258	−420	1148	112	1220	1.20
	6	164.5	On	−15.40	.043	.004	6,000	306	17.40	141.47	−.897	−.441	−.053	.456	20.48	.740	415.0	125	495	−915	−55	−975	1.00
12a	1	204.0	Rated	−4.80	.057	.007	6,000	239	6.76	11.62	−.344	−.280	.120	.167	13.44	.566	18.0	271	220	−813	−44	−835	1.10
	2	198.5	Rated	−5.20	.061	.007	6,000	239	7.25	53.20	−.392	−.258	.137	.218	12.60	.589	65.0	252	315	−728	−59	−780	1.20
	3	197.5	Rated	5.30	.062	.007	6,000	−267	−9.66	−3.55	.580	.381	−.200	.292	−14.84	−.652	−49.0	−346	−370	870	−8	855	.90
	4	198.5	Rated	4.00	.061	.007	6,000	−276	−9.66	−92.20	.765	.381	−.177	−.283	−18.20	−.669	−77.0	−385	−452	843	31	898	.95
15	1	199.0	On	−8.70	.032	.004	6,000	313	9.34	89.47	−.618	−.336	.143	.222	14.70	.580	13.0	220	345	−872	−40	−890	.70
	2	198.5	On	7.00	.032	.004	6,000	−343	−12.08	−99.80	.876	.482	------	−.215	-----	−.730	−115.0	−510	−608	1020	−45	919	.55
24	1	299.5	On	4.50	.018	.003	6,000	−368	−6.41	−63.24	.819	.311	−.085	.263	−9.56	−.930	−20.0	−475	−455	1255	−20	1235	.35
	2	299.0	On	−4.00	.018	.003	6,000	339	5.50	68.67	−.866	−.294	.085	.294	9.56	.720	90.0	597	640	−1180	152	−990	.50
24	7	159.0	Off	19.97	---	---	6,000	−420	−26.56	−125.91	.862	.661	.192	.297	−29.76	−.987	−85.0	−460	−540	1095	−25	1050	1.40
	8	154.0	Off	−15.65	---	---	6,000	446	28.17	189.46	−1.065	−.588	−.043	.353	29.76	.678	135.0	528	630	−960	33	−880	1.10
12a	5	198.0	Off	−4.00	---	---	6,000	221	10.95	16.94	−.494	−.336	.103	−.406	16.80	.621	27.0	286	263	−808	−30	−832	.60
	6	200.5	Off	−5.00	---	---	6,000	254	10.95	93.62	−.698	−.358	.114	−.363	15.68	.550	102.0	383	475	−761	−14	−775	.65
	7	197.0	Off	5.40	---	---	6,000	−321	−10.47	−58.24	.599	.437	−.057	−.699	−14.56	−.863	−50.0	−305	−300	862	139	1010	.60
	8	200.0	Off	5.10	---	---	6,000	−313	−9.90	−149.30	.627	.358	−.057	−.046	−12.60	−.643	−57.0	−301	−358	750	115	847	.65
15	3	198.0	Off	−8.55	---	---	6,000	304	13.52	109.33	−.804	−.414	.125	.261	20.72	.651	103.0	395	500	−1012	50	−920	.70
	4	199.5	Off	5.80	---	---	6,000	−354	−10.63	−110.88	.715	.392	------	−.215	−16.80	−.847	−100.0	−385	−500	990	−5	975	1.05
24	3	290.0	Off	5.00	---	---	6,000	−420	−6.18	−48.86	.740	.316	−.075	−.305	−9.56	−.773	−65.0	−455	−395	1215	−130	1085	>3.20
	4	288.5	Off	−4.75	---	---	6,000	332	6.41	63.74	−.709	−.271	.043	−.315	9.56	.693	77.0	450	422	−1163	155	−1018	>2.70

[a] Initial steady-flight value (increment from wings-level trim).

TABLE IV.—RUDDER KICKS (IN WHICH NO LOADS WERE MEASURED)

Flight	Run	V_e (mph)	Power	$\Delta\beta$ (deg) (a)	T_c	Q_e	Altitude (ft)	ΔF_r (lb)	$\Delta\delta_r$ (deg)	$\dot{\delta}_r$ (deg/sec)	$\ddot{\psi}_1$ (rad/sec²)	$\dot{\psi}$ (rad/sec)	$\dot{\theta}$ (rad/sec)	$\ddot{\theta}_1$ (rad/sec²)	$\Delta\beta$ (deg)	$\ddot{\psi}_2$ (rad/sec²)	Δt (sec)
6	1	102	On	0	0.117	0.007	10,000	−28	−6.50	−34.16	0.172	0.111	−0.138	−0.143	−4.28	------	>1.40
	2	100	On	0	.122	.007	10,000	86	8.13	70.94	−.341	−.255	.087	.164	-----	------	.80
	3	100	On	0	.122	.007	10,000	−29	−4.88	−18.21	.133	.089	−.153	−.139	−3.31	------	>1.60
	5	100	On	0	.122	.007	10,000	−97	11.06	111.59	−.375	−.300	.102	.204	11.32	------	1.10
	8	100	On	0	.122	.007	10,000	---	7.15	35.34	−.254	−.166	.041	.061	8.29	------	>1.30
6a	1	100	Rated	0	.480	.029	10,000	−159	−8.37	−79.56	.311	.187	−.268	−.217	−9.52	−0.282	1.30
	2	100	Rated	0	.480	.029	10,000	−174	−10.30	−106.18	.276	.176	−.241	−.217	−9.11	−.289	1.20
	3	100	Rated	0	.480	.029	10,000	153	10.95	51.28	−.408	−.275	.102	.194	13.81	.520	.80
	4	100	Rated	0	.480	.029	10,000	219	17.71	18.07	−.549	−.374	.107	.203	15.19	.562	.80
8	1	200	Rated	0	.060	.007	6,000	−157	3.87	−35.38	.299	.204	−.214	−.196	−8.98	−.333	1.90
	3	200	Rated	0	.060	.007	6,000	102	2.90	10.70	−.193	−.143	.032	.109	4.14	.175	2.05
	5	200	Rated	0	.060	.007	6,000	−280	−8.53	−19.83	.564	.330	−.321	−.356	-----	−.553	1.65
	6	200	Rated	0	.060	.007	6,000	−287	−13.01	−65.82	.850	.478	−.471	−.483	-----	−.809	1.50
	7	200	Rated	0	.060	.007	6,000	234	7.08	23.91	−.420	−.319	.064	.180	-----	.858	.70
	8	200	Rated	0	.060	.007	6,000	261	7.41	53.95	−.501	−.308	.064	.136	-----	.664	.80
8a	1	200	Rated	0	.060	.007	6,000	282	7.73	35.12	------	−.330	.064	.156	15.19	------	.80
	2	200	Rated	0	.060	.007	6,000	350	8.69	41.81	------	−.352	.086	.215	16.85	------	1.00
	3	200	Rated	0	.060	.007	6,000	---	−6.93	−46.38	.427	.275	−.310	−.272	−15.47	−.955	1.30
8b	4	200	On	0	.032	.004	6,000	−290	−9.98	−77.28	.675	.385	−.257	−.369	−13.43	−.741	.60
11	1	300	On	0	.024	.004	6,000	−261	−4.19	−37.10	.541	.224	−.160	−.209	−7.60	−.870	.70
	2	300	On	0	.024	.004	6,000	−229	−3.22	−22.61	.458	.190	−.160	−.204	−7.32	−.874	.80
	3	300	On	0	.024	.004	6,000	234	3.95	26.80	−.497	−.157	.057	.143	6.35	.762	.90
	4	300	On	0	.024	.004	6,000	195	3.06	8.15	−.278	−.174	.068	.106	5.80	.683	.80
15	5	325	On	0	.024	.004	6,000	−267	−2.90	------	.576	.218	------	−.258	−5.80	−.678	.50
4	1	99	Off	0	---	---	6,000	32	5.69	11.23	−.083	−.122	.026	.033	6.62	------	>3.20
	2	100	Off	0	---	---	6,000	−23	−7.80	−18.80	.100	.200	−.010	−.007	−8.84	------	>3.30
	3	100	Off	0	---	---	6,000	----	------	------	.081	.161	0	−.004	−9.11	------	-----
	4	100	Off	0	---	---	6,000	70	14.23	93.85	−.195	−.178	.020	.062	7.18	------	>1.80
	5	100	Off	0	---	---	6,000	−59	−14.47	−125.23	.324	.272	−.010	−.007	−8.29	------	>1.60
4a	1	100	Off	0	---	---	6,000	---	−15.20	−133.98	.330	.266	0	−.049	−9.39	------	>2.70
	2	100	Off	0	---	---	6,000	89	24.07	161.48	−.337	−.220	.050	.036	9.39	------	.30
	3	100	Off	0	---	---	6,000	51	13.50	66.54	−.215	−.189	.026	.045	5.52	------	>1.50
	4	100	Off	0	---	---	6,000	−42	−13.01	−63.46	.214	.222	−.026	−.021	−6.91	------	2.10
	5	100	Off	0	---	---	6,000	59	12.85	102.03	−.219	−.200	.031	.031	6.91	------	1.55
4b	5	100	Off	0	---	---	5,500	−77	−21.46	−150.03	.309	.333	------	−.009	−10.50	------	1.30
5_1	1	102	Off	0	---	---	6,000	−45	−13.01	−77.39	.215	.250	−.010	−.013	−8.84	------	>1.70
	2	100	Off	0	---	---	6,000	58	14.96	89.50	−.245	−.220	.020	.043	6.08	------	>1.80
	3	101	Off	0	---	---	6,000	−65	−15.93	−26.43	.225	.278	------	−.024	−9.67	------	>1.70
	4	99	Off	0	---	---	6,000	79	18.86	25.78	−.244	−.266	.026	.043	11.05	------	>1.50
	5	99	Off	0	---	---	6,000	82	17.89	39.39	−.254	−.278	.031	.074	8.29	------	>1.60
5_2	1	100	Off	0	---	---	6,000	---	−21.48	−185.92	.335	.278	------	−.019	−6.91	------	.85
	6	100	Off	0	---	---	6,000	74	−17.89	122.07	−.251	−.278	.031	.063	12.98	------	>1.90
	7	100	Off	0	---	---	6,000	−43	−13.01	−29.59	.173	.266	−.020	−.010	-----	------	>2.00
7	1	200	Off	0	---	---	6,000	---	−9.43	−71.85	.388	.194	−.066	−.064	−8.15	−.344	1.50
	2	200	Off	0	---	---	6,000	---	7.80	45.46	−.257	−.155	.026	.030	6.91	.231	>1.40
	3	205	Off	0	---	---	6,000	---	7.97	−14.73	.233	.167	−.082	−.059	−8.01	−.305	1.40
	4	198	Off	0	---	---	6,000	---	6.88	13.63	−.230	−.133	.010	.024	5.80	.167	1.55
	5	192	Off	0	---	---	5,000	---	------	------	------	.006	------	−.008	-----	------	-----
	6	202	Off	0	---	---	5,000	---	−17.07	−97.65	.736	.344	−.233	−.218	−13.26	−.603	>1.00
7a	1	200	Off	0	---	---	6,000	−140	−8.05	−26.28	.309	.297	−.187	−.192	−9.67	−.664	.90
	2	200	Off	0	---	---	6,000	180	8.37	17.48	−.442	−.297	.054	.153	7.87	------	>.90
	3	200	Off	0	---	---	6,000	−157	−8.86	−63.79	.478	.352	−.268	−.236	−10.50	−.612	>1.00
	4	200	Off	0	---	---	6,000	202	9.01	33.97	−.525	−.297	.054	.188	6.91	------	.80
	5	200	Off	0	---	---	6,000	−159	−9.34	−63.12	.588	.319	−.214	−.261	−12.15	−.921	1.00
7b	1	200	Off	0	---	---	6,000	---	−11.59	−70.20	------	-----	−.257	−.314	−11.88	------	>1.10
11	5	300	Off	0	---	---	6,000	−205	−3.38	−14.04	.336	.140	−.057	−.150	−6.21	−.320	1.40
	6	300	Off	0	---	---	6,000	−218	−3.22	−16.42	.403	.168	−.114	−.131	−6.91	−.777	.90
	7	300	Off	0	---	---	6,000	190	3.38	23.28	−.399	−.157	.057	.133	5.94	.460	1.20
	8	300	Off	0	---	---	6,000	223	3.86	12.50	−.404	−.213	.046	.104	6.49	.726	.80
11a	5	300	Off	0	---	---	6,000	---	−4.51	−39.62	.526	.168	−.086	−.152	−8.56	−1.117	.60
12	1	200	On	−5.25	.033	.004	6,000	228	7.08	22.26	−.382	−.308	.114	------	12.60	.504	.62
	2	200	On	−5.45	.033	.004	6,000	313	8.69	71.89	−.510	−.347	.114	------	13.72	.597	.70
	3	200	On	5.95	.033	.004	6,000	---	−9.66	−71.54	.757	.420	−.171	------	−16.24	−.621	.50
	4	200	On	3.65	.033	.004	6,000	---	−8.37	−82.40	.606	.336	−.114	------	−13.72	−.574	.70

a Initial steady-flight value (increment from wings-level trim).

TABLE V.—FISHTAIL MANEUVERS

[Altitude, 6000 ft]

Flight	Run	Speed (mph)	Power	Initial $\Delta\delta$ (deg)	Mean $\Delta\delta$ (deg)	Max. load first cycle (lb)	Max. load (lb)	Max. rudder load (lb)	Max. fin load (lb)	Remarks
16	1	150	On	8.0	9.0	−600	−670	−160	−660	Attempt to maximize loads (high side-slip amplitude).
	2	151	Off	13.5	14.0	−450	570	125	630	
18a	1	151	Rated	−11.5	11.0	960	1070	−420	−780	Attempt to maximize loads (rudder kick against swing).
	2	154	Rated	13.0	11.5	−780	−1070	−300	−730	
	3	151	Off	−14.0	16.0	720	940	350	660	
	4	153	Off	11.0	11.0	−610	−930	270	−710	
25a	1	199	Rated	−8.5	7.5	880	−1200	−290	−970	ze loads (high
	2	198	Off	−8.2	7.5	1000	1130	290	860	
26	1	200	Rated	−6.5	3.15	580	640	−230	650	Natural mil l fishtail.
	2	250	Rated	−3.1	2.00	470	600	−200	620	
	3	300	Rated	−2.3	1.65	750	810	210	810	
	4	345	Rated	−2.2	1.50	640	−840	−230	−760	